RICE UNIVERSITY

Negative Feedback Mechanisms Regulating Neurotransmitter Release at the Drosophila Neuromuscular Junction

by

Chun-Jen (Curtis) Lin

A THESIS SUBMITTED
IN PARTIAL FULFILLMENT OF THE
REQUIREMENTS FOR THE DEGREE

DOCTOR OF PHILOSOPHY

APPROVED, THESIS COMMITTEE:

Michael Stern, Professor
Biochemistry and Cell Biology

George N. Bennett, Professor
Biochemistry and Cell Biology

Charles R. Stewart, Professor
Biochemsitry and Cell Biology

James A. McNew, Associate Professor
Biochemsitry and Cell Biology

Robert Raphael, Associate Professor
Bioengineering

HOUSTON, TEXAS
May 2011

Abstract

Homeostasis is an indispensable phenomenon in the maintenance of living organisms. Genetic defects which disrupt negative feedback processes can impact homeostatic regulation, potentially resulting in disease. To uncover the molecular mechanisms governing these and other diseases potentially related to defective homeostasis, I used the Drosophila neuromuscular junction as a model system. I characterized two potential mechanisms that regulate homeostasis within the nervous system. First, in Drosophila larval motor neurons, ligand activation of Drosophila metabotropic glutamate receptor A (DmGluRA) mediates a Phosphoinositide 3-kinase (PI3K)-dependent downregulation of neuronal activity, but the mechanism by which mGluR activates PI3K remains incompletely understood. Here, I identified Ca^{2+}/Calmodulin-dependant protein kinase II (CaMKII) and the Focal adhesion kinase (DFak) as critical intermediates in the DmGluRA-dependent activation of PI3K at Drosophila motor nerve terminals. I found that transgene-induced CaMKII inhibition or the *DFak*^{CG1} null mutation each block the ability of glutamate application to activate PI3K in larval motor nerve terminals, whereas transgene-induced CaMKII activation increases PI3K activity

in motor nerve terminals in a DFak-dependent manner, even in the absence of glutamate application. I conclude that the activation of PI3K by DmGluRA is mediated by CaMKII and DFak. Second, I observed that Push, a putative E3-ubiquitin ligase and Ca^{2+}/Calmodulin binding protein, regulates both neurotransmitter release and retrograde signaling in the Drosophila neuromuscular junction. I found that RNAi-mediated Push inhibition in the neuron increases but, in the muscle decreases, neurotransmitter release. Similar results were obtained from RNAi knock down of PLCβ and IP3R, which mediates Ca^{2+} release from the endoplasmic reticulum. I conclude that Push mediation of the ubiquitin proteasome system may be important in the regulation of PLCβ /IP3R-mediated intracellular Ca^{2+} release, and that this Ca^{2+} release in the neuron inhibits neurotransmitter release, but in the muscle activates neurotransmitter release via a retrograde signal.

Acknowledgments

I would specially like to thank my advisor, Dr. Michael Stern. He was very patient in teaching me many things, both in science and American culture. He also allowed me to try and learn many techniques. Because of his wonderful guidance, I gradually grew up and became an independent researcher during my graduate career. I would also like to thank my committee members, Dr. George N. Bennett, Dr. Charles R. Stewart, Dr. James A. McNew, Dr. Richard Gomer, and Dr. Robert Raphael, for all the suggestions they gave throughout my graduate period.

I really appreciate that Dr. Eric Howlett taught me Drosophila electrophysiology, William Lavery taught me electron microscopy, Magdalena Walkiewicz gave me many scientific suggestions, and Cassidy Johnson and James Summerville helped me on my research. I would also like to thank former and current lab members in Dr. McNew's lab for all your assistances on my experiments: Dr. Song Liu, Tyler Moss, Joseph Faust, and Avani Verma. In addition, I also thank all of you gave me a lot of fun in my graduate career.

Thanks to everybody who also helped me on my research or in life, including Dr. Huey Huang and Dr. Yen Sun who helped me with the Microforge; Dr. Yu-Chang Tsai and Dr. Fu-Jung Lin who gave me great support on my

experiments and in life; Dr. Tom Guu, Andrew Chang, and Yen-Fei Chen who shared a lot of happiness with me and who helped me through good and bad; and the many friends who have participated in my life.

This dissertation is dedicated to my farther, Yung-Shan Lin, my mother, Pao-Luan Cheng, and my brother, Zi-Jing Lin, for their love, encouragement, and life-long support. This dissertation is also particularly dedicated to commemorate my dear mom. Even though cancer took her away from us, I know she will always stay with me and give me great support. Without all your support, I will never have made it this far. Thank you again to my dear family.

Table of Contents

List of Figures and Tables

Tables

List of Abbreviations

AMPA	α-amino-3-hydroxy-5-methyl-4- isoxazolepropionic acid
ASD	Autism spectrum disorders
Brat	Brain tumor
CaMKII	Ca^{2+}/Calmodulin-dependent protein kinase
Camta	Calmodulin-binding transcription activator
ChIP	Chromatin Immunoprecipitation
CNS	Central nervous system
DAG	Diacylglycerol
DIGE	Difference in gel electrophoresis
EJP	Excitatory junction potential
EphA4	Ephrin type-A receptor 4
ER	Endoplasmic reticulum
ERAD	Endoplasmic reticulum-associated protein degradation
Fak	Focal adhesion kinase
FAT	Focal adhesion targeting
FERM	Protein 4.1, ezrin, radixin and moesin homology
Foxo	Forkhead box O
Gbb	Glass bottom boat
GPCR	G-protein couple receptor
IP3	Inositol 3 phosphate
IP3R	Inositol 3 phosphate receptor
LTD	Long term depression
LTF	Long term facilitation
LTP	Long term potentiation
mEJC	Miniature excitatory junction current
mGluR	Metabotropic glutamate receptors
MAP	Microtubule-associated protein
NMJ	Neuromuscular junction

Nos	Nanos
Para	Paralytic
PDK1	Phosphoinositide-dependent protein kinase-1
PI3K	Phosphatidylinositol 3-kinases
PIP2	Phosphatidylinositol- 3,4-bisphosphate
PIP3	Phosphatidyl-inositol-3,4,5-triphosphate
PLCβ	Phospholipase C beta
Pten	Tensin homologue deleted on chromosome10
Pum	Pumilio
RNAi	RNA interference
S6K	S6 kinase
Sax	Saxophone
SH2	Src-homology 2
SH3	Src-homology 3
SNARE	Soluble N-ethylmaleimide-sensitive factor activating protein receptor
SR	Sarcoplasmic reticulum
TAP	Tandem affinity purification
TGF-β	Transforming growth factor *beta*
Tkv	Thickveins
Tor	Target of Rapamycin protein
UAS	Upstream activation sequence
UPS	Ubiquitin-proteosome protein degradation system
Wit	Wishful thinking

Chapter 1: Introduction

1.1 Significance

Homeostatic regulation has been observed as a response to maintain the proper function of the nervous system. When a system under homeostatic regulation is perturbed, neuronal physiology, including synaptic function and cellular depolarization, will be altered to compensate for the changes (Davis and Goodman, 1998; Desai et al., 1999). However, if balance cannot be restored, the result might be neurological disease, such as autism, epilepsy, and schizophrenia. In addition, the defects of Phosphatidylinositol 3-kinases (PI3K) and type II metabotropic glutamate receptors (mGluR) have been implicated in causing these neurological diseases (Kwon et al., 2006; Li et al., 2002; Ogawa et al., 2007; Schoepp, 2001). The observation that altered PI3K or mGluR activity might underlie these diseases raised the possibility that these molecules might participate in homeostatic regulation. If so, our research on mGluR/PI3K feedback-associated homeostatic signaling can further elucidate the linkage between PI3K/mGluR activity and physiological responses. This study may also

be able to assist with the development of new therapeutic strategies for treating these neurological diseases.

1.2 Homeostasis and negative feedback control in neuronal systems

Homeostasis is an internal equilibrium mechanism that maintains and adjusts physiological processes in the living organism. In the nervous system, homeostatic signaling also controls and maintains the stability of neuronal excitability and growth (Marder and Prinz, 2002; Turrigiano and Nelson, 2004). The nervous system can be treated as a complicated electrical circuit. When this circuit is simplified, the whole circuit can be divided into three parts: inward signal, outward signal, and integrative feedback; further, the outward signal contains the set point output and actual output (Figure 1.2.1) (Yi et al., 2000). In a perfectly controlled circuit system, the input will be equal to the set point output. However, in the nervous system, exogenous factors such as nutritional and genetic inputs, cause signal error (Davis, 2006a). The difference between actual output and set point output signal system utilizes integrative feedback to rectify this error. Recently, two different types of mechanisms have been proposed to control

neuronal homeostasis by maintaining a neuron's intrinsic electrical properties. First, activity-independent coupled expression regulates the homeostasis of excitability through the expression, posttranslational processing, or modification of ion channels (MacLean et al., 2005).

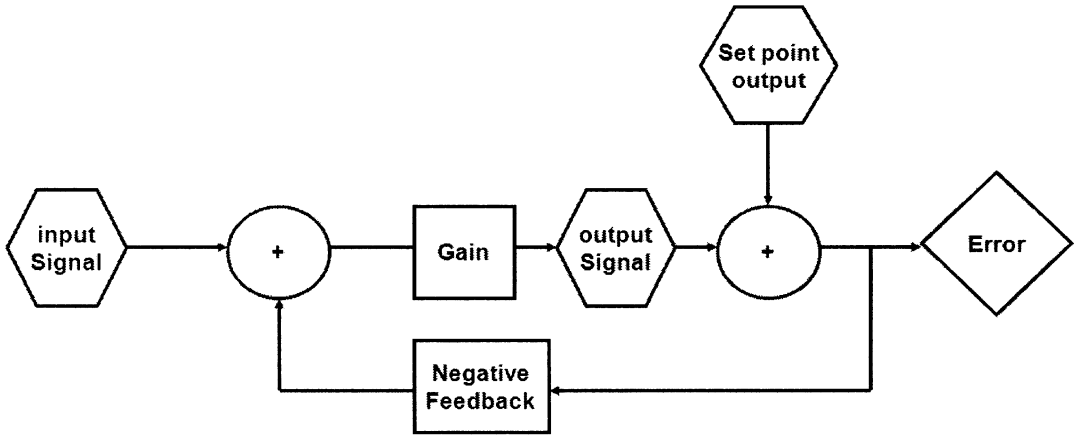

Figure 1.2.1: The block diagram of integrative feedback control circuit can represent the environment for controlling proper neuronal homeostasis in the nervous system. The synaptic microenvironment can be described as circuit. When the neurotransmitters are released from presynaptic area (input signal) the postsynaptic region (gain) will relay and amplify the signal (output signal). However, if the output signal is not equal as set point output, the error will be generated; furthermore, the negative feedback will adjust the presynaptic input to rectify the error and maintain proper homeostasis.

Second, negative feedback can be triggered by signaling molecules that

sense neuron firing, which maintain homeostasis through transcriptional and translational regulatory machinery. This is also called activity-dependent regulation (Davis and Bezprozvanny, 2001; Desai et al., 1999). These phenomena provide us with starting points to study neuronal homeostasis.

1.3 Action potential propagation and synaptic transmission

1.3.1 The biophysical properties of passive neuronal membrane and resting potential

The cell membrane is a specialized structure that separates the internal environment from the outside environment. The membrane is composed of a phospholipid bilayer and embedded proteins. The phospholipids are bipolar organic molecules which contain hydrophobic "tail" regions and hydrophilic "head" regions. These amphipathic phospholipids will form a continuous lipid bilayer and the arrangement of phospholipids in the lipid bilayer results in very low permeability to polar solutes. This resting potential of the passive neuronal membrane is determined by the most permenable ion, uaually K^+. In neurons, the

resting potential is generated by the distribution of three major ions, which are potassium (K^+), sodium (Na^+), and chloride (Cl^-). These ions all have different distributions across the membrane. For example, in mammalian spinal motor axon, the electrochemical potential of K^+ across a semi-permeable membrane can be derived using the Nernst Equation (Equation 1.3.1). Based on this equation, the Nernst potential of K^+ is -90 mV (Ganong WF, 2005).

$$E_{ion} = \frac{RT}{ZF} \ln \frac{[Ion]_{extracellular}}{[Ion]_{\text{int } racelluar}} \quad \text{(Equation 1.3.1)}$$

R = universal gas constant

T = absolute temperature

Z = valence

F = Faraday constant

Ion	Extra Cellular Fluid (mM)	Intra Cellular Fluid (mM)	Nernst Potential (mV)
Potassium (K+)	5.5	150.0	-90
Sodium (Na+)	150.0	15.0	60
Chloride (Cl-)	125.0	9.0	-70

Table 1.3.1. Extracellular and intracellular ionic distribution of the major ions across the passive neuronal membrane of the mammalian spinal motor axon (Moore and Adelman, 1961, Ganong WF, 2005).

In addition, the individual electrochemical potentials and the permeability of each of the relevant ion species (K^+, Na^+, and Cl^-) can be used for calculating the actual resting membrane potential inside the neurons. The mathematical model which is used to describe the resting membrane potential is Goldman-Hodgkin-Katz voltage equation (Equation 1.3.2). Based on this equation and the different distributions of K^+, Na^+, and Cl^- across the membrane of mammalian spinal motor axon, the resting potential is -70 mV (Ganong WF, 2005).

$$Vm = \frac{RT}{ZF} \ln \frac{P_k[K^+]_o + P_{Na}[Na^+]_o + P_{Cl}[Cl^-]i}{P_k[K^+]i + P_{Na}[Na^+]_i + P_{Cl}[Cl^-]_0} \quad \text{(Equation 1.3.2)}$$

P= permeability

R = universal gas constant

T = absolute temperature

Z = valence

F = Faraday constant

1.3.2 Action potential propagation

In the absence of perturbations, the neurons are typically maintained at a negative resting potential. When synaptic inputs stimulate at the hillock which is

part of the cell body of neuron and connects to the axon, a small depolarization of the membrane will be generated. If this small depolarization is successfully above the stimulation threshold (minimum membrane potential for inducing action potential), it will initiate the opening of voltage-gated Na^+ channels which allow Na^+ ions to flow into the cell, thus resulting in further depolarization of the membrane potential (Figure 1.3.1). Subsequently, the depolarization spreads outwards from the local region and triggers the opening of other voltage-gated Na^+ channels as a positive feedback to create the continuous wave of depolarization moving down to the axon terminal. Following depolarization of the membrane, the opening of voltage-gated K^+ channels occurs and increases permeability of K^+ ions to flux from the intracellular region. Once Na^+ influx reaches the maxima (the peak of action potential) (Figure 1.3.1), K^+ efflux then repolarizes the cell (Figure 1.3.1). A hyperpolarization of the membrane potential subsequently occurs, which is caused by an excess of K^+ efflux (Figure 1.3.1). To reset the membrane potential back to equilibrium, Na^+ and K^+ channels close and Na^+/K^+ pumps utilize ATP as energy source to transport Na^+ and K^+ acrossing membrane.

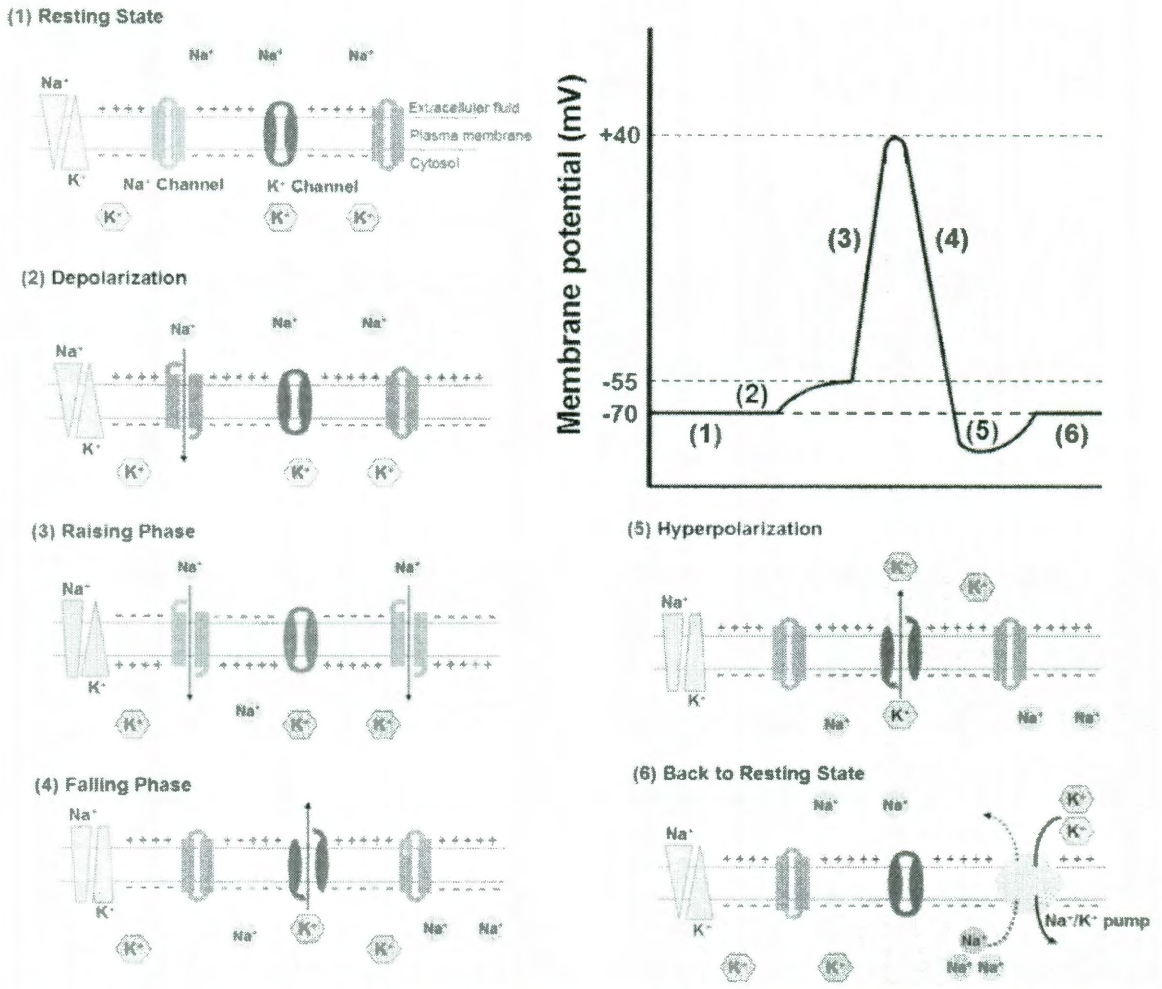

Figure 1.3.1: The mechanism of action potential propagation. (1) Resting state: Both [Na^+] and [K^+] across the membrane maintain the resting potential. (2) Depolarization: the electrical signal triggers Na^+ channel opening. The Na^+ enters the intracellular region and increases the Na^+ concentration. (3) Rising Phase: more Na^+ channels open and allow more Na^+ to flow into intracellular region. The [Na^+] increase results in further depolarization. This stage also initiates K^+ channel opening. (4) Falling phase: the Na^+ channels begin to close and K^+ start to leave cell via K^+ channels. (5) Hyperpolarization: extra K^+ release from the intracellular to extracellular. K^+ channels begin to close. (6) Back to resting state: both Na^+ and K^+ channels close and Na^+/K^+ pumps utilize ATP as energy source to transport Na^+ and K^+ acrossing membrane and reset the membrane potential back to equilibrium.

1.3.3 Neurotransmitter release

When the action potential reaches to the nerve terminal, the depolarization triggers the opening the voltage-gated Ca^{2+} channels and allows the Ca^{2+} to flow from extracellular regions into the axon terminal (Figure 1.3.2). The increase of $[Ca^{2+}]$ induces the vesicles containing either excitatory or inhibitory neurotransmitter to release from the active zone into the synapse. The released neurotransmitters diffuse across the synaptic cleft and bind to target receptors on the postsynaptic region of the target dendrite or muscle (Figure 1.3.2). In summary, these electrical and chemical changes in the nervous system provide the powerful machinery needed to control communication among tissues inside living organisms.

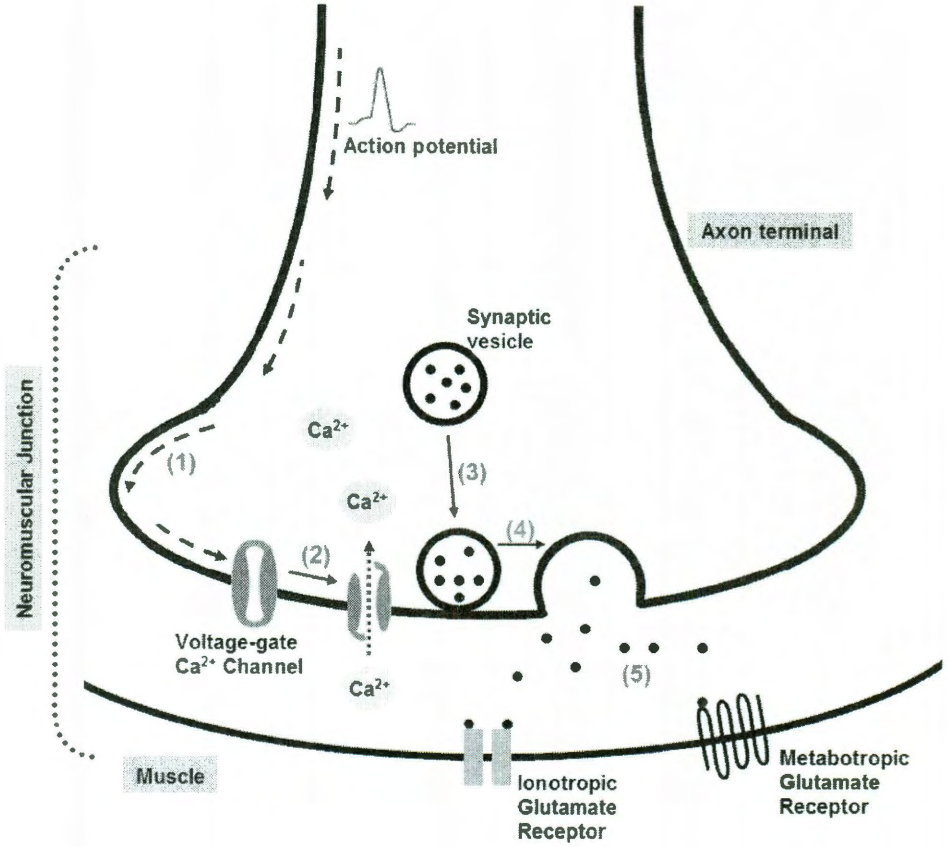

Figure 1.3.2. The mechanism of neurotransmitter release in the neuromuscular junction. (1) The action potential travels to the presynaptic area of neuromuscular junction and triggers opining of voltage-gated Ca^{2+} channels. (2) The opened Ca^{2+} channels allow Ca^{2+} flux into the nerve terminal and increases Ca^{2+} concentration. (3) The increased [Ca^{2+}] initiates the membrane fusion process mediated by V- and T-SNAREs. (4) The neurotransmitters are released into the synaptic cleft by exocytosis. (5) The neurotransmitters diffuse and bind to target receptors and induce responses.

1.4 Neurological disorders involving mGluR/PI3K-mediated homeostatic defects

Metabotropic glutamate receptors (mGluRs), which are G protein coupled receptors for which glutamate is ligand, mediate aspects of synaptic plasticity in mammalian and invertebrate systems. In several regions of the mammalian brain, including the hippocampus, the cerebellum, the prefrontal cortex and others, ligand activation of group I mGluRs induces a long-term depression of synaptic activity, termed mGluR-mediated LTD (Luscher and Huber, 2010). Induction of mGluR-mediated LTD both activates and requires the activation of the lipid kinase PI3 Kinase (PI3K) and the downstream kinase Tor (Hou and Klann, 2004). Several genetic diseases of the nervous system are predicted to increase sensitivity to activation of mGluR-mediated LTD. For example, increased sensitivity to induction of mGluR-mediated LTD has been observed in the mouse model for Fragile X (Bear et al., 2004). Furthermore, the genes affected in tuberous sclerosis (Tsc1 and Tsc2) and Neurofibromatosis (Nf1) encode proteins that downregulate Tor activity (Dasgupta et al., 2005; Gao et al., 2002). These observations raise the possibility that hyperactivation of mGluR-mediated LTD

plays a causal role in the neurological phenotypes of Fragile X, Neurofibromatosis and tuberous sclerosis (Kelleher and Bear, 2008). Because these diseases are each associated with an extremely high incidence of autism spectrum disorders (ASD), and because several lines of evidence suggest that elevated PI3K activity is associated with ASD (Cusco et al., 2009; Kwon et al., 2006; Mills et al., 2007; Serajee et al., 2003), it has been hypothesized that hyperactivation of this pathway might be responsible for ASD as well.

1.5 mGluR/PI3K-dependant signal transduction pathway

Glutamate is the major excitatory neurotransmitter in the mammalian central nervous system (CNS) and at the insect neuromuscular junction (NMJ) (Jan and Jan, 1976), and activates two distinct types of receptors; ion-channel-associated (ionotropic) and G-protein-coupled (metabotropic) glutamate receptors (Enz, 2007). The N-terminal domain of mGluR is located in the extracellular region and is about 600 amino acids long. In mammals, there are eight mGluR subtypes divided into three groups, which each activate different downstream signaling pathways (Enz, 2007). Previous work demonstrated that the C-terminal domains

vary in length (Enz, 2007). The C-termini are the key sites for interaction with different proteins to regulate different signaling pathways (Perroy et al., 2001). PI3K is a conserved lipid kinase that contains two subunits and mediates several physiological functions, including cell survival, cell cycle progression, protein synthesis, and aging (Engelman et al., 2006). PI3K is activated most prominently by receptor tyrosine kinases. PI3K phosphorylates phosphatidylinositol-3,4-bisphosphate (PIP2) to phosphatidyl-inositol-3,4,5-triphosphate (PIP3). As mentioned in section 1.4, mGluR has been implicated in the activation of PI3K-mediated signaling pathways (Hou and Klann, 2004). When PIP3 is present on the membrane, the pleckstrin homolgy domain containing proteins, which can bind phosphatidylinositol lipids, phosphoinositide-dependent protein kinase-1 (PDK1) and protein kinase B (PKB/AKT), are recruited to the membrane, and AKT is phosphorylated by PDK1. The phospho-AKT then regulates through phosphorylation many downstream effectors, such as the forkhead box transcription factor FOXO, mammalian target of rapamycin (mTOR), and S6 kinase (S6K). These downstream effectors can further control different physiological functions (Engelman et al., 2006) (Figure 1.5.1). Foxo has been implicated in the regulation of cell survival (Burgering and Medema, 2003) and

S6K is an important factor in controlling protein synthesis and cell growth (Klann and Sweatt, 2008).

In addition, the phosphatase and tensin homologue deleted on chromosome10 (PTEN) function as a negative effector, to dephosphorylate PIP3 to PIP2 and inhibit the activation of PI3K. PTEN has two structural domains; the phosphatase and C2 domains. The phosphatase domain of PTEN can dephosphorylate PIP3 to PIP2. Therefore, PI3K and PTEN can function together to adjust PIP3 levels and maintain proper level of AKT-mediated signaling (Gericke et al., 2006) (Figure 1.5.1). In conclusion, the mGluR/PI3K signaling pathway has important roles in the regulation of synaptic plasticity and neuronal homeostasis. Therefore, the mGluR/PI3K-mediated signaling pathway becomes one key mechanism to understand the cause of ASD, Fragile X, Neurofibromatosis and tuberous sclerosis

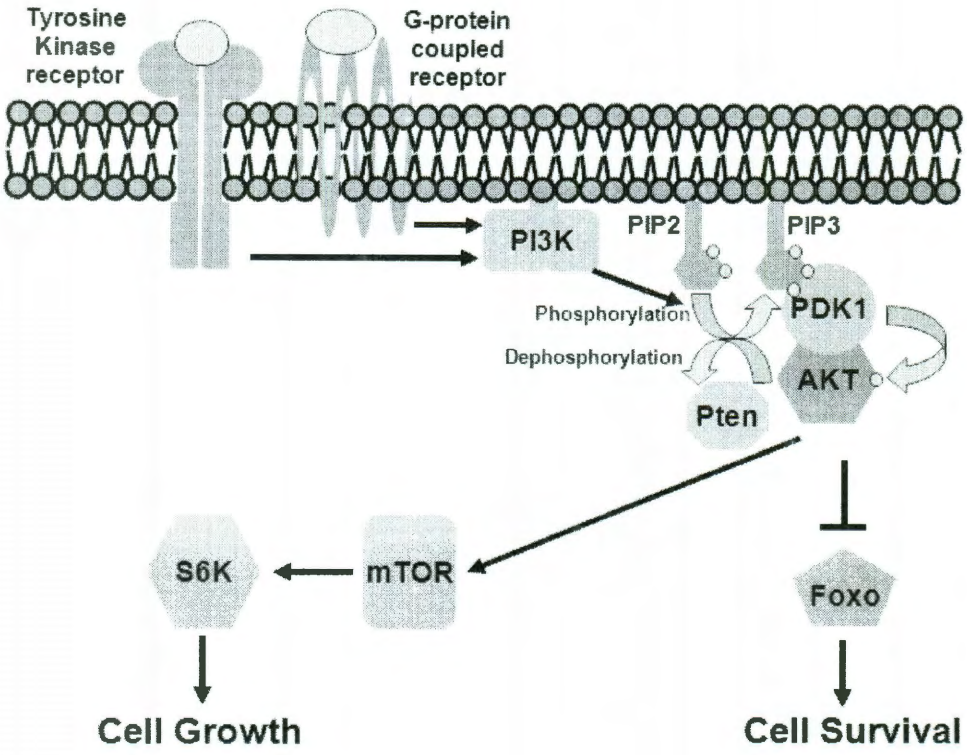

Figure 1.5.1. The PI3K signaling pathway regulates many physiological events by interacting with different downstream effectors. PI3K can be activated by different types of upstream receptors including tyrosine kinase receptors and GPCRs. Active PI3K phosphorylates PIP2 to PIP3. Next, PIP3 recruits PDK1 and AKT and PDK1 phosphorylates AKT (p-AKT). The p-AKT further regulates downstream effectors, such as Foxo and S6K, to control cell survival and cell growth, respectively.

1.6 Drosophila GAL4/UAS system

Drosophila GAL4/UAS system is a genetic tool to express genes temporally and spatially. GAL4 is a protein containing 881 amino acids and first identified in

Saccharomyces cerevisiae. GAL4 is a transcriptional activator and regulates transcription by directly binding to a specific DNA sequence called upstream activation sequence (UAS) (Giniger et al., 1985). Molecular biological and transgenic methodologies are used to create the transgenic flies that carry either *gal4* or target genes sequence downstream of UAS into the Drosophila genome randomly. To active specific UAS target gene transcription, GAL4 fly lines (also called drivers), which are under control of tissue specific promoters, will mate with responder lines (which call UAS-drives transgenes) to express target genes (Figure 1.6.1). The expression patterns of target genes will reflect the GAL4 pattern of the respective driver (McGuire et al., 2004; Phelps and Brand, 1998). Because of these special characters of the Gal4/UAS system, we can study the molecular mechanism of nervous system by expressing the target proteins and measuring the change of neurological properties.

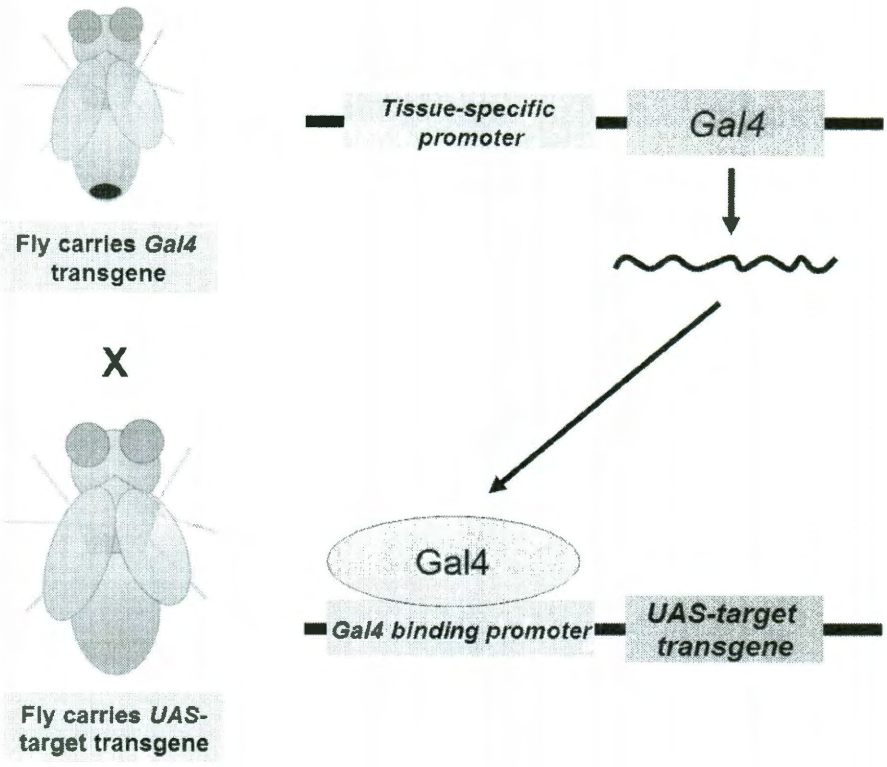

Figure 1.6.1. The Drosophila GAL4/UAS system. Flies carrying yeast transcription factor Gal4 with a specific expression pattern are crossed to flies carrying target genes under the control of UAS (UAS-target gene). The progeny will carry both Gal4 and UAS-target gene and express target gene in the expression pattern of the Gal4. (Fly pictures are generously provided by Cassidy Johnson)

1.7 Drosophila larval nervous system for studying neuronal function.

Drosophila melanogaster is a simple and popular genetic model system for biological studies, including aging, growth, and neuroscience. There are several

advantages in using Drosophila for neuronal studies. The Drosophila genome and gene variations are simple compared to vertebrate systems. Drosophila gene expression can be easily manipulated both spatially and temporally. The anatomy of the Drosophila neuromuscular system is very well-understood. Drosophila is a proven system for the study of electrophysiology, development, and behavior (Jan and Jan, 1976; Jan and Jan, 1978; Mackay, 2009). In addition, only a few motor neurons innervate Drosophila body wall muscles, and synapses are accessible for both physiological and developmental studies (Budnik et al., 1990). The synapses, also called boutons, in the NMJ develop during late embryonic stages and then grow significantly during larval development (Prokop, 2006). The neuronal growth exhibits increases in branching, bouton number, and active zones per bouton (Marques et al., 2002). In summary, the Drosophila larva provides a great platform to study electrophysiology and growth in motor neurons.

1.8 Excitatory junction potential (EJP) as a reflection for measuring Drosophila neurotransmitter release.

As mentioned in Section 1.3.3, an action potential is propagated to the nerve

terminal and causes transmitter release at the neuromuscular junction. The neurotransmitter subsequently induces the depolarization of the muscle membrane, called the excitatory junction potential (EJP) (Jan and Jan, 1976). EJP amplitude can represent the amount of transmitter release. In addition, at low [Ca^{2+}], Ca^{2+} is limiting for transmitter release, and mutations that alter Ca^{2+} influx have significant effects on EJP amplitude (Ganetzky and Wu, 1982; Huang and Stern, 2002). For example, increasing the activity of Phosphatidylinositol 3-kinase (PI3K) attenuates the amount of neurotransmitter release and results in a decrease in EJP amplitude (Howlett et al., 2008), whereas decreasing the activity of PI3K increases the amount of neurotransmitter release and results in an increase in EJP amplitude (Howlett et al., 2008). Therefore, measuring EJP amplitude within genotypes that have altered neurotransmitter release could provide information to elucidate the signaling pathways that regulate neuronal activity.

1.9 Long term facilitation (LTF) as a reflection for measuring Drosophila neuronal excitability

LTF is a form of synaptic plasticity induced when a larval motor neuron is subjected to a train of repetitive nerve stimulations at low external [Ca^{2+}]. At a certain point during the stimulus train, a threshold is reached, and subsequent stimulations elicit EJPs greatly increased in amplitude and duration. This facilitation (termed LTF) results from increased and asynchronous neurotransmitter release, which in turn results from increased duration of nerve terminal depolarization (Jan and Jan, 1978). The number of stimulations required to reach this LTF threshold (LTF onset rate) is decreased by increased neuronal excitability (Jan and Jan, 1978; Mallart et al., 1991; Poulain et al., 1994; Schweers et al., 2002; Stern and Ganetzky, 1989; Stern et al., 1990). For example, manipulation of molecules that increase activities of K^+ channel, such as *Hyperkinetic* (*Hk*) and *ether-a-go-go* (*eag*) or decrease activities of Na+ channel, such as *paralytic* (*para*) decreases the rate of onset of LTF (Figure 1.9.1). This phenomenon is defined as hypoexcitability (Figure 1.9.1). In contrast, manipulation of molecules that decrease activities of K^+ channel or increase activities of Na^+ channel decrease the rate of onset of LTF. This phenomenon is defined as hyperexcitability (Figure 1.9.1) (Cardnell et al., 2006; Stern and Ganetzky, 1989; Stern et al., 1990). By measuring LTF onset rate, the genotypes

that reveal either hyperexcitability or hypoexcitability could provide information to map the signaling pathways that regulate neuronal activity.

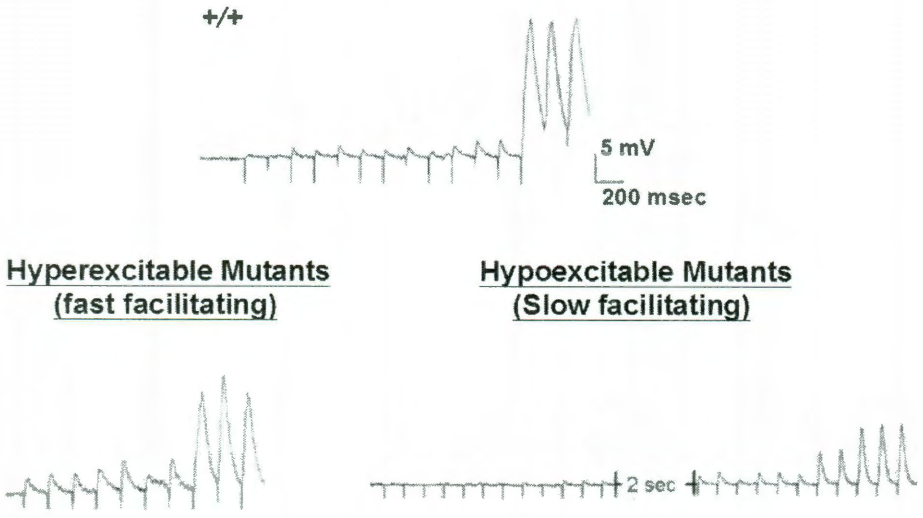

Figure 1.9.1. Drosophila neuronal excitability. LTF is elicited by applying high-frequency stimulus train (10 Hz in this figure) at low external [Ca^{2+}]. Hyperexcitability is defined as an increase in the rate of onset of LTF. On the contrary, hypoexcitability is defined as a decrease of the rate of onset of LTF (image is adopted and modified from Doctoral thesis of Eric Howlett).

Based on this phenomenon in Drosophila nervous system, the Parmentier lab first reported that elimination of Drosophila mGluR (*DmGluRA*) by the null mutation *DmGluRA*^{112b}, or by RNAi-mediated *DmGluRA* knockdown specifically in motor neurons, increases neuronal excitability (Bogdanik et al., 2004). DmGluRA

is required for the regulation of neuronal excitability and presynaptic growth (Bogdanik et al., 2004). Later, our lab found that the mGluR-associated PI3K/AKT signaling pathway is a negative feedback to maintain homeostasis in the glutamatergic synapse (Howlett et al., 2008). Our data provided several evidences. First, *DmGluRA*^{112b} and the inhibition of PI3K pathway by motor neuron-specific overexpression of either the phosphatase *PTEN*, which opposes the effect of PI3K, or the dominant-negative *PI3K* (*PI3K*^{DN}) increased the rate of onset of LTF. Second, the constitutive activation of PI3K and elimination of transcription factor Foxo by *Foxo* null mutation (*Foxo*^{21}/*Foxo*^{25}) both decreases neuronal excitability. Third, *DmGluRA*^{112b} blocked the elevation of phospho-AKT during the glutamate application. Finally, the dominant-negative *S6K* (*S6K*^{DN}), a downsteam signal molecule of PI3K/AKT, prevented the constitutive activation of PI3K inducing neuronal overgrowth (Howlett et al., 2008). Therefore, the defect of *DmGluRA* increased motor neuron excitability via PI3K and the downstream FOXO and decreased neuronal arborization via PI3K and the downstream the S6K (Figure 1.9.2) (Howlett et al., 2008). Even though mGluR, PI3K and downstream effectors, which are involed in the regulation of neuronal excitability and growth, are characterized, the molecular intermediates in the communication

between mGluR and PI3K, and between Foxo and target genes remained unidentified.

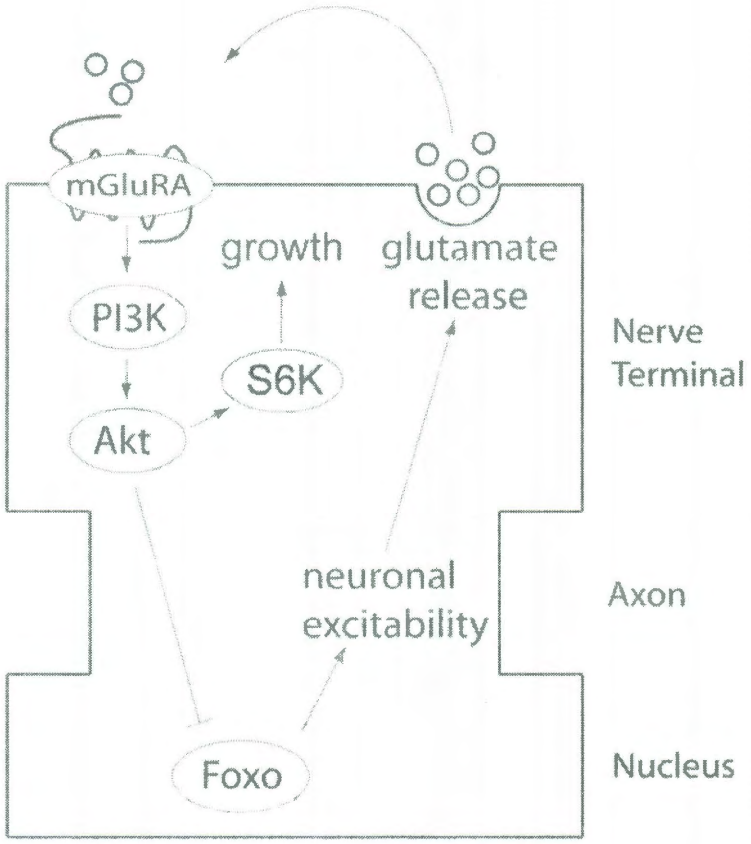

Figure 1.9.2: A proposed mechanism for the DmGluRA-dependent activation of PI3K. We suggest that glutamate released from motor nerve terminals as a consequence of neuronal activity activates DmGluRA autoreceptors located in motor nerve terminals. PI3K activation decreases neuronal excitability by inhibiting the transcription factor Foxo, and increases synapse number by activating S6 kinase.

1.10 Drosophila retrograde signaling at the neuromuscular junction

In the Drosophila neuromuscular junction (NMJ), three basic events have been observed to enable maintenance of neuronal homeostasis. First, anterograde communication, such as action potential propagation and neurotransmitter release, directly controls the change of membrane potential and vesicle release (see section 1.3) (Marques, 2005). Second, presynaptic negative feedback regulation, such as mGluR/PI3K-mediated negative feedback, adjusts the neuronal excitability and transmitter release (see section 1.5) (Bogdanik et al., 2004; Howlett et al., 2008). This negative feedback-mediated inhibition can be in response to excessive vesicle release at motor nerve terminal and reset the system (Davis, 2006b). Third, post-synaptic retrograde signaling, such as TGF-β signaling-mediated retrograde signaling, affects and regulates pre-synaptic neurotransmitter release. This effect of post-synaptic retrograde signaling will be described in detail in this section (Koh et al., 2000; Marques, 2005; Marques et al., 2002).

TGF-β-mediated retrograde signaling is a well-understood mechanism which controls the number of vesicle release (also called quantal content) at Drosophila

NMJ (Marques, 2005; Marques et al., 2002; McCabe et al., 2003). The process of retrograde signaling initiates with the secretion of Glass bottom boat (Gbb), a bone morphogenetic protein and the ligand of TGF beta type II receptors, from the muscle (McCabe et al., 2003). Gbb diffuses from the muscle site (post-synaptic) to the nerve terminal (pre-synaptic) and binds to the type II receptor Wishful thinking (Wit) at the nerve terminal (Aberle et al., 2002; McCabe et al., 2004; McCabe et al., 2003; Rawson et al., 2003); moreover, this binding event induces the Ser/Thr kinase activity of Wit (Figure 1.10.1). This Gbb/Wit binding complex recruits and phosphorylates one of the type I receptors, either Saxophone (Sax) or Thickveins (Tkv) (Rawson et al., 2003). The phosphorylation of Sax or Tkv activates their own kinase activities, and then phosphorylates the presynaptic transcription factor Mad (Aberle et al., 2002; Marques et al., 2002). Following phosphorylation, phospho-Mad transports from the axon terminal to the nucleus and forms a complex with the co-Smad Medea (Med) (Aberle et al., 2002; Marques et al., 2002). This active transcription factor complex then modulates the expression of target genes and adjusts the quantal content of transmitter release (Figure 1.10.1) (Aberle et al., 2002; Marques et al., 2002; McCabe et al., 2004; McCabe et al., 2003; Rawson et al., 2003).

However, several lines of evidence have shown that TGF-β-mediated retrograde signaling is not the sole pathway to control the retrograde signaling in the Drosophila NMJ. In Drosophila, cell adhesion molecules, such as homophilic cell adhesion molecule Fasciclin II (FasII) are required for retrograde signaling (Kazama et al., 2007). They reported that postsynaptic overexpession of constitutive calcium/calmodulin-dependent protein kinase II (CaMKII) induced the retrograde signaling by increasing the number of active zones, and the frequency of miniature excitatory junction currents (mEJCs) but these CaMKII-mediated retrograde signaling were blocked in *fasII* mutation backgrounds (Kazama et al., 2007). The results suggested that the modulation of retrograde signaling is initiated by CaMKII and independent of the TGF-β signaling-mediated retrograde signaling (Kazama et al., 2007). However, the microenvironmental changes including the alteration of cell adhesion still remain unclear. Therefore, the examination of cell adhesion in the regulation of retrograde signaling is also important for understanding the neuronal homeostasis.

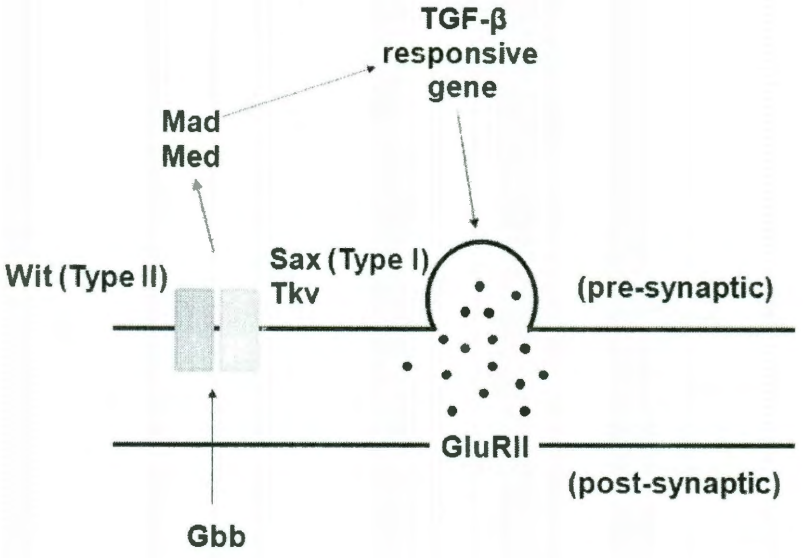

Figure 1.10.1. A TGF-β signaling pathway regulates retrograde signaling in the Drosophila NMJ. Gbb is secreted from muscle (post-synaptic) and then diffuses to the nerve terminal (pre-synaptic). Once Gbb binds to TGF beta type II receptor (Wit), Wit will recruit and activate the TGF beta type II receptor (Sax or Tkv). Furthermore, the activation of Sax of Tkv will regulate the activity of the transcription factor complex (Mad and Med) and control neurotransmitter release in the nerve terminal.

1.11 Structure and function of Ca^{2+}/Calmodulin protein kinase II

1.11.1 The role of Calcium in cells

Calcium (Ca^{2+}) is a key element regulating a large number of intracellular responses, including glycogenolysis, endocytosis, mitochondrial respiration,

transcription, and neurotransmitter release (Hudmon and Schulman, 2002). Ca^{2+} also acts as a second messenger. When membrane receptors are activated by outside signal molecules, including hormones and neurotransmitters, these active membrane receptors couple to second messengers and convey the extracellular stimuli with correspondent cellular responses (Hudmon and Schulman, 2002). The signaling processes that are mediated by Ca^{2+} are essential for neuron physiology, including vesicle fusion, neurotransmitter release, and synaptic transmission, and also for muscle contraction (Hudmon and Schulman, 2002). To achieve these events, a change in $[Ca^{2+}]$ is executed within the cells. Cells typically maintain relatively low intracellular $[Ca^{2+}]$ levels (10^{-7} M) compared with extracellular $[Ca^{2+}]$ levels (10^{-3} M) (Chin and Means, 2000). By increasing intracellular $[Ca^{2+}]$ levels from extracellular and intracellular Ca^{2+} storage (ER and mitochondria), the elevation of $[Ca^{2+}]$ level can trigger the Ca^{2+}-mediated signaling pathways (Chin and Means, 2000).

1.11.2 Inositol 3 phosphate (IP3)-mediated Calcium released signaling transduction pathway

As mentioned in the section 1.11.1, cells maintain a lower cytoplasmic [Ca^{2+}] level and accomplish many physiological processes including neurotransmitter release and muscle contraction by elevating cytoplasmic [Ca^{2+}] level, especially from intracellular Ca^{2+} storage (ER and mitochondria). One of the important signaling pathways to elevate intracellular [Ca^{2+}] is the IP3-mediated Calcium release pathway. When GPCRs that are specific for mediating intracellular Ca^{2+} release receive outside signals, these active GPCRs activate downstream G-proteins. The active G-proteins stimulate Phospholipase C beta (PLCβ). Once PLCβs are activated, PLCβ will induce the hydrolysis of PIP2 to IP3 and DAG. Because IP3 is soluble, IP3 will diffuse and bind to the IP3R to trigger Ca^{2+} release from ER to the cytoplasm (Figure 1.11.1) (Berridge, 1993; Berridge et al., 2000).

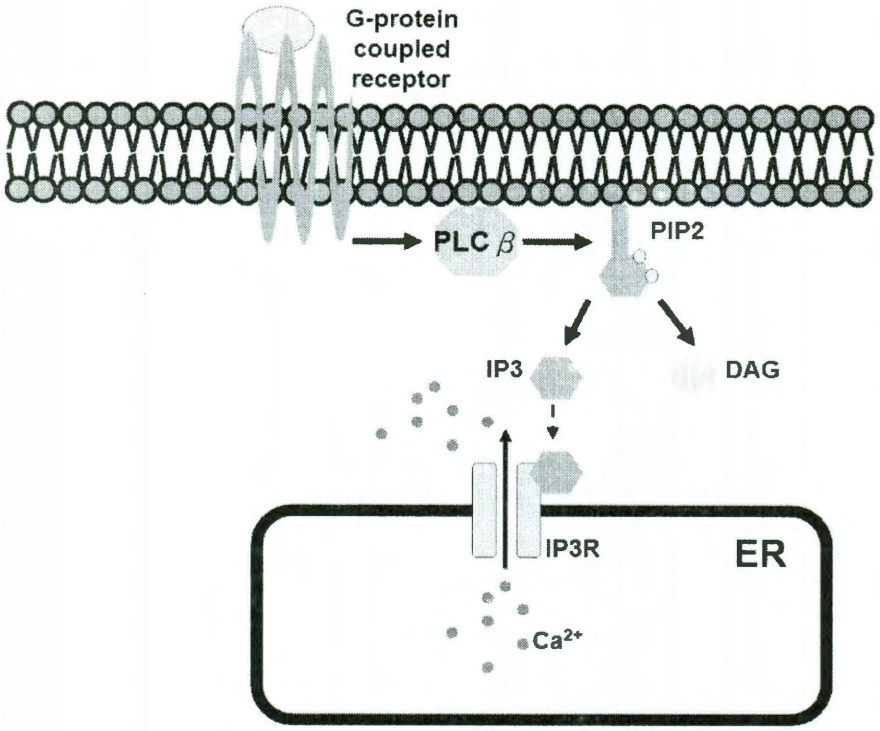

Figure 1.11.1. The PLCβ/IP3R-mediated signaling is important in the regulation of Ca^{2+} release from ER. PLCβ can be activated by GPCR. The active PLCβ hydrolyzes PIP2 to IP3 and DAG. Furthermore, IP3 binds to IP3R and induces the channel opening of IP3R. The opened IP3R allows Ca^{2+} to release from ER to cytoplasm and increase the cytoplasmic Ca^{2+} concentration.

1.11.3 The mechanism of CaMKII in regulating Calcium concentration

CaMKII is a Ca^{2+}/Calmodulin-dependent protein and a Ser/Thr protein kinase. CaMKII consists of three functional domains; a catalytic domain, a regulatory

domain, and an association domain (Figure 1.11.2) (Griffith, 2004; Kolb et al., 1998; Shen and Meyer, 1998). CaMKII activity is regulated by autophosphorylation. CaMKII ordinarily exists as a multimeric structure within cells. When [Ca^{2+}] is increased, Ca^{2+} and Calmodulin form an active Ca^{2+}/CaM complex and then bind to the CaM-binding domain inside the regulatory domain of CaMKII. When this binding occurs, the active CaMKII subunit will phosphorylate the Threonine (Thr) 286 of the adjacent subunit, which switches on kinase activity. When all the Thr 286 in the subunits of CaMKII are phosphorylated and all active CaMs are trapped due to [Ca^{2+}] increase, the dissociation rate of Ca^{2+}/CaM increases more than 1000 fold (Griffith, 2004; Hudmon and Schulman, 2002). Next, the dissociation of Ca^{2+}/CaMs from CaMKII subunits subsequently induce the phosphorylation on Thr 306 and Thr 307 of adjacent subunits. The phosphorylation of Thr 306/307 prevents CaMKII activities and also allows specific phospatases of CaMKII to remove the phosphate groups on Thr286/306/307 and inactivate CaMKII (Figure 1.11.2). The autophosphorylation of CaMKII can regulate CaMKII-mediated signaling efficiently and also maintain the Ca^{2+}-related neuronal responses properly (Griffith, 2004; Hudmon and Schulman, 2002; Kemp et al., 1996; Lou and Schulman, 1989; Miller et al., 1988).

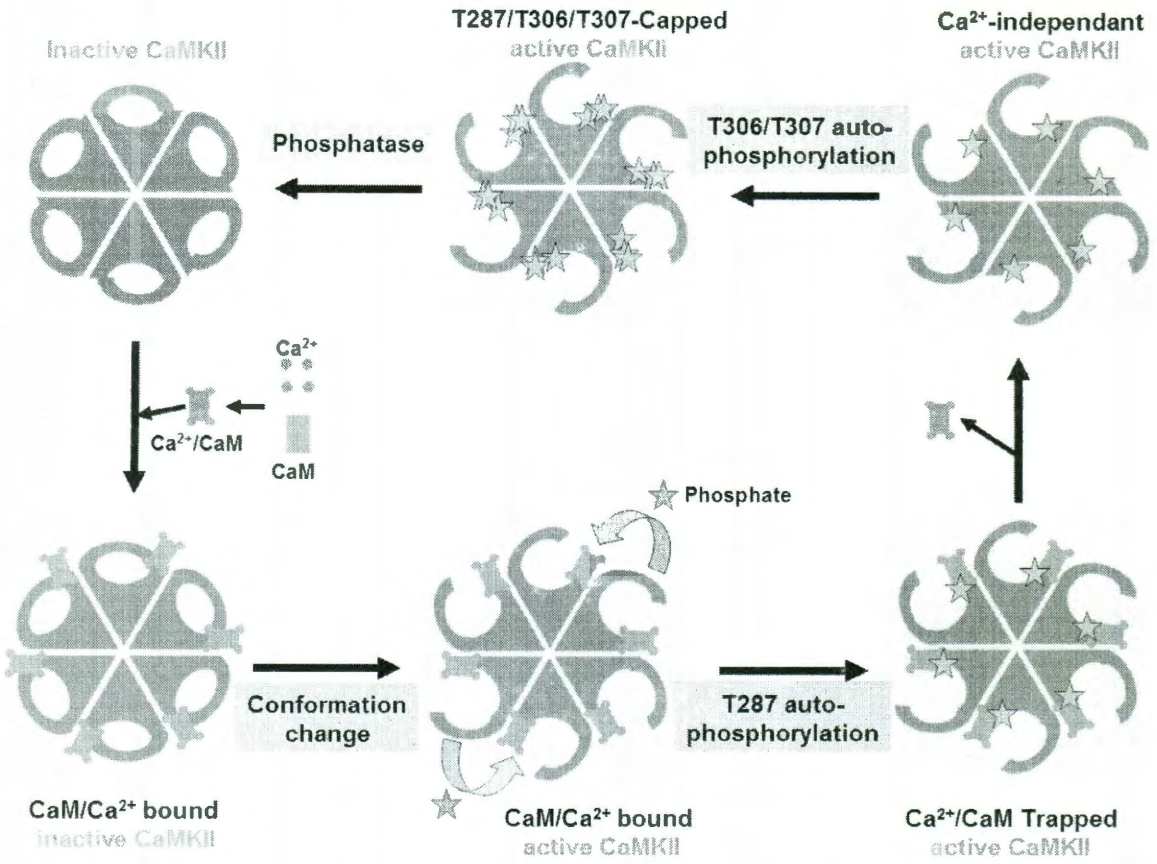

Figure 1.11.2. The autophosphorylation mechanism regulating CaMKII activity in Drosophila. When intracellular [Ca^{2+}] increases, inactive CaMKII will bind to the Ca^{2+}/CaM complex. This binding induces a conformational change in CaMKII and CaMKII trans-phosphorylates adjacent CaMKII on threonine 287 (T287). The CaMKII with T287 phosphorylation becomes Ca^{2+} independent and begins to release Ca^{2+}/CaM complex; furthermore, CaMKII with T287 phosphorylation triggers autophosphorylation on threonine 306 and 307(T306/T307). This T287/T306/T307-capped CaMKII becomes Ca^{2+} insensitive and phosphatase which is CaMKII specific will dephosphorylate on T287, T306, and T307 and brings CaMKII back to inactive state.

1.11.4 The physiological role of CaMKII in nervous system

CaMKII is one of the most abundant proteins in the nervous system. For example, CaMKII comprises up to 2% of total proteins in the mammalian hippocampus and 1% of total protein in the mammalian forebrain (Onodera et al., 1990). Because of the high expression level of CaMKII in the forebrain and hippocampus and the alteration of CaMKII activity associated with long term potentiation (LTP) and long term depression (LTD), a long-lasting enhancement and reduction in signal transmission, respectively, this information implicates the importance of CaMKII in regulating forms of learning and memory (Bear and Malenka, 1994; Erondu and Kennedy, 1985; Hudmon and Schulman, 2002; Malenka and Bear, 2004; Riedel and Reymann, 1996).

In Drosophila, it was previously found that motor neuron expression of *CaMKII*^{T287D} increased synapse number and decreased excitability in motor neurons (Park et al., 2002); both of these phenotypes are also exhibited in larvae expressing the constitutively active *PI3K-CAAX* (Howlett et al., 2008; Martin-Pena

et al., 2006). In conclusion, these results support the notion that levels of PI3K activity are specified, at least in part, by activity of CaMKII.

1.12 Structure and function of Focal adhesion kinase

1.12.1 The functional domains of Focal adhesion kinase

Focal adhesion kinase (Fak) is a 125-kDa non-receptor tyrosine kinase which is expressed ubiquitously. Fak not only provides signalling and scaffolding functions at sites of integrin adhesion but is also involved in the regulation of integrin-mediated assembly and disassembly processes in cell-matrix attachment (Schlaepfer et al., 2004). Fak is composed of a protein 4.1, ezrin, radixin and moesin homology (FERM) domain, a kinase domain, proline-rich regions, and a focal adhesion targeting (FAT) domain (Figure 1.12.1A) (McLean et al., 2005; Schlaepfer et al., 2004). The functions of Fak domains will be discussed in two separate sections; 1) the domains involved in the association of integrins, and 2) the domains regulating Fak activation and catalytic activity.

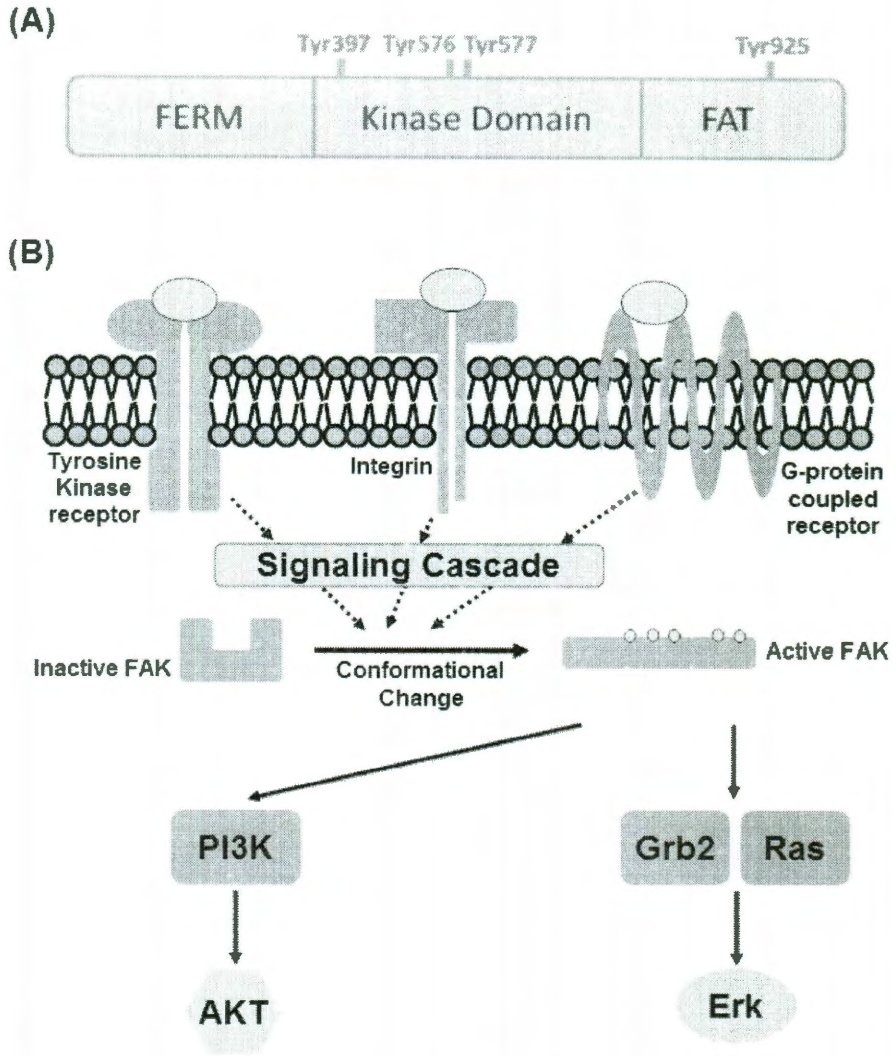

Figure 1.12.1. Fak can activate PI3K and MAPK signaling cascades via Tyrosine kinase receptor, integrin, and GPCR-mediated singaling pathways. (A) Fak contains three functional domains, including a protein 4.1, ezrin, radixin and moesin homology (FERM) domain, a kinase domain, and a focal adhesion targeting (FAT) domain. (B) Fak can be activated by different types of upstream receptors, including integrins, tyrosine kinase receptors and GPCRs. These activations will induce Fak autophosphorylation on tyrosine 397, and the consequent conformational change activates Fak. Moreover, active Fak can activate PI3K or MAPK signaling cascades.

1.12.2 The integrin-association domains in Fak

The FERM domain of Fak performs as a signalling linkage of receptor tyrosine kinases including integrins or growth factor receptors (Sieg et al., 2000). The FAT domain is located in the C-terminal region of Fak and consists of multiple motifs which mediates the association with integrin-associated proteins including paxillin and talin (Hildebrand et al., 1993; Schlaepfer et al., 2004). Because previous studies have shown that Fak cannot directly bind to integrins (Chen et al., 1995), the integrin-associated proteins, such as Paxillin, serve as linkage for integrins to activate Fak (Schlaepfer et al., 1999; Schlaepfer and Hunter, 1997). In addition, two proline-rich regions in the C-terminal domain of Fak serve as binding sites for Src-homology 3 (SH3)-domain-containing proteins (Mitra et al., 2005). The Integrin-mediated activation of Fak can regulate the cytoskeleton, cell adhesion and membrane morphogenesis to control cell movement (Mitra et al., 2005).

1.12.3 Regulation of FAK activation and catalytic activity

When Fak receives an input signal from cell surface-associated receptors such as integrins, G-protein couple receptors, and receptor protein tyrosine kinases, the autophosphorylaltion process will occur either in *cis* or *trans* to phosphorylate Tyr397 (Toutant et al., 2002). Tyr397 phosphorylation of Fak induces a conformational change in Fak and subsequently recruits Src homology 2 (SH2)-containtig proteins, such as Src-family kinase (SFKs), p120 RasGAP, and the p85 subunit of phosphatidylinositol 3-kinase (PI3K) (Figure 1.12.1B) (Hanks et al., 2003; Schlaepfer et al., 2004). This phosphorylation of Tyr397 is required for the activation of Fak. Once Src binds to Fak, Src phosphorylates Fak on Tyr576 and Tyr577 within the catalytic domain. The phosphorylation of Tyr576 and Tyr577 increases the binding affinity between two Faks and induces the intermolecular phosphorylation of Tyr861 and Tyr925 on Fak (Figure 1.12.1B) (Ruest et al., 2000; Schlaepfer et al., 2004). Moreover, Fak ,phosphorylated on Tyr861 and Tyr925 can become the docking site for SH2 domain adaptor proteins, such as Grb2 (an upstream signaling molecule of Ras and ERK), and induce the activation of multiple intracellular signaling cascades (Figure 1.12.1B) (Schaller, 2001; Schlaepfer et al., 1994; Schlaepfer et al., 1999; Schlaepfer and Hunter, 1997).

1.12.4 CaMKII and FAK may both serve as molecular intermediates in the mGluR/PI3K pathway to regulate neuronal excitability.

Because of the variation of C-terminal domains within different metabotropic glutamate receptor (mGluR) groups, each group activates different second messengers (Enz, 2007). For example, mammalian type I mGluR evokes Ca^{2+} via small G protein (Gαq)-mediated phospholipase Cβ (PLCβ) activation and IP3-dependent release of Ca^{2+} from intracellular stores. However, in Drosophila, there is only one mGluR (which is DmGluRA). Even though DmGluRA is more similar to mammalian group II mGluR, which inhibit adenylate cyclase, DmGluRA may also play the roles of group I and III mGluR since it is the sole mGluR in Drosophila (Bogdanik et al., 2004). In addition, in 2002, the Griffith group published that neuronal overexpression of *CaMKII*^{T287D}, which mimics CaMKII constitutive activation, resulted in failure of action potential propagation and increase in the number of boutons (Park et al., 2002). These results are similar to the phenotype of constitutive activation of PI3K (Howlett et al., 2008). In addition, Ueda et al. (2008) recently reported that the *DFak null* mutation *DFak*^{CG1} exhibits

neuronal hyperexcitability (Ueda et al., 2008), which might reflect inability to activate PI3K. Based on these researches, we believe Ca^{2+}/Calmodulin-dependent Kinase II (CaMKII) and Focal adhesion kinase (FAK), the substrate of CaMKII and activator of regulatory subunit of PI3K, may be the bridge between mGluR and PI3K. Therefore, the roles of CaMKII and Fak in the mGluR/PI3K signaling pathway need to be further characterized.

1.13 The functions of the transcription factor Foxo

Foxo proteins are composed of conserved DNA-binding domain (the Forkhead box, or FOX) and belong to the subgroup class 'O' of the Forkhead family of transcription factors. Foxo has been shown to be regulated by the PI3K/AKT signaling pathway and regulates many physiological events including cell death, reactive oxygen species detoxification, DNA repair, cell cycle arrest, glucose metabolism, and energy homeostasis (Kops et al., 2002; Medema et al., 2000; Nakae et al., 2001; Salih and Brunet, 2008). The mechanism by which *Foxo* controls life span is particularly well understood. In C. elegans, the Foxo homolog daf-16 is required to decrease insulin/PI3K/AKT signaling and promotes longevity

(Hsu et al., 2003; Libina et al., 2003; Murphy et al., 2003). Foxo is not only involved in the regulation of life span, but also in maintaining muscle function and neuronal excitability (Howlett et al., 2008). Recently, one study implicated Foxo and its target 4E-BP (a signaling molecule involved in protein synthesis) in preserving the function of proteostasis and delaying the decay of muscle function (Demontis and Perrimon). In addition, our data also implicated Foxo in the nervous system. In a Drosophila *Foxo null* mutant, the motor axon terminal showed a hypoexcitable phenotype (Howlett et al., 2008). This result suggested that Foxo is important in maintaining neuronal homeostasis and regulating neuronal excitability. Because Foxo is one of the downstream effectors of PI3K/AKT, Foxo also participates in the mGluR/PI3K/AKT singling pathway to regulate neuronal excitability (Howlett et al., 2008). However, the target genes of Foxo in the regulation of neuronal excitability still remain unknown.

1.14 The functions of translational repressor Pumilio

The Pumilio (Pum) proteins are Puf domain-containing proteins and highly conserved in several organisms including yeast, Drosophila, Xenopus, plants, and

mammals (Spassov and Jurecic, 2003). Pum functions as a translational repressor. In Drosophila, previous studies have shown that Pum is essential in regulating several physiological events, including embryogenesis and neuronal function (Sonoda and Wharton, 1999; Wreden et al., 1997). During embryogenesis, Pum binds directly to specific sequences in the 3' untranslated region (UTR) of hunchback (hb) mRNA (known as nanos-response elements or NREs) (Sonoda and Wharton, 1999; Wreden et al., 1997) and then recruits at least two other proteins, Nanos (Nos) and Brain Tumor (Brat) (Murata and Wharton, 1995; Sonoda and Wharton, 1999; Sonoda and Wharton, 2001), by protein-protein interactions to inhibit the initiation of protein translation; this translational inhibition controls the posterior development of Drosophila embryos (Macdonald, 1992).

In addition, Pum protein also plays an important role in the regulation of several neuronal events, such as neuronal excitability (Mee et al., 2004; Muraro et al., 2008; Schweers et al., 2002), dendrite morphogenesis (Ye et al., 2004), and postsynaptic protein translation (Menon et al., 2009; Menon et al., 2004; Salazar et al., 2010). For example, previous studies indicated that *pum* mutants exhibit

neuronal hyperexcitability (Schweers et al., 2002) and significantly elevated *paralytic* (Para; a Na^+ channel) mRNA (Mee et al., 2004; Muraro et al., 2008). Therefore, these results suggested that Pum regulates neuronal excitability by acting as the translational repressor of *para* mRNA. In conclusion of section 1.11 and 1.12, *Foxo* mutants exhibit neuronal hypoexcitability and *pum* mutants exhibit neuronal hyperexcitability. In addition, Pum is required in the regulation of the proper quantities of Para. Therefore, Foxo may regulate neuronal excitability by repressing transcription of *pum* and these indirectly control the translation of Para.

1.15 Drosophila push and the ubiquitin-proteosome protein degradation system

The ubiquitin-proteosome protein degradation system (UPS) is highly conserved from yeast to mammals. One of the major functions of UPS is a cellular quality control system that tags misfolded proteins by labeling them with multiple ubiquitins, a small protein with 76 amino acids, for refolding or degradation (Hershko and Ciechanover, 1998). Three major proteins catalyze this reaction sequentially: a ubiquitin activating enzyme (E1), a ubiquitin conjugating enzyme

(E2), and a ubiquitin ligase (E3) (Glickman and Ciechanover, 2002). Once the UPS system is triggered, the reactive site of ubiquitin is modified by E1 in a process requiring ATP as an energy source. Following the activation, ubiquitin is transferred from E1 to the active site of E2 and then E2 binds to E3 and transfers the ubiquitin in two ways. One is a direct transfer of ubiquitin from E2 to the substrate protein, and the other one is via formation of the E3-ubiquitin intermediate followed by transfer of ubiquitin to the substrate protein (Figure 1.15.1). After the substrate protein is tagged with a poly-ubiquitin chain, this protein can be rapidly degraded by the 26S-proteasome into small peptides (Figure 1.15.1) (Glickman and Ciechanover, 2002). The UPS system is also involved in regulating synapse development, presynaptic function, and neurotransmitter release (Yi and Ehlers, 2005).

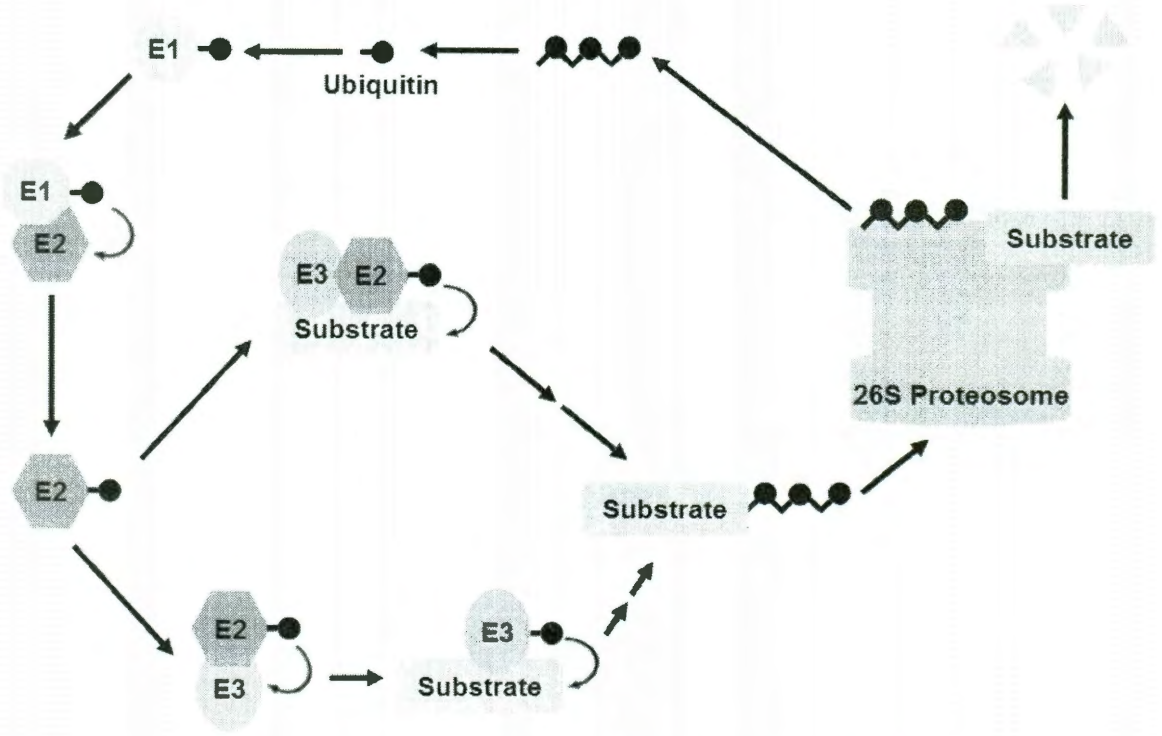

Figure 1.15.1. The ubiquitin-proteasome (UPS) pathway. The activation of UPS begin with the transformation of ubiquitin from E1 to the active site of E2. Next, E2 binds to target E3 and transfers the ubiquitin in two ways. One is a direct transfer of ubiquitin from E2 to the substrate protein. The other one is via formation of the E3-ubiquitin intermediate followed by transfer of ubiquitin to the substrate protein. Once the substrate protein is tagged with a poly-ubiquitin chain, this protein will be rapidly degraded by the 26S-proteasome into small peptides and ubiquitin will be recycled.

Drosophila Push is a large, ~570 kD protein and is the suspected ortholog of the mammalian P600/UBR4 protein. Based on previous characterizations of Push and P600/UBR4, Push has been suggested to function as a Ca^{2+}/Calmodulin-binding protein (Porter et al., 1995; Yager et al., 2001), as an E3-ubiquitin ligase

(Tasaki et al., 2005), and as an ER binding protein (Shim et al., 2008) and therefore may participate in many physiological events. P600/UBR4 belongs to the UBR family, a family of proteins involved in protein refolding and degradation (Tasaki et al., 2005), which are involved in membrane morphogenesis and in the prevention of anoikis, a type of programmed cell death that is induced by improper cell-matrix interaction (Nakatani et al., 2005). Drosophila Push has been implicated in the regulation of neurotransmitter release (Richards et al., 1996), chromatin scaffolding, male spermatogenesis (Richards et al., 1996), and perineurial glia growth (Yager et al., 2001). Even though push has been indicated in the regulation of many physiological events, the cellular locations and functional properties of push are totally unclear and needed more examination.

Chapter 2: CaMKII and DFak as critical intermediates in metabotropic glutamate receptor-mediated activation of PI3K

2.1 Synopsis

In Drosophila larval motor neurons, glutamate activation of the single mGluR, called DmGluRA, downregulates neuronal excitability (Bogdanik et al., 2004); glutamate both activates PI3K and requires PI3K activity for this downregulation (Howlett et al., 2008). Because glutamate is the excitatory neurotransmitter at the Drosophila neuromuscular junction (NMJ) (Jan and Jan, 1976), it was hypothesized that this DmGluRA-mediated downregulation of neuronal excitability carried out a negative feedback on activity: glutamate released from motor nerve terminals would activate DmGluRA autoreceptors, which would then depress excitability.

Here we identify additional molecular components that mediate the activation of PI3K by DmGluRA in Drosophila larval motor nerve terminals. We find that activity of the Calcium/calmodulin-dependent kinase II (CaMKII) is necessary for glutamate application to activate PI3K, and expression of the constitutively active

CaMKII^{T287D} (Jin et al., 1998) is sufficient both to activate PI3K even in the absence of glutamate and to confer several other neuronal phenotypes consistent with PI3K hyperactivation. We also find that CaMKII^{T287D} requires the nonreceptor tyrosine kinase DFak for this PI3K activation: the *DFak*^{CG1} null mutation (Grabbe et al., 2004) blocks the ability of glutamate application to activate PI3K, and prevents CaMKII^{T287D} from hyperactivating PI3K. Finally, *CaMKII*^{T287D} expression completely suppresses the hyperexcitability conferred by the *DmGluRA* null mutation *DmGluRA*^{112b}. We conclude that ligand activation of DmGluRA activates PI3K via CaMKII and DFak.

2.2 Materials and Methods

2.2.1 Drosophila stocks

For all experiments, Drosophila larvae were reared on standard cornmeal/ agar media at 22-23°. The *D42* Gal4 driver (Brand and Perrimon, 1993; Parkes et al., 1998), which expresses in motor neurons, was provided by Tom Schwarz

(Harvard Medical School, Boston, Massachusetts). Flies carrying the *UAS-PI3K^{DN}* (D954A) and *UAS-PI3K-CAAX* transgenes (Leevers et al., 1996), encoding dominant-negative and constitutively active PI3K, respectively, were provided by Sally Leevers (London Research Institute, London, UK). Flies carrying the *UAS-ala*, *UAS-CaMKII^{T287A}* and *UAS-CaMKII^{T287D}* transgenes, which encode a CaMKII inhibitor peptide, calcium/calmodulin-dependent CaMKII, and calcium/calmodulin-independent CaMKII, respectively (Griffith et al., 1994; Park et al., 2002), were provided by Leslie C. Griffith (Brandeis University, Waltham, Massachusetts). Flies carrying the *DFak^{CG1}* deletion mutation and *UAS-DFak^{+}* transgene (Grabbe et al., 2004) were provided by Ruth Palmer (Umeå University, Umeå, Sweden). Flies carrying the *DmGluRA^{112b}* deletion mutation (Bogdanik et al., 2004) were provided by Marie-Laure Parmentier (Unité Propre de Recherche Centre, Montpelier, France). All other fly stocks were provided by the Drosophila stock center (Bloomington, IN).

2.2.2 Immunocytochemistry

Larvae were grown to the wandering third-instar stage in uncrowded half-pint bottles. Larvae were collected for experimentation only during the first and second days after the initial wandering third-instar larvae appeared. For basal phosphorylated Akt (p-Akt) measurements, larvae were dissected in Schneider's Drosophila media (Gibco) and fixed in Schneider's Drosophila media containing 4% paraformaldehyde. For experiments involving glutamate application, larvae were dissected and then incubated for 1 minute in Schneider's Drosophila media containing 100 μM glutamate prior to the fixation procedure described above. Fixed larval tissues were incubated with a rabbit anti-Drosophila p-Akt (Ser505) polyclonal primary antibody (1:500 dilution, Cell Signaling Technologies). The antibody used was from a different lot from the antibody used in a previous report (Howlett *et al.*, 2008) and thus might not have identical properties. Larvae were then incubated with Rhodamine Red conjugated goat anti-rabbit IgG (1:500 dilution, Jackson ImmunoResearch), and Cy-2 conjugated antibodies against horseradish peroxidase (1:200 dilution, Jackson ImmunoResearch). Immuno-labeled larval tissues in standard Phosphate Buffered saline (PBS, 0.128

M NaCl, 2.0 mM KCl, 4.0 mM $MgCl_2$, 0.34 M sucrose, 5.0 mM HEPES, pH 7.1, and 0.15 mM $CaCl_2$) containing 50% glycerol were mounted onto slides. Care was taken to treat all samples identically during this procedure. Neuromuscular junctions (NMJs) from muscles 6 and 7 in segments A3, A4, A5 or A6 were imaged on a Zeiss LSM 510 confocal microscope system (Zeiss, Oberkochen, Germany) with a 20X objective. Optical sections were 10 μm thick, which encompassed the entire NMJ. Optical parameters, including pinhole, gain, contrast, and brightness, were held constant for each experimental set. NMJs (marked by anti-HRP) were traced using the Image-J (NIH, Bethesda, MD) freehand selection tool and the selection was transferred to the anti-p-Akt image where pixel intensity value was quantified. Background was obtained by averaging p-Akt intensity from muscles 6 and 7 from the same abdominal hemisegment, excluding the muscle nuclei and the neuromuscular junction. This background was then subtracted from the mean motor nerve terminal p-Akt pixel intensity. This p-Akt pixel intensity was then normalized to the mean p-Akt pixel intensity of wild type motor nerve terminals obtained in experiments performed in parallel.

To measure synaptic bouton number, larvae were grown, selected and dissected as described above, fixed in standard PBS containing 4% paraformaldehyde and labeled with Cy-2 conjugated antibodies against horseradish peroxidase (1:200 dilution). Images were obtained as described above. The LSM Image Browser was used for quantifying bouton numbers and obtaining surface area of muscle 6 and 7 from abdominal segment A3 and A4. The number of boutons was counted manually.

2.2.3 Transmission electron microscopy

Transmission electron microscopy was performed as described previously (Howlett et al., 2008; Lavery et al., 2007). Briefly, larvae were grown, selected, and dissected as described above, fixed with glutaraldehyde and paraformaldehyde, stained with 0.5% OsO_4 and 2% uranyl acetate, and embedded in an eponate 12-araldite mixture. Ultrathin cross-sectional slices (pale gold, 120-nm-thick) were cut with an ultramicrotome, poststained with uranyl acetate and Reynolds lead citrate, and analyzed with a JEOL 1230 (JEOL Ltd.,

Tokyo, Japan) transmission electron microscope at 80 kV. Carl Zeiss Axioversion software (Zeiss, Oberkochen, Germany) was used for analyzing axon diameter. Each experimental set was analyzed from the five largest axons (motor axons) from more than five different nerves from at least two different larvae.

2.2.4 Electrophysiology

Larvae were grown and selected as described above and dissected in Jan's buffer (128 mM NaCl, 2.0 mM KCl, 4.0 mM $MgCl_2$, 34 mM sucrose, 4.8 mM HEPES, pH 7.1, and $CaCl_2$ concentration as specified in the text). Peripheral nerves were cut immediately posterior to their exit from the ventral ganglion, and were stimulated with a suction electrode at a 5V stimulus intensity. Muscle recordings were taken from muscle 6 in abdominal sections 3–5. Stimulus duration, approximately 0.05 msec, was adjusted to 1.5 times threshold which reproducibly stimulates both axons innervating muscle 6. Intracellular recording electrodes for muscle potentials were pulled with a Flaming/Brown micropipette puller to a tip resistance of 10–40 MΩ and filled with 3M KCl. Rate of onset of long

term facilitation (LTF) and excitatory junction potential (EJP) amplitude are reported as geometric means because the data show a positive skew. For all long-term facilitation (LTF) experiments, the bath solution contained 0.15 mM [Ca^{2+}] and 100 μM quinidine, which is a potassium channel blocker that sensitizes the motor neuron and enables LTF to occur and measured even in hypoexcitable neurons.

2.3 Results

2.3.1 CaMKII regulates PI3K activity in Drosophila motor nerve terminal

Metabotropic glutamate receptors (mGluRs) are G-protein-coupled receptors for which glutamate is ligand. In Drosophila, the *DmGluRA*^{112b} null mutation in the single mGluR increases motor neuron excitability by preventing activation of the lipid kinase PI3K (Bogdanik et al., 2004; Howlett et al., 2008). Given that glutamate is the major excitatory neurotransmitter at neuromuscular junctions (NMJs) in insects such as Drosophila (Jan and Jan, 1976), it was

suggested that DmGluRA in motor neurons participates in a negative feedback: glutamate released from motor nerve terminals as a consequence of neuronal activity activates DmGluRA autoreceptors in motor nerve terminals. DmGluRA activation downregulates subsequent neuronal activity by activating PI3K. In this view, *DmGluRA*^{112b} increases excitability by preventing PI3K activation and thus severing this negative feedback. This view is supported by the observation that transgene-induced PI3K inhibition increases neuronal excitability in a manner similar to *DmGluRA*^{112b}, whereas transgene-induced PI3K activation decreases neuronal excitability (Howlett et al., 2008). However, the molecular mechanism by which glutamate-DmGluRA activates PI3K was not elucidated.

We initially hypothesized that the Calcium/calmodulin-dependent kinase II (CaMKII) might be an essential intermediate in DmGluRA-mediated PI3K activation. Although the possibility that CaMKII can activate PI3K has only recently been reported (Ma et al., 2009), altered CaMKII activity alters certain motor neuron phenotypes in Drosophila in a manner similar to altered PI3K activity (Griffith et al., 1994; Park et al., 2002). One way that CaMKII activity can be altered is by expression of the constitutively active *CaMKII*^{T287D}: this variant is

rendered active even in the absence of calcium or calmodulin by the phosphomimetic T287D substitution in the autophosphorylation site (Fong et al., 1989). It was previously found that motor neuron expression of *CaMKII*^{T287D} increased synapse number and decreased excitability in motor neurons (Park et al., 2002); both of these phenotypes are also exhibited in larvae expressing the constitutively active *PI3K-CAAX* (Howlett et al., 2008; Martin-Pena et al., 2006). Similarly, CaMKII inhibition accomplished by transgenic expression of the CaMKII inhibitory peptide "ala" (Joiner MI and Griffith, 1997) increases motor neuron excitability and decreases synapse number (Park et al., 2002); both of these phenotypes are also exhibited in transgenic larvae in which PI3K activity is blocked. Taken together, these results support the notion that levels of PI3K activity are specified, at least in part, by activity of CaMKII.

To test the prediction that altered CaMKII activity would alter PI3K activity in Drosophila larval motor nerve terminals, we used the *D42* motor neuron *Gal4* driver to express transgenes encoding either the nonactivated *CaMKII*^{T287A} (which acts equivalently to wildtype in all assays performed to date), the constitutively-active *CaMKII*^{T287D} or the CaMKII inhibitory peptide *ala* in motor

neurons, and then evaluated effects of these transgenes on PI3K activity. We monitored PI3K activity with an antibody against the phosphorylated form of the kinase Akt (p-Akt), which increases upon PI3K activation and is a well-established readout for PI3K activity (Colombani et al., 2005; Dionne et al., 2006; Palomero et al., 2007). We found that expressing the activated *CaMKII*^{T287D}, but not the non-phosphorylatable *CaMKII*^{T287A}, increased p-Akt levels in motor nerve terminals about 40% (Figure 2.3.1, p=0.002, n=29), which is similar to, but less extreme, than the two-fold increase in p-Akt conferred by transgene-induced PI3K activation (Howlett et al., 2008). The magnitude of this response is similar to the magnitude of the p-Akt increase induced during mGluR-mediated LTD in the mouse hippocampus (Hou and Klann, 2004), consistent with the possibility that the p-Akt increases in the Drosophila and mammalian systems occur via a common pathway.

The previous study in which this approach was used (Howlett et al., 2008) was not able to distinguish possible differences in basal p-Akt levels among genotypes because of high sample errors. However, by significantly increasing sample size and by including data normalization to accommodate signal

variability, we were able to show that CaMKII inhibition via *ala* expression decreased basal p-Akt about 25% (Figure 2.3.1, p=0.033, n=16). These results support the notion that CaMKII activity specifies PI3K activity in larval motor neurons.

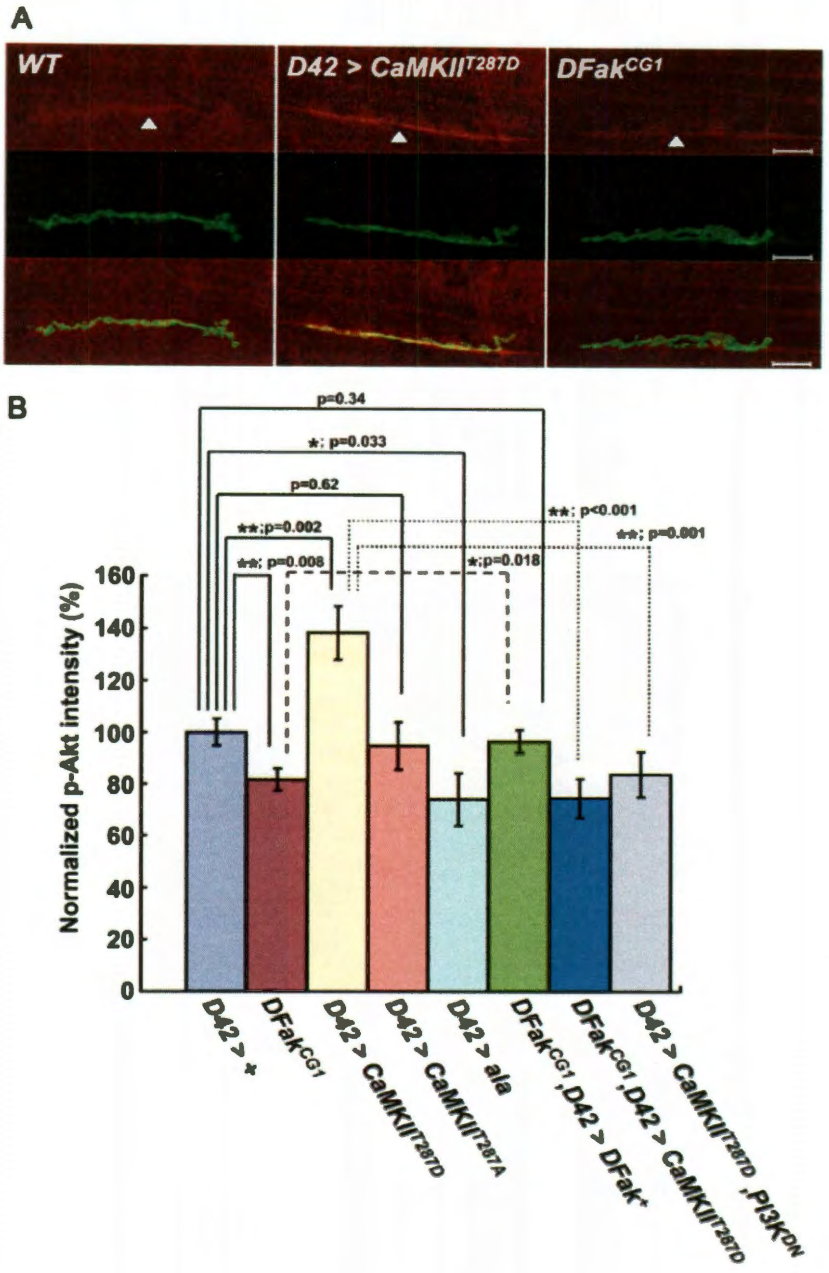

Figure 2.3.1: CaMKII activity increases levels of p-Akt in larval motor nerve terminals in a DFak-dependent manner. (A) Representative confocal images of third instar larval neuromuscular junctions of wildtype (*WT*), *D42>CaMKII^{T287D}* and *DFak^{CG1}* stained with anti-pAkt (upper panels), anti-HRP (center panels), and merged images (lower panels). All images are taken from muscles 7 and 6 from abdominal segment A3, A4, A5 or A6. Scale bar is 20 µm. (B) Mean normalized p-Akt intensity (Y axis) +/- SEM for the following genotypes (X axis): *D42>+*,

DFak^{CG1}, *D42>CaMKII*^{T287D}, *D42>CaMKII*^{T287A}, *D42>ala*, *DFak*^{CG1}*; D42>DFak*$^{+}$, *DFak*^{CG1}*; D42>CaMKII*^{T287D} and *D42>CaMKII*^{T287D}*, PI3K*^{DN}. Anti-HRP was applied to outline nerve terminals. Pixel intensities were quantified using ImageJ software and background subtraction was performed as described in the Methods section. The normalized p-Akt intensities are shown as a ratio change compared to wild type. From left to right, n = 65, 70, 29, 30, 16, 84, 35, 18 respectively, for each genotype. One-way ANOVA and Fisher's LSD were performed for statistical analysis and gave the following differences: For *D42>+*; vs. *DFak*^{CG1}, p=0.008; vs. *D42>CaMKII*^{T287D}, p=0.002; vs. *D42>CaMKII*^{T287A}, p=0.62; vs. *D42>ala*, p=0.033; vs. *DFak*^{CG1}*; D42>DFak*$^{+}$, p=0.34. For *DFak*^{CG1}; vs. *DFak*^{CG1}*; D42>DFak*$^{+}$, p=0.018; vs. *DFak*^{CG1}*; D42>CaMKII*^{T287D}, p=0.40. For *D42>CaMKII*^{T287D}; vs. *DFak*^{CG1}*; D42>CaMKII*^{T287D}, p<0.001; vs. *D42>CaMKII*^{T287D}*, PI3K*^{DN}, p=0.001. *P* values <0.05 were considered statistically significant.

2.3.2 Focal Adhesion Kinase (DFak) is required for CaMKII to activate PI3K

Next we wanted to identify molecules that might serve as intermediates linking activated CaMKII with PI3K activation. We hypothesized that the nonreceptor tyrosine kinase Focal Adhesion Kinase (DFak) might play such a role: DFak is the single Drosophila orthologue of the family which in mammals consists of both Fak and the closely related Pyk2. In mammals, CaMKII phosphorylates Pyk2 on multiple serine residues on the C terminus, which leads to Pyk2 tyrosine phosphorylation and activation by mechanisms that are incompletely understood (Della Rocca et al., 1997; Fan et al., 2005; Heidinger et al., 2002; Montiel et al., 2007; Soltoff, 1998; Zwick et al., 1999). CaMKII also phosphorylates mammalian Fak on C terminal serine residues, although the functional significance of these phosphorylations remain unknown (Fan et al., 2005). Furthermore, both Pyk2 and Fak are capable of activating PI3K (Avraham et al., 2000; Chen et al., 1996; Chen and Guan, 1994; Dikic et al., 1996; Guinebault et al., 1995; Montiel et al., 2007; Rocic et al., 2001; Schlaepfer et al., 1994). Two CaMKII phosphorylation sites on Fak, serines 843 and 910, are

conserved in DFak (Figure 2.3.2), raising the possibility that CaMKII phosphorylates DFak at these serine positions, which leads to DFak, and then PI3K, activation (Grabbe et al., 2004).

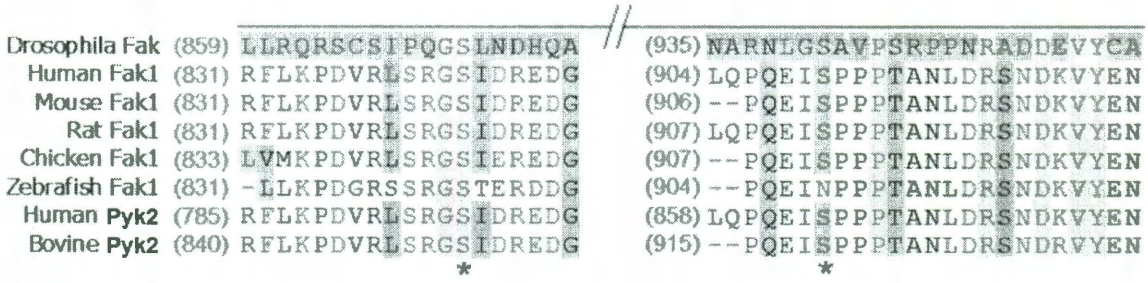

Figure 2.3.2: Two CaMKII phosphorylation sites on DFak are conserved. Portion of Focal adhesion kinase alignmemt among different animal speices was analyzed by Clustalw. Asterisks indicate two conserved serine.

If DFak acts downstream of CaMKII, then the *DFak* null mutation $DFak^{CG1}$ is predicted to decrease motor nerve terminal PI3K activation, and prevent $CaMKII^{T287D}$-dependent PI3K activation. As shown in Figure 2.3.1, PI3K activity in motor nerve terminals, as monitored by levels of p-Akt, was decreased in $DFak^{CG1}$ to 80% of wildtype (p=0.008, n=70). Furthermore, this decrease was rescued by motor neuron expression of a $DFak^{+}$ transgene (Figure 2.3.1), demonstrating that this effect of $DFak^{CG1}$ resulted from loss of DFak specifically within motor neurons.

Furthermore, *DFak*^{CG1} larvae expressing CaMKII^{T287D} in motor neurons did not exhibit the increased p-Akt levels in motor nerve terminals observed when CaMKII^{T287D} was expressed in an otherwise wildtype background (Figure 2.3.1, $p<0.001$). Rather, p-Akt levels were decreased to levels similar to those observed in *DFak*^{CG1} larvae in the absence of CaMKII^{T287D} expression ($p=0.4$). Similarly, co-expression with the dominant-negative *PI3K*^{DN} (Leevers et al., 1996) blocked the ability of *CaMKII*^{T287D} to increase p-Akt levels (Figure 2.3.1). Taken together, these results confirm that both DFak and PI3K activities are required for CaMKII to increase p-Akt levels.

2.3.3 CaMKII and DFak are required for PI3K activation by glutamate application

It was previously demonstrated that application of glutamate to larval NMJs in filleted third instar larval preparations activates PI3K, as monitored by glutamate-induced increases in p-Akt levels in motor nerve terminals (Howlett et al., 2008). Furthermore, these glutamate-evoked p-Akt increases were blocked by the null mutation *DmGluRA*^{112b}, or by presynaptic inhibition of either DmGluRA or

PI3K (Howlett et al., 2008), which demonstrated that glutamate activated PI3K via DmGluRA autoreceptors. If CaMKII and DFak are critical intermediates in glutamate/DmGluRA-induced PI3K activation, then inhibition of either molecule is predicted to block this glutamate-induced PI3K activation. To test this possibility, we applied 0.1 mM glutamate to *DFak*^{CG1} larvae, or to larvae expressing the CamKII inhibitory peptide *ala* in motor neurons. We found that wildtype larvae showed a robust glutamate-induced PI3K activation, as monitored by immunocytochemistry against p-Akt (Figure 2.3.3, p=0.001), following 1 minute of glutamate application. This percent increase is similar to the increase reported during mGluR-mediated LTD in the mouse hippocampus (Hou and Klann, 2004) in which a 5 minute application of a glutamate analog evoked about a 50% increase in p-Akt levels. In contrast, blocking either CaMKII or DFak blocked this increase (Figure 2.3.3, p=0.64 and p=0.77, respectively). Furthermore, the motor neuron expression of *UAS-DFak*$^{+}$ restored normal glutamate sensitivity to *DFak*^{CG1} (Figure 2.3.3).

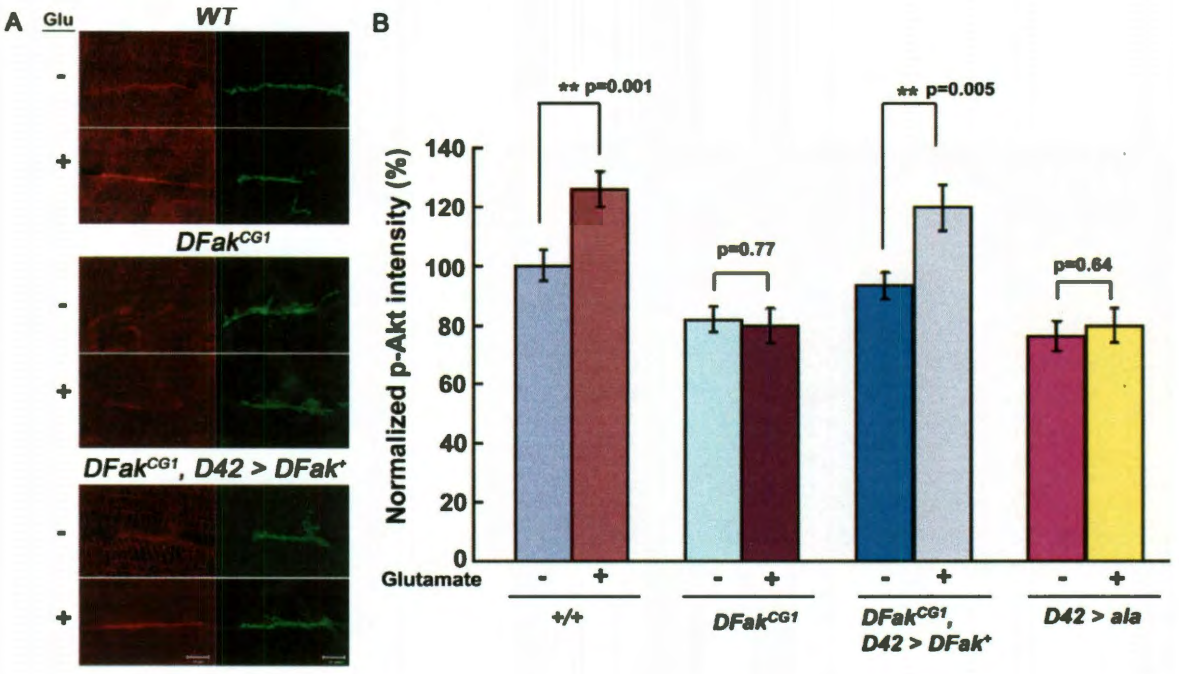

Figure 2.3.3: The glutamate-evoked increase in presynaptic p-Akt levels requires CaMKII and DFak. (A) Representative confocal images of third instar larval neuromuscular junctions of wildtype (WT or *+/+*), *DFak^{CG1}* and *DFak^{CG1}; D42>UAS-DFak^{+}* either prior to (-) or 1 min following (+) application of 100 µM glutamate. Larvae were stained with anti-p-Akt (left panel) and anti-HRP (right panel). All images are from muscles 7 and 6 of abdominal segment A3, A4, A5 or A6. Scale bar is 20 µm. (B) Mean normalized p-Akt intensity (Y axis) +/- SEM, both prior to and following 1 min glutamate application, for the following genotypes (X axis): *D42>+*, *DFak^{CG1}*, *D42>ala*, and *DFak^{CG1}; D42>DFak^{+}*. Anti-HRP was applied to outline nerve terminals. Pixel intensities were quantified using ImageJ software and background subtraction was performed as described in the Methods section. The normalized p-Akt intensities are shown as a ratio change compared to wild type. From left to right, n = 65, 56, 70, 48, 84, 24, 32, 36, respectively, for each genotype. One-way ANOVA and Fisher's LSD were performed for statistical analysis. *P* values <0.05 were considered statistically significant.

2.3.4 CaMKII promotes synapse formation via DFak-dependent PI3K activation

CaMKII activity was previously shown to promote arborization and increase synapse number at the larval NMJ (Park et al., 2002) by phosphorylating discs-large and thus decreasing levels of Fas2 (Koh et al., 1999). The observation that CaMKII acts downstream of integrins for this control of synapse structure (Beumer et al., 2002) is consistent with a role for DFak in this process as well. In addition, arborization and synapse number are regulated by PI3K activity: activating PI3K by expressing the constitutively-active *PI3K-CAAX* increases synapse number about 2.5-fold, whereas blocking PI3K by expressing the dominant-negative $PI3K^{DN}$ decreases synapse number about two-fold (Howlett et al., 2008; Martin-Pena et al., 2006). From these data and the results shown above, we hypothesized that CaMKII promotes synapse formation at least in part by activating PI3K in a DFak-dependent manner. We confirmed the previous findings of Park et al. (Park et al., 2002), that expressing $CaMKII^{T287D}$, but not $CaMKII^{T287A}$, in motor neurons increased bouton number about 30% (Figure 2.3.4, p=0.001), an increase similar to, though less extreme, than the increase conferred

by *PI3K-CAAX*. We found that this *CaMKII*^{T287D}-dependent increase required PI3K activity: in larvae co-expressing *PI3K*^{DN} and *CaMKII*^{T287D}, the *CaMKII*^{T287D}-dependent increase in bouton number was completely suppressed, and in fact was decreased to a value indistinguishable from that conferred by *PI3K*^{DN} alone (Figure 2.3.4).

To determine if DFak is a required intermediate in this CaMKII-dependent PI3K activation, we measured synapse number in *DFak*^{CG1} larvae both in the presence and absence of *CaMKII*^{T287D} expression. We found that in the absence of *CaMKII*^{T287D} expression, synapse number in *DFak*^{CG1} larvae was highly variable and therefore differences with wildtype failed to reach statistical significance ($p=0.051$). However, there was a tendency for *DFak*^{CG1} synapse number to decrease, rather than increase, compared to wildtype (Figure 2.3.4). Thus we were unable to confirm the finding of Tsai et al. (2008), who reported that DFak inhibition increases synapse number at the larval NMJ. However, *DFak*^{CG1} completely suppressed the increased synapse number conferred by *CaMKII*^{T287D} expression (Figure 2.3.4, $p=0.001$); synapse number in *DFak*^{CG1} larvae expressing *CaMKII*^{T287D} was indistinguishable from synapse number in *DFak*^{CG1}

alone (Figure 2.3.4, p=0.89). These data support the notion that CaMKII activates PI3K in a DFak-dependent manner.

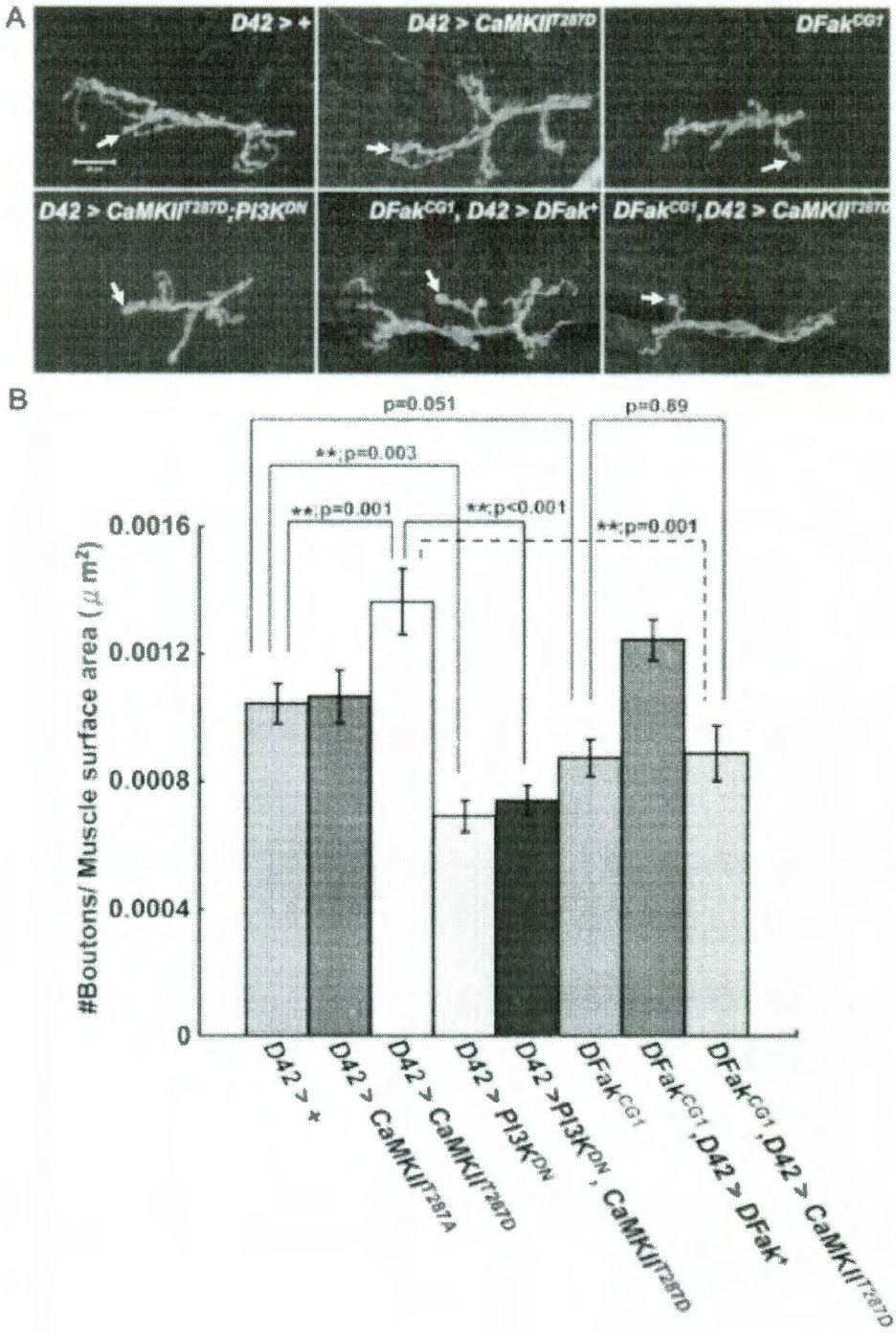

Figure 2.3.4: The increase in motor neuron synapse number conferred by CaMKII^{T287D} expression requires DFak and PI3K. (A) Representative confocal images of third instar larval neuromuscular junctions of *D42>+*, *D42>CaMKII^{T287D}*, *DFak^{CG1}*, *D42>CaMKII^{T287D}*, *PI3K^{DN}*, *DFak^{CG1}; D42>DFak^{+}*, and *DFak^{CG1};*

D42>CaMKII^{T287D}. Nerve terminals were visualized by staining with anti-HRP. Scale bar is 20 μm. (B) Means +/- SEMs of synaptic bouton number normalized to the total surface area of muscle (Y axis) for the following genotypes (X axis): *D42>+*, *D42>CaMKII*^{T287A}, *D42>CaMKII*^{T287D}, *D42>PI3K*^{DN}, *D42>PI3K*^{DN}, *CaMKII*^{T287D}, *DFak*^{CG1},*DFak*^{CG1}; *D42>DFak*$^{+}$, and *DFak*^{CG1}; *D42>CaMKII*^{T287D}. All measurements were performed on nerve terminals on muscles 6 and 7 from abdominal segment A3. From left to right, n = 25, 12, 18, 8, 16, 26, 28, 17, respectively, for each genotype. The white arrow indicates one single bouton. One-way ANOVA and Fisher's LSD were performed for statistical analysis.

We also found that blocking CaMKII in motor neurons by expressing the CaMKII-inhibitor peptide *ala* decreased synapse number about two-fold (Figure 2.3.5, $p<0.001$). If this decrease were a consequence of failure to activate PI3K, then expression of the constitutively active (and hence CaMKII-independent) *PI3K-CAAX* would be predicted to suppress these effects of CaMKII inhibition. We confirmed this prediction: the *ala*-dependent decrease in synapse number was completely suppressed by co-expression with *PI3K-CAAX*: synapse number in larvae expressing both *ala* and *PI3K-CAAX* was significantly increased compared to synapse number in larvae expressing *ala* alone (Figure 2.3.5, $p<0.001$), and was indistinguishable from synapse number in larvae expressing *PI3K-CAAX* alone (Figure 2.3.5, $p=0.53$). In addition, we found that synapse number in larvae expressing *PI3K-CAAX* was similarly unaffected by the presence of $DFak^{CG1}$ (Figure 2.3.5). Taken together, these results suggest that CaMKII increases synapse number by the DFak-dependent activation of PI3K.

Certain genotypes exhibited altered bouton morphology in addition to altered bouton number. For example, boutons in $DFak^{CG1}$ mutants often appear to be larger in size than wildtype. The $DmGluRA^{112b}$ mutation was similarly found to

increase bouton size (Bodganik *et al.*, 2004). These observations are consistent with the possibility that DFak activation is attenuated in the absence of *DmGluRA*.

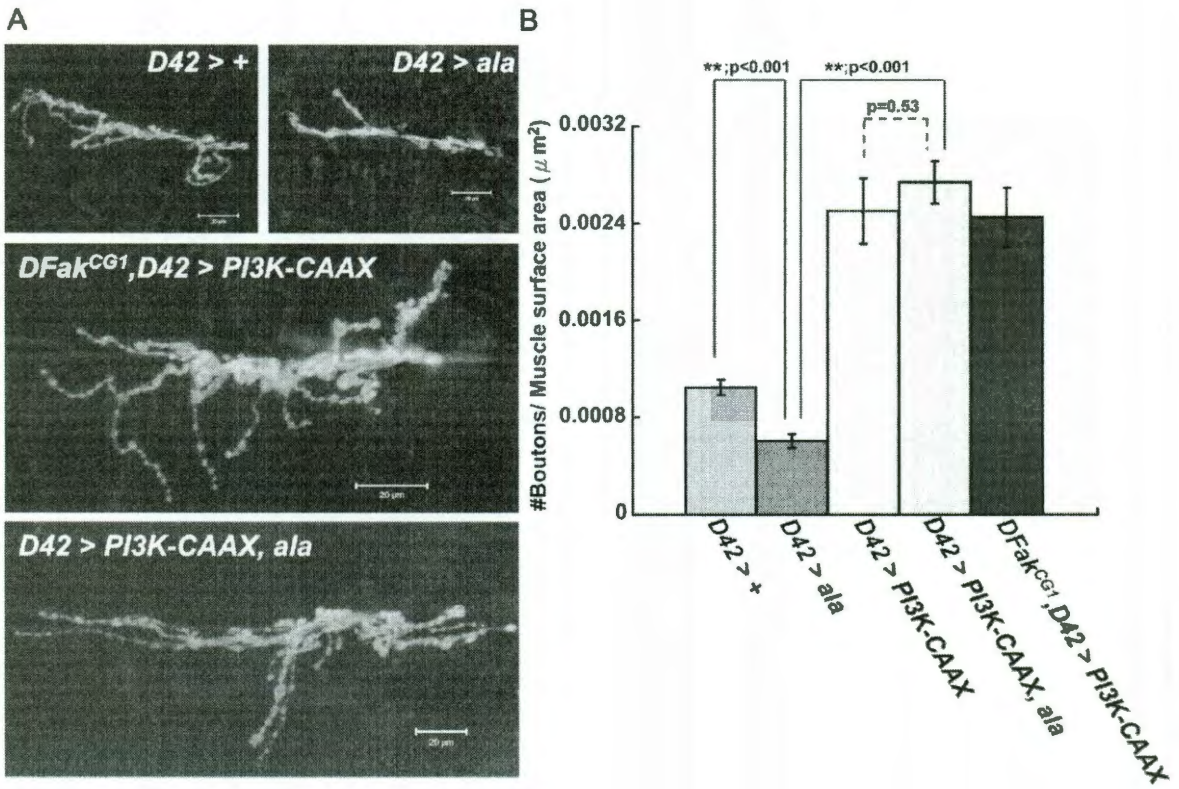

Figure 2.3.5: Constitutive PI3K activation suppresses the decrease in synapse number conferred by CaMKII or DFak inhibition. (A) Representative confocal images of third instar larval neuromuscular junctions of *D42>+*, *D42>ala*, *D42>ala, PI3K-CAAX* and *DFak^{CG1}; D42>PI3K-CAAX*. Nerve terminals were visualized by staining with anti-HRP. Scale bar is 20 μm. (B) Means +/- SEMs of synaptic bouton number normalized to the total surface area of muscle (Y axis) for the following genotypes (X axis): *D42>+*, *D42>ala*, D42>PI3K-CAAX, *D42> ala, PI3K-CAAX,* and *DFak^{CG1}; D42>PI3K-CAAX*. All measurements were performed on nerve terminals on muscles 6 and 7 from abdominal segment A3. From left to right, n = 25, 12, 15, 8, 10, respectively, for each genotype. One-way ANOVA and Fisher's LSD were performed for statistical analysis.

2.3.5 CaMKII activity increases motor axon diameter by the DFak-dependent activation of PI3K

Larval motor axon diameter is specified by the level of PI3K activity: expressing constitutively active *PI3K-CAAX* increases motor axon diameter about 75% (0.8 μm to 1.4 μm), whereas expressing the dominant-negative $PI3K^{DN}$ decreases motor axon diameter (Howlett et al., 2008). To determine if CaMKII similarly regulates motor axon diameter, we expressed $CaMKII^{T287D}$ in motor axons and found as predicted significantly increased (about 40%) motor axon diameters (Figure 2.3.6, p=0.001), an increase similar to, but less extreme than, the increase conferred *PI3K-CAAX*. In addition, the $CaMKII^{T287D}$-dependent increase, but not the *PI3K-CAAX*-dependent increase, in axon diameter was blocked by $DFak^{CG1}$ (Figure 2.3.6, p=0.004). Taken together, these results suggest that CaMKII increases motor axon diameter by the DFak-dependent activation of PI3K.

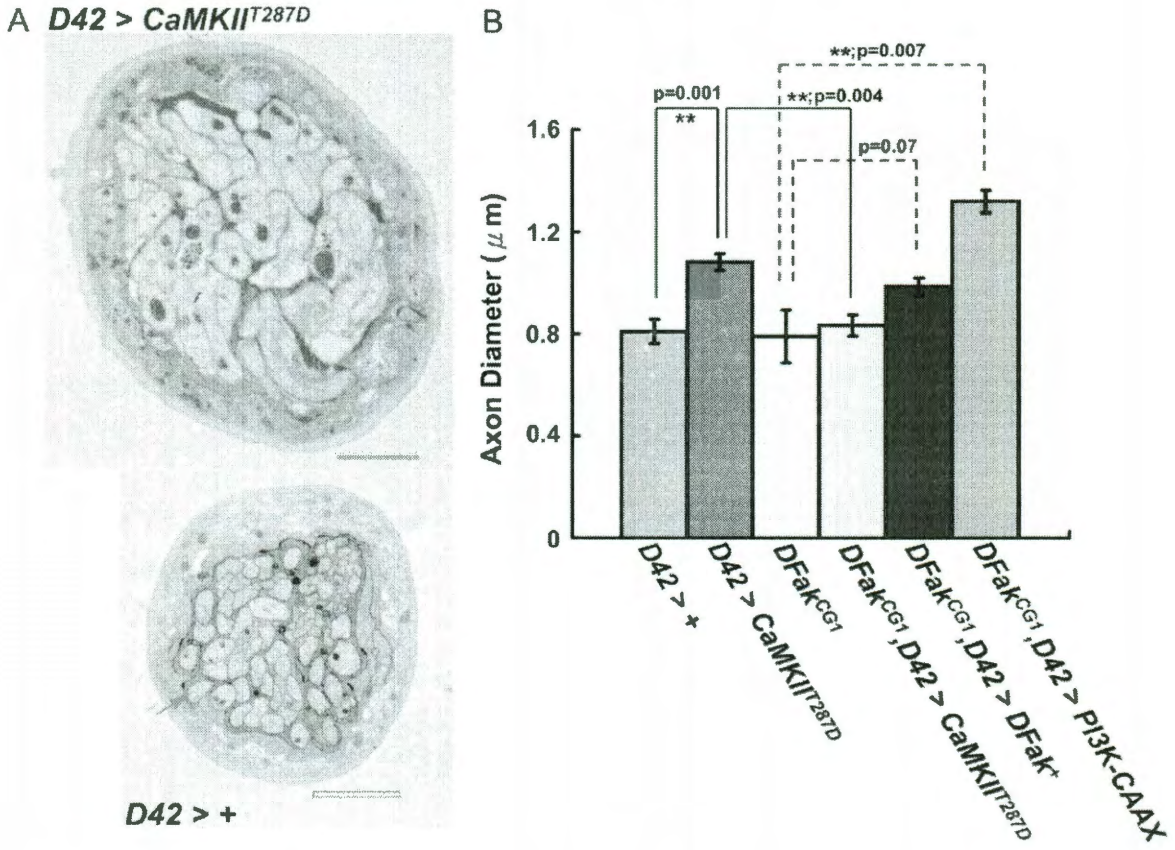

Figure 2.3.6: DFak is required for the increased motor axon diameter conferred by CaMKII, but not PI3K. (A) Representative transmission electron micrographs of cross sections of peripheral nerves from *D42>+* and *D42>CaMKII^{T287D}* larvae. The ~80 motor and sensory axons within the nerve are surrounded by at least two layers of glia. Diameter of the motor axons, the largest axons in the nerve, are considerably increased in *D42>CaMKII^{T287D}*. An axon is marked with an arrow. Scale bar is 2 μm. (B) Mean axon diameter +/- SEMs of the five largest axons (which are motor axons) from each nerve (Y axis) for the following genotypes (X axis): *D42>+*, *D42>CaMKII^{T287D}*, *DFak^{CG1}*, *DFak^{CG1}; D42>CaMKII^{T287D}*, *DFak^{CG1}; D42>DFak^{+}*, and *DFak^{CG1}; D42>PI3K-CAAX*. Nerves from at least two different larvae were scored for these axon measures. From left to right, n = 6, 7, 5, 5, 7, 5, nerves respectively, for each genotype. One-way ANOVA and Fisher's LSD were performed for statistical analysis.

2.3.6 Altered CaMKII and DFak activities alter motor neuron excitability

PI3K activity regulates motor neuron excitability: transgene-induced PI3K activation decreases neuronal excitability, whereas transgene-induced PI3K inhibition increases neuronal excitability (Howlett et al., 2008). Additional reports have demonstrated that CaMKII and DFak also regulate Drosophila neuronal excitability (Griffith et al., 1994; Park et al., 2002; Ueda et al., 2008), raising the possibility that CaMKII, DFak and PI3K might regulate excitability via a common pathway. However, in each previous report, different sets of excitability assays were used, which complicates attempts to assign the effects of these three genes to specific pathways.

To address this complication, we monitored motor neuron excitability in *DFak*^{CG1} and in larvae expressing the constitutively active *CaMKII*^{T287D} with the same assay previously employed to monitor excitability in larvae with altered PI3K activity. With this assay, the larval neuromuscular preparation (Jan and Jan, 1976), transmitter release from motor neurons is evoked by nerve stimulation, and the amount of transmitter released is inferred from the amplitude of the muscle

depolarization (termed the excitatory junction potential, or EJP). Using this assay, we employed the same readouts to evaluate neuronal excitability in *DFak*^{CG1} larvae, and in larvae expressing *CaMKII*^{T287D}, that were previously employed for altered PI3K (Howlett et al., 2008).

First, we measured rate of onset of a phenomenon termed "long term facilitation" (LTF) (Jan and Jan, 1978). LTF is a form of synaptic plasticity induced when a larval motor neuron is subjected to a train of repetitive nerve stimulations at low external [Ca^{2+}]. At a certain point during the stimulus train, a threshold is reached, and subsequent stimulations elicit EJPs greatly increased in amplitude and duration. This long term facilitation results from increased and asynchronous neurotransmitter release, which in turn results from increased duration of nerve terminal depolarization (Jan and Jan, 1978). The number of stimulations required to reach this LTF threshold (LTF onset rate) is decreased by increased neuronal excitability (Jan and Jan, 1978; Mallart et al., 1991; Poulain et al., 1994; Schweers et al., 2002; Stern and Ganetzky, 1989; Stern et al., 1990). Both the *DmGluRA*^{112b} null mutation and transgene-induced inhibition of *PI3K* greatly decrease the number of nerve stimulations required to reach LTF and thus greatly increase LTF

onset rate (Bogdanik et al., 2004; Howlett et al., 2008). This increased LTF onset rate indicates increased excitability in these genotypes. The possibility that DFak is required for DmGluRA-dependent PI3K activation predicted that *DFak*^{CG1} would prevent this PI3K activation and similarly increase the LTF onset rate. This prediction was confirmed (Figure 2.3.7). This increased LTF onset rate was rescued by motor neuron-dependent expression *DFak*$^{+}$, confirming that DFak is required in the motor neuron for this effect. In contrast, the possibility that CaMKII^{T287D} constitutively activates PI3K would predict that *CaMKII*^{T287D} expression would decrease LTF onset rate, which we also confirmed (Figure 2.3.7).

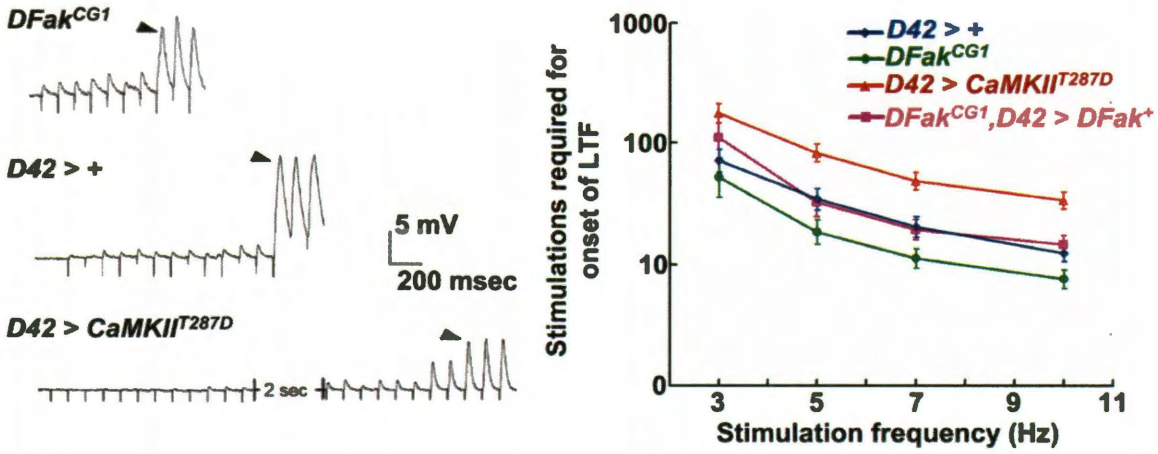

Figure 2.3.7: CaMKII and DFak regulate motor neuron excitability. The larval neuromuscular preparation (Jan and Jan, 1976) was used for all recordings. Left panel: representative traces showing increased rate of onset of LTF in *DFak^{CG1}*, and decreased rate of onset of LTF in larvae overexpressing CaMKII^{T287D} in motor neurons. Arrowheads indicate the increased and asynchronous EJPs, indicative of onset of LTF. The bath solution contained 0.15 mM [Ca^{2+}] and 100 µM quinidine. Right panel: Geometric means +/- SEMs of the number of stimulations required to evoke LTF (Y axis) at the indicated stimulus frequencies (X axis) for the following genotypes *D42>+*, *DFak^{CG1}*, *D42>CaMKII^{T287D}*, and *DFak^{CG1}; D42>DFak^{+}*. From top to bottom, n = 7, 8, 18, and 6, respectively, for each genotype. One-way ANOVA and Fisher's LSD gave the following differences, at 10 Hz, 7 Hz, 5 Hz and 3 Hz, respectively: for *D42>+* vs. *DFak^{CG1}*, p=0.028, 0.022, 0.016, 0.127; vs. *D42>CaMKII^{T287D}*, p=0.001, 0.006, 0.007, 0.011; vs. *DFak^{CG1}; D42>DFak^{+}*, p=0.503, 0.876, 0.859, 0.327. *P* values <0.05 were considered statistically significant.

Second, we measured EJP amplitude evoked by single nerve stimulations at low external [Ca^{2+}]. At these low [Ca^{2+}], Ca^{2+} is limiting for transmitter release, and mutations that alter excitability, and hence Ca^{2+} influx, have significant effects

on EJP amplitude (Ganetzky and Wu, 1982; Huang and Stern, 2002). In particular, transgene-induced PI3K activation decreases EJP amplitude, whereas transgene-induced PI3K inhibition increases EJP amplitude (Howlett et al., 2008). The possibility that DFak is required for DmGluRA-dependent PI3K activation predicted that *DFak*^{CG1} would prevent this PI3K activation and similarly increase EJP amplitude. We found that *DFak*^{CG1} significantly increased EJP amplitude at 0.15 mM and 0.2 mM [Ca^{2+}] (Figure 2.3.8), but was not significantly different from wildtype at 0.1 mM [Ca^{2+}], at which transmitter release is the smallest and errors are the greatest. This increased EJP amplitude was rescued by motor neuron-dependent expression *DFak*$^{+}$, confirming that DFak is required in the motor neuron for this effect.

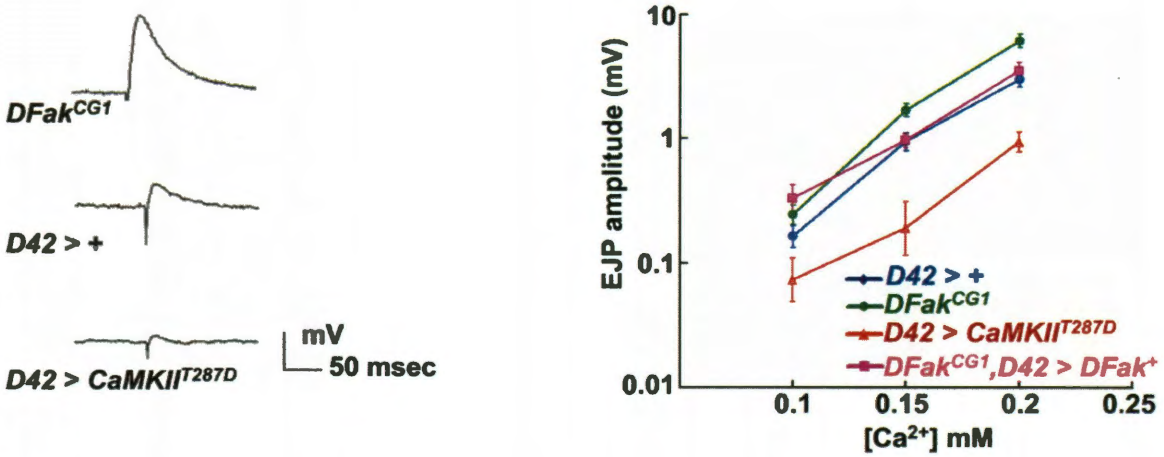

Figure 2.3.8: CaMKII and DFak regulate motor neuron excitability. Left panel: representative traces showing the increased excitatory junction potential (EJP) amplitude in *DFak^{CG1}* larvae, and the decreased EJP amplitude in larvae overexpressing CaMKII^{T287D} in motor neurons, at a bath [Ca^{2+}] of 0.15 mM. Right panel: mean EJP amplitudes +/- SEMs (Y axis) at the indicated [Ca^{2+}] (X axis), from the following genotypes: *D42>+*, *DFak^{CG1}*, *D42>CaMKII^{T287D}*, and *DFak^{CG1}; D42>DFak^{+}*. Larval nerves were stimulated at a frequency of 1 Hz, and 10 responses were measured and averaged from each nerve. n = (6, 6, 6), (14, 8, 9), (6, 6, 6), and (10, 6, 6), respectively, for each genotype and [Ca^{2+}] (0.2 mM, 0.15 mM, 0.1 mM). One-way ANOVA and Fisher's LSD gave the following differences at 0.2 mM, 0.15 mM and 0.1 mM [Ca^{2+}], respectively: for *D42>+* vs. *DFak^{CG1}*, p=0.021, 0.012, 0.21; vs. *D42>CaMKII^{T287D}*, p=0.001, 0.005, 0.484; vs. *DFak^{CG1}; D42>DFak^{+}*, p=0.375, 0.941, 0.040. *P* values <0.05 were considered statistically significant.

To confirm that these effects on EJP amplitude reflected altered transmitter release rather than altered responsiveness of the muscle to transmitter, we compared the amplitude of miniature EJPs (mEJPs), which reflect the

spontaneous release of individual vesicles of neurotransmitter, in wildtype larvae vs. *DFak*^{CG1} larvae and *DFak*^{CG1} larvae expressing *DFak*$^{+}$ in motor neurons (Figure 2.3.9). We found that mEJP amplitude was unaffected in these three genotypes. Thus the increased EJP amplitude observed in *DFak*^{CG1} reflects increased neurotransmitter release.

The possibility that *CaMKII*^{T287D} constitutively activates PI3K would predict that *CaMKII*^{T287D} expression would decrease EJP amplitude. We found that as predicted, *CaMKII*^{T287D} expression decreases EJP amplitude at each [Ca^{2+}] tested (Figure 2.3.8) while having no significant effect on mEJP amplitude (Figure 2.3.9). This observation supports the conclusion that decreased neurotransmitter release underlies the decreased EJP amplitude conferred by *CaMKII*^{T287D}.

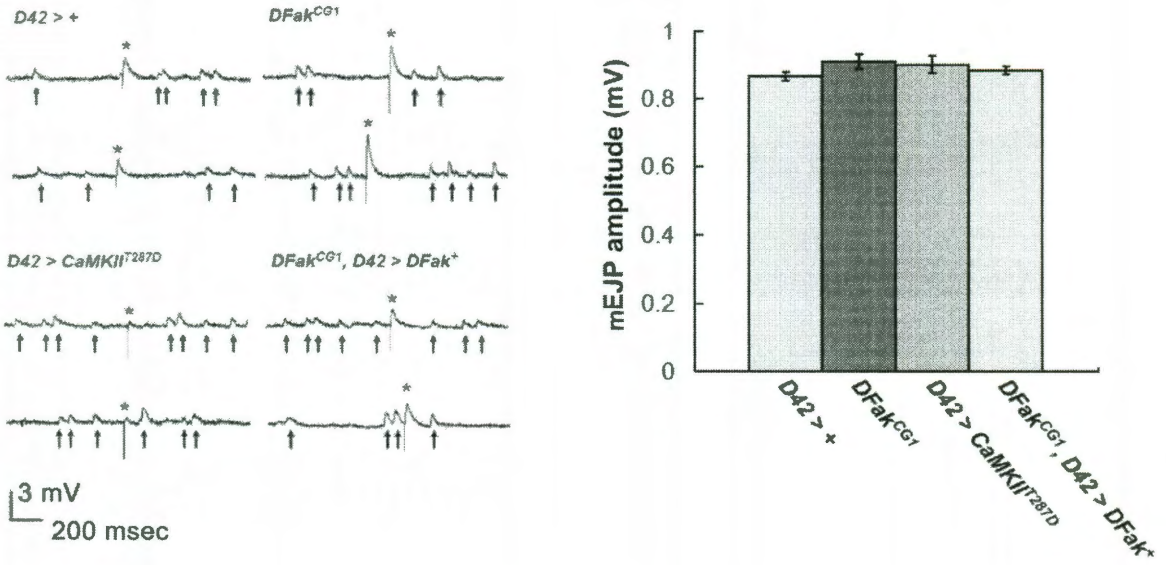

Figure 2.3.9: The mEJPs are not affected in *D42 > +*, *DFak^{CG1}*, *D42 > CaMKII^{T287D}*, and *DFak^{CG1}, D42 > DFak^{+}*. Left panel: representative traces showing mini EJPs (mEJP, marked by arrows) in *D42>+*, *DFak^{CG1}*, *D42>CaMKII^{T287D}*, and *DFak^{CG1}; D42>DFak^{+}*. Two traces from each genotype are from two different larvae. The asterisks indicate EJPs evoked by single stimulations. Right panel: Mean mEJP amplitudes +/- SEMs (Y axis) for the indicated genotypes (X axis): *D42>+*, *DFak^{CG1}*, *D42>CaMKII^{T287D}*, and *DFak^{CG1}; D42>DFak^{+}*. Recordings were collected from five different larvae from each genotype in a bath [Ca^{2+}] of 0.15 mM, and 30 responses were measured and averaged from each larva. One-way ANOVA and Fisher's LSD gave the following differences; For *D42>+* vs. *DFak^{CG1}*, p=0.127; vs. *D42>CaMKII^{T287D}*, p=0.265; vs. *DFak^{CG1}; D42>DFak^{+}*, p=0.354. For *DFak^{CG1}* vs. *D42>CaMKII^{T287D}*, p=0.788; vs. *DFak^{CG1}; D42>DFak^{+}*, p=0.332. For *D42>CaMKII^{T287D}* vs. *DFak^{CG1}; D42>DFak^{+}*, p=0.572. *P* values <0.05 were considered statistically significant.

2.3.7 Activating CaMKII prevents hyperexcitability of the DmGluRA^{112b} null mutant

The *DmGluRA^{112b}* null mutant exhibits extreme neuronal hyperexcitability, as shown by a greatly increased rate of onset of LTF (Bogdanik et al., 2004; Howlett et al., 2008). This hyperexcitability is completely suppressed by expression of the constitutively active *PI3K-CAAX* and thus reflects failure to activate PI3K (Howlett et al., 2008). If this failure to activate PI3K is a consequence of failure to activate CaMKII, then this hyperexcitability is predicted to be suppressed by transgene-induced expression of the constitutively active *CaMKII^{T287D}*. To test this prediction, we compared rate of onset of LTF in *DmGluRA^{112b}* mutants and in *DmGluRA^{112b}* mutants expressing *CaMKII^{T287D}* in motor neurons. We found that *CaMKII^{T287D}* expression completely suppressed the hyperexcitability of *DmGluRA^{112b}*, and decreased excitability to a level indistinguishable from the hypoexcitabiliy in larvae in which *CaMKII^{T287D}* was expressed in a *DmGluRA^{+}* background (Figure 2.3.10). These results support the notion that CaMKII is a critical intermediate in the ability of ligand-activated DmGluRA to activate PI3K.

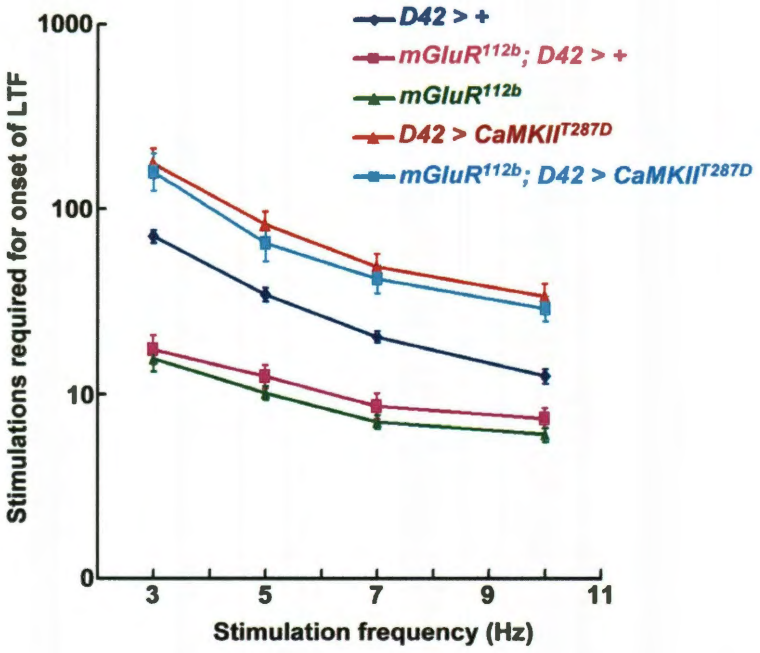

Figure 2.3.10: The increased excitability conferred by *DmGluRA^{112b}* is suppressed by expression of the activated CaMKII^{T287D}. Mean number of stimulations (geometric means +/- SEMs) required to induce LTF (Y axis) at the indicated stimulus frequencies (X axis). The bath solution contained 0.15 mM [Ca^{2+}] and 100 µM quinidine. From top to bottom (*D42>+*, *DmGluRA^{112b}; D42>+*, *DmGluRA^{112b}*, *D42>CaMKII^{T287D}*, and *DmGluRA^{112b}; D42>CaMKII^{T287D}*), n = 7, 8, 6, 18, and 18 respectively, for each genotype. One-way ANOVA and Fisher's LSD gave the following differences, at 10 Hz, 7 Hz, 5 Hz and 3 Hz, respectively: For *D42>+* vs. *DmGluRA^{112b}*, p=0.001, <0.001, <0.001, <0.001; vs. *DmGluRA^{112b}; D42>+*, p=0.031, 0.007, 0.002, <0.001; vs. *D42>CaMKII^{T287D}*, p=0.001, 0.006, 0.007, 0.011; vs. *DmGluRA^{112b}; D42>CaMKII^{T287D}*, p=0.016, 0.013, 0.045, 0.011. For *DmGluRA^{112b}; D42>+* vs. *DmGluRA^{112b}*, p=0.203, 0.256, 0.218, 0.650; vs. *DmGluRA^{112b}; D42>CaMKII^{T287D}*, p<0.001, <0.001, <0.001, <0.001. For *DmGluRA^{112b}; D42>CaMKII^{T287D}* vs. *D42>CaMKII^{T287D}*, p=0.725, 0.745, 0.642, 0.897. *P* values <0.05 were considered statistically significant.

2.4 Summary

In both mammalian central synapses and Drosophila larval motor neurons, activation by glutamate of the metabotropic glutamate receptor (mGluR) activates the lipid kinase PI3K, but the mechanism by which this activation occurs has not been elucidated. Here we identify the Calcium/calmodulin-dependent kinase II (CaMKII) as a critical intermediate in the ability of the single Drosophila mGluR (DmGluRA) to activate PI3K, and show that the ability of both activated DmGluRA and CaMKII to activate PI3K requires the nonreceptor tyrosine kinase Focal adhesion kinase (DFak) (Figure 2.3.11). These results provide novel insights into the mechanism by which DmGluRA activation triggers the observed down-regulation of subsequent neuronal activity in Drosophila motor neurons. These results might also be relevant to the mechanism by which mGluR activates PI3K in mammalian central synapses, a process implicated in fragile X, autism spectrum disorders (ASD), Neurofibromatosis and tuberous sclerosis (Kelleher and Bear, 2008).

How might CaMKII lead to the DFak-dependent activation of PI3K? Although the ability of CaMKII to activate PI3K has only recently been reported (Ma et al.,

2009), it has been well established in mammals that CaMKII phosphorylates both Fak and Pyk2 on multiple serines on the C terminus. These phosphorylation events can activate Pyk2 by enabling subsequent tyrosine phosphorylations (particularly at Tyr402) via mechanisms that are incompletely understood (Della Rocca et al., 1997; Fan et al., 2005; Heidinger et al., 2002; Montiel et al., 2007; Soltoff, 1998; Zwick et al., 1999). It has also been well established that Fak and Pyk2, when activated by tyrosine phosphorylation, are each able to activate PI3K: tyrosine-phosphorylated Fak binds p85, the PI3K regulatory subunit, via both the SH3 and SH2 domains (Chen et al., 1996; Chen and Guan, 1994; Guinebault et al., 1995). In addition, both tyrosine-phosphorylated Fak and Pyk2 are capable of activating Ras via the conserved Grb2-SoS pathway (Avraham et al., 2000; Dikic et al., 1996; Rocic et al., 2001; Schlaepfer et al., 1994), which could in principle lead to the Ras-dependent, p85-independent activation of PI3K. These observations raise the possibility that Drosophila CaMKII might similarly activate PI3K by directly phosphorylating and activating DFak. Alternatively, DFak might function in a more indirect fashion, perhaps as a scaffold linking CaMKII and PI3K in a signalling complex. This alternative possibility would suggest that additional intermediates linking CaMKII and PI3K activation exist but are currently

unidentified.

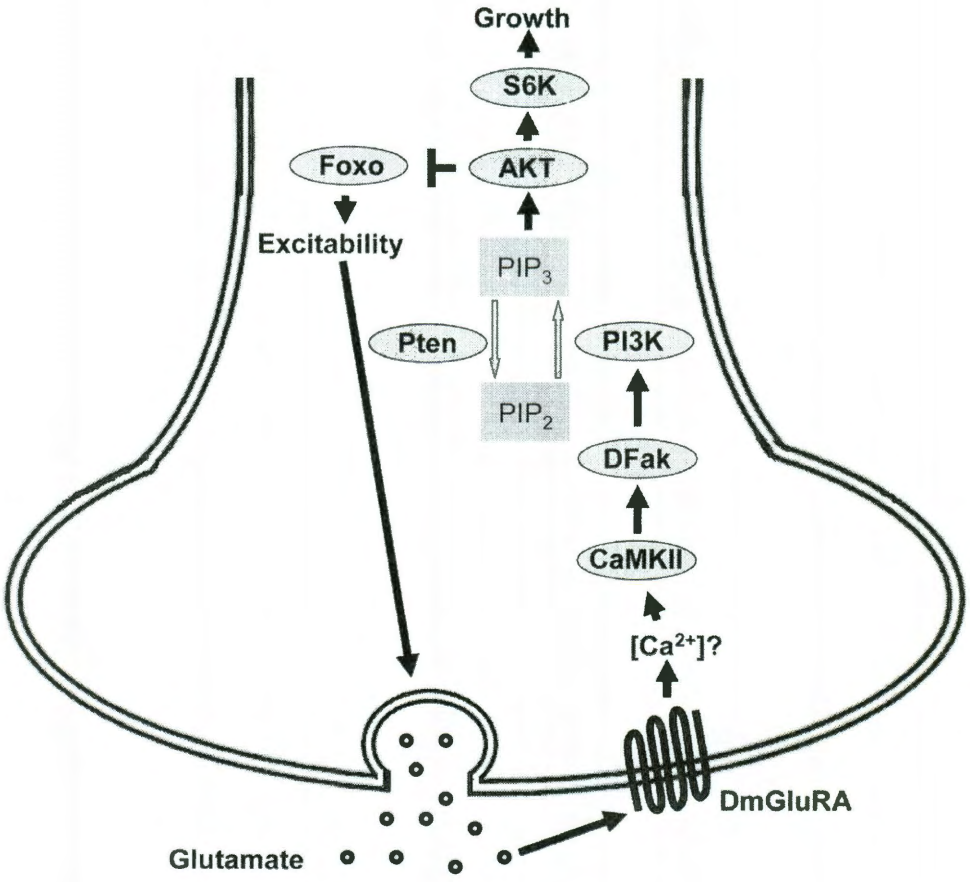

Figure 2.3.11: A proposed mechanism for the DmGluRA-dependent activation of PI3K via CaMKII and DFak. We suggest that glutamate released from motor nerve terminals as a consequence of neuronal activity activates DmGluRA autoreceptors located in motor nerve terminals. This DmGluRA activation then activates CaMKII, which phosphorylates and activates DFak. The formation of phospho-tyrosylated DFak recruits and activates PI3K, either via the p85 regulatory subunit or via Ras. The ability of DmGluRA to activate CaMKII implies that DmGluRA activation increases intracellular [Ca^{2+}], although this possibility has not been tested. As shown previously (Howlett et al., 2008), PI3K activation decreases neuronal excitability by inhibiting the transcription factor Foxo, and increases synapse number by activating S6 kinase.

The observation that DmGluRA-mediated activation of PI3K requires CaMKII implies that DmGluRA activation increases intracellular Ca^{2+} levels in Drosophila motor nerve terminals as a necessary step in PI3K activation. The source of Ca^{2+} for this activation is not known. However, it is well established that in mammals, activation of group I mGluRs, which are responsible for mGluR-mediated LTD in the hippocampus and cerebellum, induce phospholipase C and IP3-mediated Ca^{2+} transients (Pin et al., 1994): which are essential intermediates in cerebellar mGluR-mediated LTD (Ito, 2001). Although Drosophila DmGluRA is most similar to mammalian group II mGluRs, which are not known to activate Ca^{2+} transients, given that DmGluRA is the sole mGluR in Drosophila, it seems possible that DmGluRA might carry out many of the functions carried out by each of the three groups of mGluRs in mammals, as suggested previously (Pan et al., 2008). Alternatively, it is possible that DmGluRA activation might increase intracellular Ca^{2+} via the ryanodine receptor, which was previously shown to be an essential activator of CaMKII in Drosophila larval motor nerve terminals (Shakiryanova et al., 2007).

The ability of CaMKII to activate PI3K requires the nonreceptor tyrosine

kinase DFak: the *DFak*^{CG1} null mutation completely blocks the ability of glutamate applied to motor nerve terminals to activate PI3K, completely suppresses the increase in basal p-Akt levels conferred by *CaMKII*^{T287D}, and blocks the ability of CaMKII^{T287D} to confer two additional PI3K dependent phenotypes: increased synapse number at the NMJ and increased motor axon diameter. These results identify DFak as an essential intermediate in PI3K activation by DmGluRA and CaMKII. However, *DFak*^{CG1} mutants fail to exhibit other phenotypes conferred by decreased PI3K activity: in an otherwise wildtype background, *DFak*^{CG1} larvae exhibit only minor effects on NMJ synapse number or motor axon diameters, which are each significantly decreased by decreased PI3K (Howlett et al., 2008; Martin-Pena et al., 2006). These results raise the possibility that whereas PI3K activation by DmGluRA and CaMKII is blocked in *DFak*^{CG1}, total PI3K activity is not strongly decreased because other significant routes to PI3K activation are DFak-independent. Alternatively, DFak might participate in signaling pathways distinct from the CaMKII-DFak-PI3K pathway we have identified, which would oppose the effects of PI3K on synapse number and axon diameter. In this view, CaMKII would preferentially promote the ability of DFak to activate PI3K, rather than other DFak-dependent pathways.

In several subregions of the mammalian brain, ligand activation of group I mGluRs induces a type of synaptic plasticity called long term depression (LTD). This induction both activates and requires the activity of PI3K as well as the PI3K-activated kinase Tor (Hou and Klann, 2004; Ronesi and Huber, 2008). Several lines of evidence have led to the proposal that increased sensitivity to mGluR-mediated LTD induction might underlie specific neurogenetic disorders. In particular, mice null for the gene affected in Fragile X, which is associated with an extremely high incidence of autism as well as other cogitive deficits, exhibit increased sensitivity to mGluR-mediated LTD induction in both the hippocampus (Huber et al., 2002) and cerebellum (Koekkoek et al., 2005). Furthermore, the genes identified in two additional diseases associated with a high incidence of autism, Neurofibromatosis (Nf1) and tuberous sclerosis (Tsc1 and Tsc2), each encode negative regulators of the PI3K pathway: Nf1 encodes a Ras GTPase activator protein (Xu et al., 1990), which inhibits the PI3K activator Ras (Rodriguez-Viciana et al., 1994) whereas the Tsc proteins are Tor inhibitors that are in turn inhibited by PI3K activity (Gao et al., 2002; Inoki et al., 2002). Thus loss of *Nf1* or *Tsc* might also increase sensitivity to mGluR-mediated LTD. Finally, several lines of direct evidence suggest that PI3K hyperactivation plays a causal

role in autism (Butler et al., 2005; Kwon et al., 2006; Mills et al., 2007; Serajee et al., 2003). For example, DNA copy number variants observed in individuals with autism but not unaffected individuals identify at high frequency PI3K subunits or regulators, and each genetic change is predicted to elevate PI3K activity (Cusco et al., 2009). In addition, a translocation that increases expression of the translation factor eIF-4E, which is known to be activated by the PI3K pathway (Miron et al., 2003; Puig et al., 2003), plays a direct, causal role in autism (Neves-Pereira et al., 2009). The potential involvement of mGluR-mediated LTD in these neurogenetic disorders increases interest in identifying the molecular intermediates that participate in this pathway, but these intermediates are for the most part unidentified. Thus the possibility that CaMKII and Fak might participate in mGluR-mediated PI3K activation in mammals as well as Drosophila might have significant medical interest.

Chapter 3: Pumilio may regulate neuronal excitability via the mGluR/ PI3K signal transduction pathway and transcription factor Foxo

3.1 Synopsis

According to our previous studies (Howlett et al., 2008) and chapter 2, we have found that the mGluR/PI3K pathway regulates motor neuron excitability, and we have identified CaMKII and DFak as two critical intermediates for the DmGluRA-mediated activation of PI3K. In addition, we also reported that overexpression of *Foxo*$^{+}$ increased the rate of onset of LTF, basal transmitter release and frequency of successful EJPs to a level very similar to that observed when PI3K pathway activity was decreased (Figure 3.1.1) whereas in *Foxo*^{21}/*Foxo*^{25} larvae, the rate of onset of LTF, basal transmitter release and frequency of successful EJPs were decreased to levels very similar to those observed when *PI3K-CAAX* was expressed in motor neurons (Figure 3.1.1) (Howlett et al., 2008). Therefore, these results suggest the transcription factor Foxo acts as a downstream effecter of PI3K to regulate motor neuron excitability

(Howlett et al., 2008). In summary, in response to nerve stimulation, the consequent release of glutamate (the excitatory neurotransmitter) from motor nerve terminals down-regulates neuronal excitability by activating metabotropic glutamate receptors (mGluRs) in the same nerve terminal, and furthermore, this downregulation of excitability occurs by mGluR-dependent activation of PI3K and Akt and the consequent inhibition of Foxo (Figure 3.1.2) (Howlett et al., 2008). This PI3K/Foxo-mediated function serves as an activity-dependent inhibition of neuronal activity (negative feedback). However, the Foxo transcriptional targets mediating this control of neuronal excitability were not identified.

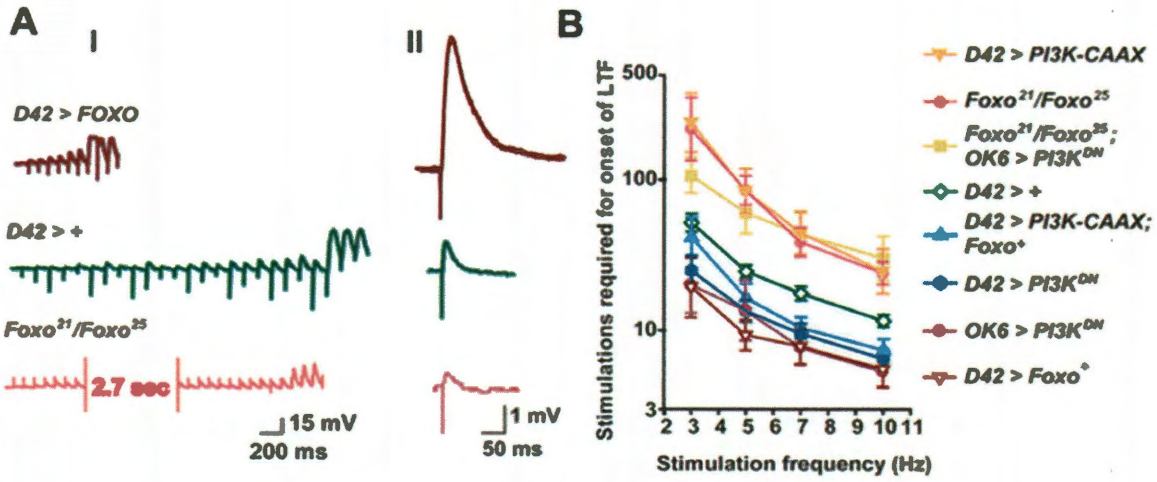

Figure 3.1.1: *Foxo* mediates the effects of *PI3K* on motor neuron excitability. The *Gal4* driver *D42* was used to drive expression of transgenes in all genotypes except for $Foxo^{21}/Foxo^{25}$; $OK6>PI3K^{DN}$, in which the motor neuron driver *OK6* was used and which behaves similarly to *D42* in this assay. For all LTF experiments, the bath solution contained 0.15 mM [Ca^{2+}] and 100 µM quinidine. A) Representative traces showing the decreased rate of onset of LTF (I) and decreased ejp amplitude (II) in $Foxo^{21}/Foxo^{25}$ larvae compared to wildtype at the indicated [Ca^{2+}], and the increased rate of onset of LTF and ejp amplitude in larvae overexpressing *Foxo*. Arrowheads indicate the increased and asynchronous ejps, indicative of onset of LTF. In (II), representative traces are averages of multiple ejps. From *top* to *bottom*, n = 23, 180, and 34 respectively. B) Number of stimulations required to induce LTF (Y axis) at the indicated stimulus frequencies (X axis). Geometric means+/−SEMs are shown. From *top* to *bottom*, n = 12, 6, 7, 18, 10, 21, 5, and 9 respectively, for each genotype. One-way ANOVA and Fisher's LSD gave the following differences, at 10 Hz, 7 Hz, 5 Hz and 3 Hz, respectively: For *D42>+* vs. $Foxo^{21}/Foxo^{25}$, p = 0.0096, 0.0069, <0.0001, 0.0007; vs. $D42>Foxo^{+}$, p = 0.0026, 0.0012, <0.0001, 0.0065. For *D42>PI3K-CAAX*, *Foxo* vs. *D42>PI3K-CAAX*, p = 0.0041, 0.0005, 0.0002, 0.0006; vs. *D42>Foxo*, p = 0.50, 0.43, 0.16, 0.14. For $Foxo^{21}Foxo^{25}$; $OK6>PI3K^{DN}$ vs. $OK6>PI3K^{DN}$, p = ; 0.0003, 0.0004, 0.0014, 0.001. vs. $Foxo^{21}Foxo^{25}$, p = 0.63, 0.74, 0.43, 0.20. *P* values <0.05 were considered statistically significant (Howlett et al., 2008).

Several previous papers have reported that alterations of the translational repressor *pumilio* (*pum*) and the sodium channel *paralytic (para)* also affect neuronal excitability in motor axons. First, in Drosophila, *pum* null mutants, motor neuron excitability is increased, and this phenotype is similar to the phenotype conferred by overexpression of Para in motor neurons (Schweers et al., 2002; Stern et al., 1990). In contrast, overexpression of Pum and loss of Para in the nervous system reduce neuronal excitability (Schweers et al., 2002; Stern et al., 1990). Second, Pum binds directly to *para* mRNA and inhibits the Para translation; which decreases sodium current and excitability in Drosophila motor neurons (Mee et al., 2004; Muraro et al., 2008). Third, I also found that there are three potential Foxo binding sequences ((G/A)TAAA(C/T)A) within 1 Kb of genomic DNA from the *pum* 5' extended gene region (Curran et al., 2009; Demontis and Perrimon, 2010; Teleman et al., 2008) (Table 3.1.1). In addition, inhibiting the mGluR/PI3K signaling pathway also increases neuronal excitability, and this phenotype is similar to *pum* null mutants (Howlett et al., 2008; Schweers et al., 2002). Therefore, I hypothesized that Pum and Para may function as downstream signaling molecules of Foxo in the mGluR/PI3K-mediated negative feedback.

Promoter Region	Foxo Binding Consensus Sequence	Position	Sequence
Pum (CG9755) promoter (3R:5063417,5064417)	(G/A)TAAA(C/T)A	(-405) (-453) (-646)	ATAAATA ATAAATA ATAAATA

Table 3.1.1: The potential Foxo binding sequences in 5' extended gene region of *pum*.

Therefore, we hypothesize that Foxo activity increases neuronal excitability by directly binding to and repressing transcription of *pum* (Figure 3.1.2). This transcriptional repression was predicted to increase neuronal excitability because Pum inhibited the transcription of *para* (Mee et al., 2004). Therefore, Foxo activity is proposed to increase sodium channel levels, conferring increased neuronal excitability (Howlett et al., 2008). To test this hypothesis, anti-Pum antibody was applied to measure the expression level of Pum in the Drosophila central nervous system (CNS). Therefore, if Foxo does inhibit the transcription of pum directly, we predict that activating PI3K or inhibiting Foxo will increase Pum protein levels.

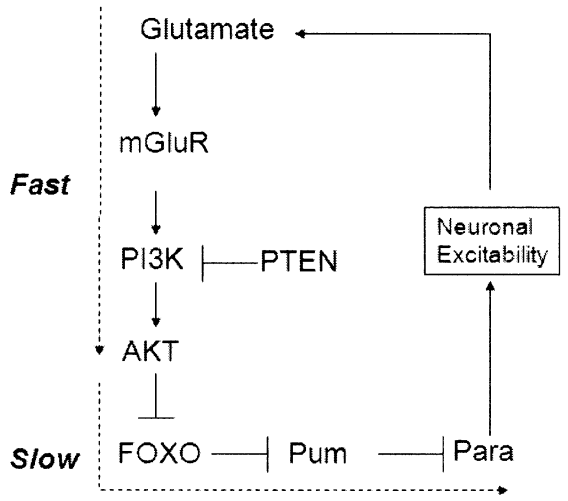

Figure 3.1.2: A proposed mechanism for the mGluR/PI3K/Foxo-mediated negative regulation of neuronal excitability via Pum and Para. Glutamate released from motor nerve terminals as a consequence of neuronal activity activates DmGluRA autoreceptors located in motor nerve terminals. This DmGluRA activation then activates PI3K. PI3K activation decreases neuronal excitability by inhibiting the transcription factor Foxo. The inhibition of Foxo activity may suppress the expression of Pum and then Para will be increased; furthermore, the alteration of Para will affect neuronal excitability and control presynaptic glutamate release.

3.2 Materials and Methods

3.2.1 Drosophila stocks

For all experiments, Drosophila larvae were reared on standard cornmeal/ agar media at 22-23°. Flies carrying the *UAS-PI3K^{DN}* (D954A) and

UAS-PI3K-CAAX transgenes (Leevers et al., 1996), encoding a dominant-negative and constitutively active PI3K, respectively, were provided by Sally Leevers (London Research Institute, London, UK). Flies carrying the *UAS-Foxo*$^{+}$ transgene was provided by Marc Tatar (Brown University, Providence, RI). Flies carrying the *Foxo*^{21} and *Foxo*^{25} were provided by Heinrich Jasper (University of Rochester, Rochester, NY). All other fly stocks were provided by the Drosophila stock center (Bloomington, IN).

3.2.2 Immunocytochemistry

Antibodies against Drosophila Pumilio (Pum) were kindly provided by Dr. Lehmann (New York University) and were used at 1:500 dilution. Dylight™ 594-conjugated goat anti-rabbit IgG (Jackson ImmunoResearch) was used at a dilution of 1:500. For ventral ganglion staining, larvae were dissected in PBS and fixed in 4% paraformaldehyde. Images were taken on a Zeiss 510 LSM with a 63× objective. Z-stacks were compiled from 2 µm serial sections to a depth adequate to encompass the 10 µm thickness for each sample. ImageJ software was used to

analyze pumilio intensities. In particular, 2D projections were created using the average pixel intensity and cell area was traced using the freehand selection tool and the selection where the mean pixel intensity value was measured. Two different areas of each sample and five samples of each genotype were selected for analyzing Pumilio. The mean intensity of Pum level of wild type was used for reference. Bars represent mean Pumilio levels +/-SEMs.

3.3 Results

3.3.1 The protein level of pumilio is increased in *Foxo* null mutants in the Drosophila ventral ganglion

Based on the model, Foxo might regulate neuronal excitability by inhibiting *pum* transcription, which results in the decrease of Pum levels. Because this translational machinery lies close to the nucleus of the cell, I hypothesize that this translational event will take place within the motor neuron cell body which is located in the Drosophila ventral ganglion. Therefore, if Foxo inhibits *pum* transcription, I predict that Pum protein level should be elevated in *Foxo* null

mutants within the motor neuron cell body. To test this hypothesis, first, I monitored the expression level of Pum following application of an antibody against Pum and measured the fluorescence intensity of Pum in the ventral ganglion in wild type and $Foxo^{21}/Foxo^{25}$ larva. As shown in Figure 3.3.1, we found that Pum levels in *Foxo* null flies were significantly increased (Figure 3.3.1).

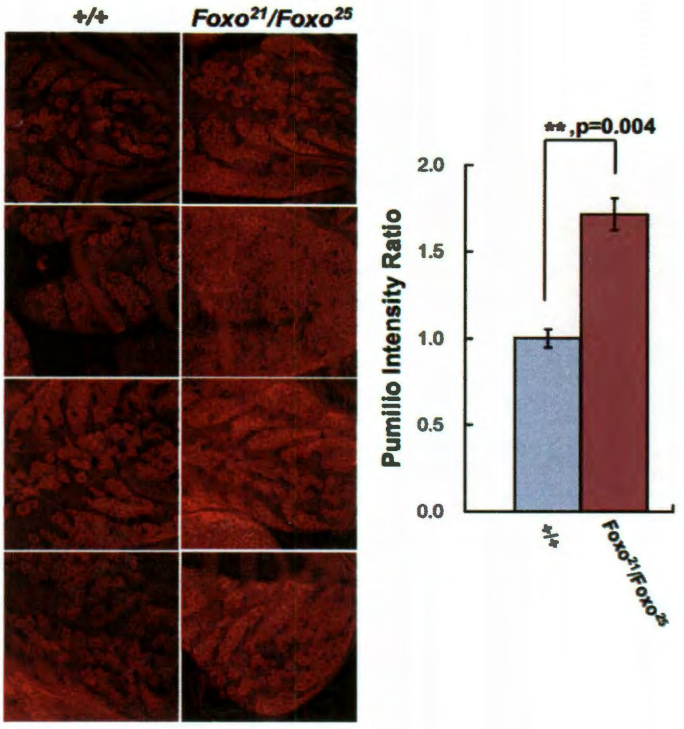

Figure 3.3.1: The inhibition of Foxo activity increases the expression of Pum. Left panel: Representative confocal images of third instar larval ventral ganglion of wildtype (*+/+*) and *Foxo^{21}/Foxo^{25}* stained with anti-Pum. All images are taken from different larvae. Right panel: Mean normalized Pum intensity (Y axis) +/- SEM for the following genotypes (X axis): *+ > +* and *Foxo^{21}/Foxo^{25}*. Pixel intensities were quantified using ImageJ software. The normalized Pum intensities are shown as a ratio change compared to wild type. From left to right, n = 5, 5, respectively, for each genotype. Student T-test was performed for statistical analysis. *P* values <0.05 were considered statistically significant.

Next, we wanted to know whether overexpression of Foxo can inhibit the Pum expression and examine whether this potential transcriptional regulation is occurring in the motor neuron. We used the motor neuron driver *D42* (Sanyal,

2009) to overexpress both Foxo^{+} and green fluorescence protein (GFP). GFP was used for labeling motor neurons. Here, we found that overexpression of Foxo suppressed the expression level of Pum in motor neurons (Figure 3.3.2). In conclusion, Foxo is a negative regulator of Pum.

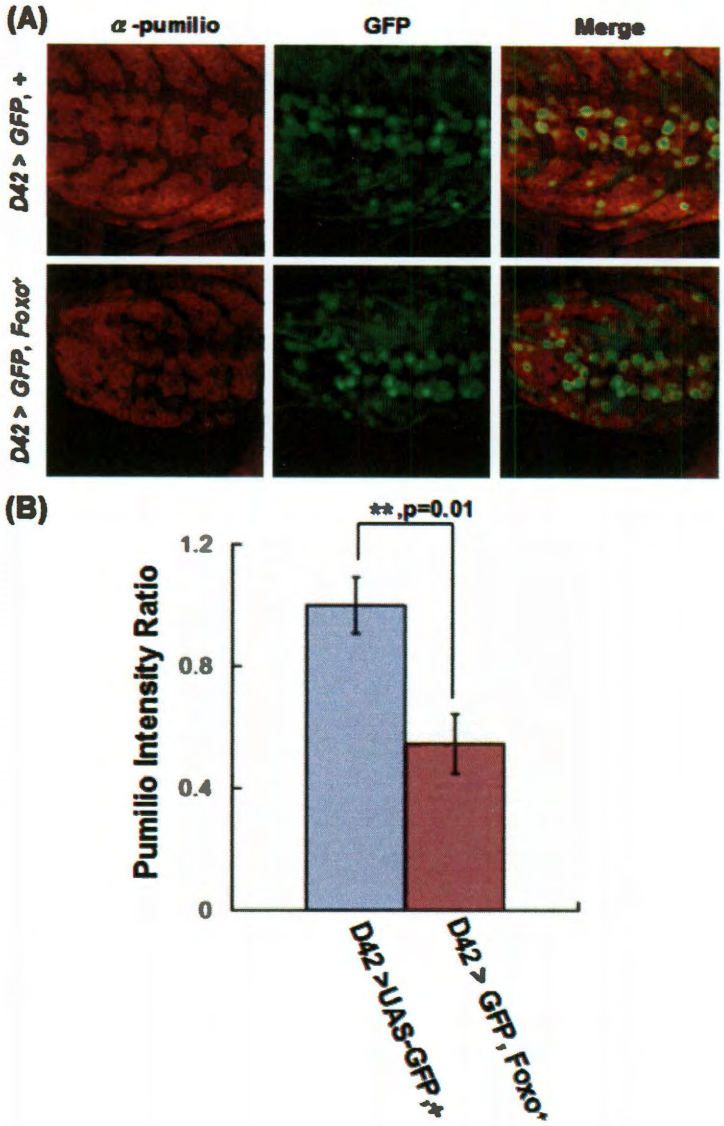

Figure 3.3.2: Foxo activity suppresses the expression of Pum. (A) Representative confocal images of third instar larval ventral ganglion of *D42 > GFP, +*, and *D42 > GFP, Foxo+* stained with anti-Pum (left panels), GFP (middle panels), and merged images (right panels). (B) Mean normalized Pum intensity (Y axis) +/- SEM for the following genotypes (X axis): *D42 > GFP, +*, and *D42 > GFP, Foxo+*. Pixel intensities were quantified using ImageJ software. The normalized Pum intensities are shown as a ratio change compared to wild type. From left to right, n = 5, 5, respectively, for each genotype. Student T-test was performed for statistical analysis. *P* values <0.05 were considered statistically significant.

3.3.2 Manipulation of the PI3K signaling pathway within the Drosophila ventral ganglion affects pumilio protein levels

As described above, the expression of pumilio is inhibited by Foxo. Foxo has also been shown to be a downstream effector of mGluR/PI3K signaling, and mGluR/PI3K/Foxo negatively regulates neuronal excitability at motor neuron terminals (Howlett et al., 2008). Therefore, we predict that the manipulation of signaling molecules within the PI3K pathway will also alter the expression of Pum. To test this prediction, we used the central nervous system driver *Elav* (Sanyal, 2009) to overexpress both $PI3K^{DN}$ and Pten. Because the overexpression of $PI3K^{DN}$ and Pten block PI3K signaling and prevent the inhibition of Foxo, I hypothesized that the expression of pum will be suppressed in both *Elav > PTEN* and *Elav* > $PI3K^{DN}$. As shown in Figure 3.3.3, the expression of pum in *Elav* > $PI3K^{DN}$ decreased about 20% and in *Elav > Pten* decreased about 15% (Figure 3.3.3). Taken together, these results confirmed that pum is required for mGluR/PI3K/Foxo-mediated negative regulation to maintain neuronal homeostasis.

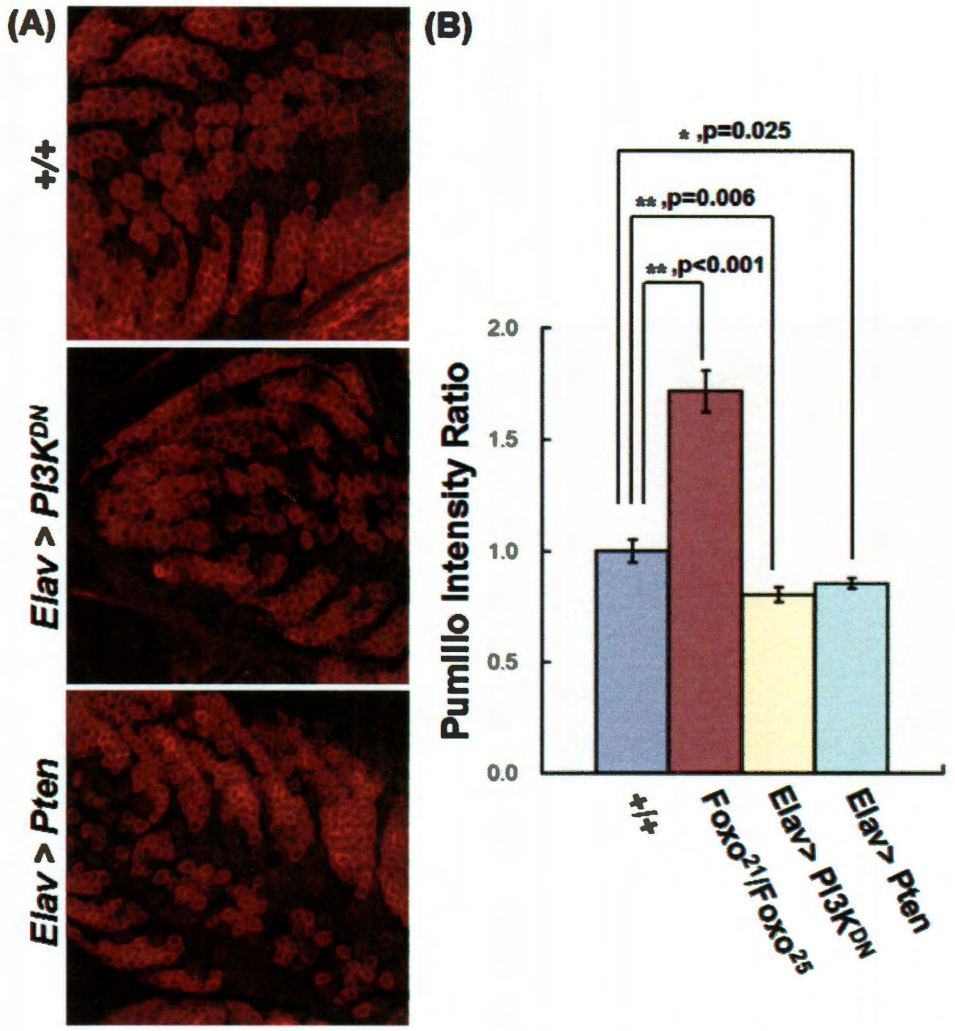

Figure 3.3.3: The decrease of PI3K activity suppresses the expression of Pum. (A) Representative confocal images of third instar larval ventral ganglion of *+/+*, *Foxo^{21}/Foxo^{25}*, *Elav > PI3K^{DN}*, and *Elav > Pten* stained with anti-Pum. (B) Mean normalized Pum intensity (Y axis) +/- SEM for the following genotypes (X axis): *+/+*, *Foxo^{21}/Foxo^{25}*, *Elav > PI3K^{DN}*, and *Elav > Pten*. Pixel intensities were quantified using ImageJ software. The normalized Pum intensities are shown as a ratio change compared to wild type. From left to right, n = 5, 5, 5, 5, respectively, for each genotype. Student T-test was performed for statistical analysis. *P* values <0.05 were considered statistically significant.

3.4 Summary and future work

Here I showed that the translational repressor *pumilio* (*pum*) may function as a downstream effector in the regulation of presynaptic neuronal homeostasis. However, there are still many questions and concerns that need to be addressed. First, to confirm that disruptions of genes involved in mGluR/PI3K/Foxo negative feedback alter the expression of Pum and Para in Drosophila ventral ganglion, Q-PCR will be performed to measure *pum* and *para* transcript level in larva that have genetic disruptions in mGluR/PI3K/Foxo-mediated signaling molecules. Second, Chromatin Immunoprecipitation (ChIP) assays will be utilized to identify the Foxo binding region in the *pum* 5' UTR. Third, Third instar larvae with pum^{bem}, $Foxo^{21}/pum^{bem}$, $Foxo^{25}$ or pum^{bem}, *D42>PI3K-CAAX* will be characterized on phenotypic changes, including neuronal excitability and neuronal arborization. These experiments may be able to elucidate the relationship of Pum and Para in mGluR/PI3K/Foxo-mediated negative feedback mechanism.

Chapter 4: Drosophila Push may regulate neuronal homeostasis and retrograde signaling in neuromuscular junction

4.1 Synopsis

The ubiquitin proteosome system (UPS) has been implicated in regulating synapse development, presynaptic function, and neurotransmitter release (Yi and Ehlers, 2005). For example, in 2001, DiAntonio's lab reported that the overexpression of the deubiquitinating protein fat facets (faf) in the Drosophila nervous system significantly increased the number of synaptic boutons and arbors (DiAntonio et al., 2001). Moreover, the overexpression of faf also decreases both the quantal content of excitatory junction potential (EJP) and the frequency of spontaneous miniature EJPs (mEJPs). Simultaneously, the data also showed that loss-of-function of highwire (*hiw*), an E3-ubiquitin ligase, had a similar phenotype to *faf* gain-of-function (DiAntonio et al., 2001). Recently, UPS and endoplasmic reticulum (ER)-associated protein degradation (ERAD) have been further implicated in the regulation of neuronal excitability. Altier et al. reported that a mammalian L-type voltage-gated calcium channel subunit, Cav1.2,

underwent robust ubiquitination by the RFP2 ubiquitin ligase and degradation by the proteasome in the absence of the accessory subunit Cavβ (Altier et al., 2010). This finding indicated that Cavβ and UPS are required to regulate the density of Cav1.2 and maintain proper neuronal activity (Altier et al., 2010). In addition, Fu et al, reported that activation of the ephrin type-A receptor 4 (EphA4) induced the degradation of GluR1, a subunit of the α-amino-3-hydroxy-5-methyl-4-isoxazolepropionic acid (AMPA) receptor (AMPAR), through ubiquitin ligase anaphase-promoting complex (APC) and proteasomes. The consequent decrease in the quantity of synaptic and surface GluR1 then resulted in a reduction of mEPSC amplitude (Fu et al., 2010). These results indicated that EphA4 regulated the density of GluR1 subunit of the AMPAR via a UPS degradation pathway (Fu et al., 2010). Based on these findings, the UPS and ERAD have emerged as important regulators in maintaining neuronal excitability and homeostasis (Kantamneni et al., 2011).

As mentioned in chapter 1, push has been predicted to be an E3-ubiqutin ligase (Yager et al., 2001). Our previous studies showed that push also plays an important role in the regulation of neuronal excitability. In *push null* mutants, both larvae and adults exhibit several severe behavioral defects, which are the

consequence of neuronal defects. Adults with *push* mutations exhibit an inability to fly, uncoordination, sluggishness, and lack of an escape response (Richards et al., 1996). Third instar larvae with *push* mutations demonstrate an increase both in neurotransmitter release (EJP amplitude increase) and in the frequency of mEJPs in the neuromuscular junction (Richards et al., 1996) (Figure 4.1.1). Even though these previous studies already indicated that Push is required to maintain neuronal homeostasis, the cellular location and functional properties of Push and Push-mediated molecular pathways remained a mystery.

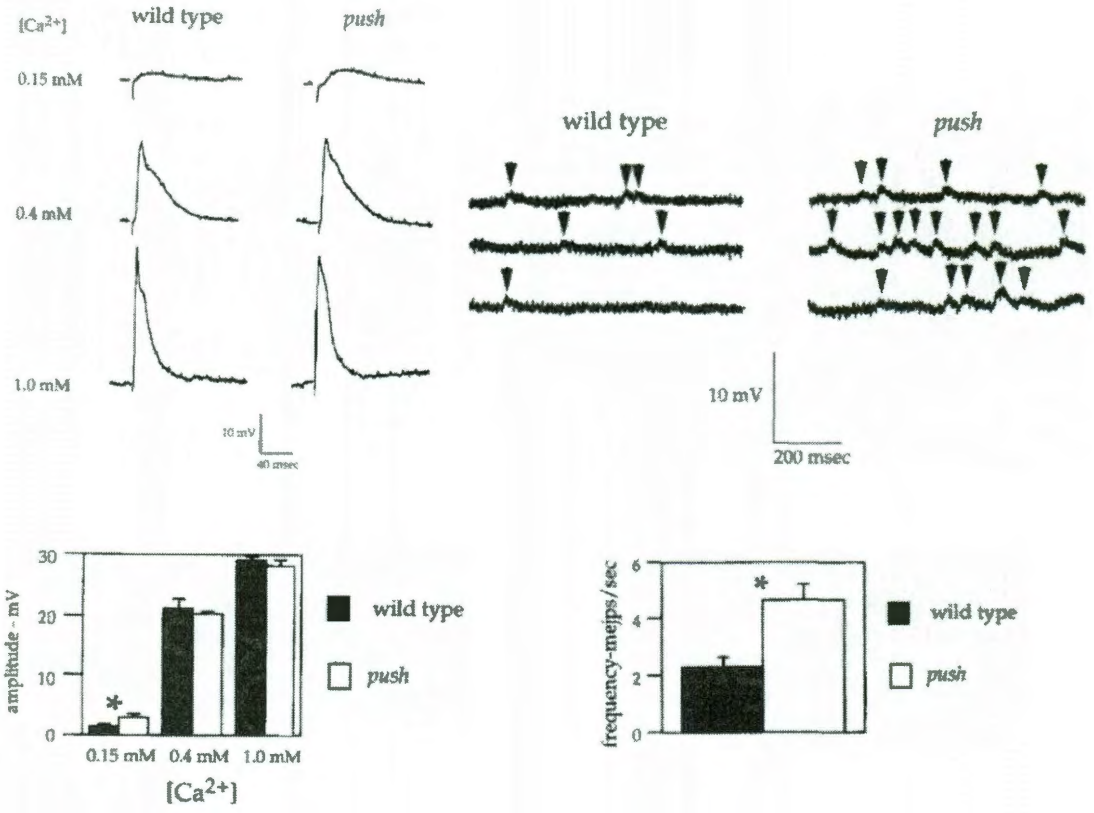

Figure 4.1.1: *push* mutations increase neurotransmitter release and the frequency of single vesicle release (represented as mEJPs) in the motor neuron. (A) Top Left panel: representative traces showing the increased excitatory junction potential (EJP) amplitude in *push*^{1}/*push*^{1} larvae at a bath [Ca^{2+}] of 0.15 mM, 0.4 mM and 1.0 mM in Jan's solution. Bottom left panel: mean EJP amplitudes +/- SEMs (Y axis) at the indicated [Ca^{2+}] (X axis), from the following genotypes: *wild type* and *push*^{1}/*push*^{1} (*push*). n = (12, 7, 5) respectively, for each genotype and [Ca^{2+}] (0.15 mM, 0.4 mM and 1.0 mM in Jan's bufffer). (B) Top right panel: representative traces showing the increased of frequency of mini EJPs in *push*^{1}/*push*^{1}. Three traces from each genotype are from three different larvae. Bottom right panel: Mean mEJP frequency +/- SEMs (Y axis) for the indicated genotypes (X axis): *wild type* and *push*^{1}/*push*^{1}. Recordings were collected from twelve different larvae from each genotype in Jan's solution with a bath [Ca^{2+}] of 0.15 mM, and total number of responses within 5 seconds period were measured and averaged from each larva. The asterisk indicated *P* values <0.05 and are considered statistically significant. (Data is adopted from Richards et al., 1996).

Therefore, in this chapter, I will be focused on characterizing the role of Push in the Drosophila neuromuscular systems. Three avenues of investigation will be described in this chapter including 1) the expression pattern of Push in Drosophila, 2) the role of push in the regulation of neurotransmitter release, and 3) the role of push in the regulation of homeostasis at the Drosophila neuromuscular junction.

4.2 Materials and Methods

4.2.1 Drosophila stocks

For all experiments, Drosophila larvae were reared on standard cornmeal/ agar media at 22-23°. *push*^{1}*/CyoGFP* (1481G and 1481C) and *push*^{2}*/CyoRoi* (S1516D) were generated in our lab (Richards et al., 1996). Flies carrying the *UAS-PI3K-CAAX* transgene (Leevers et al., 1996), encoding constitutively active PI3K, were provided by Sally Leevers (London Research Institute, London, UK). Flies carrying the *UAS-push*^{RNAi} (14472R-1), *UAS-PLCβ*^{RNAi} (4574R-1) and *UAS-IP3R*^{RNAi} (1063R-1) transgenes, were provided by National Institute of

Genetics (Shizuoka, Japan). Flies carrying the *UAS-mGluR*^{RNAi}, were provided by Marie-Laure Parmentier (Unité Propre de Recherche Centre, Montpelier, France). Flies carrying *the UAS-IP3R*^{RNAi} transgenes, were provided by Vienna Drosophila RNAi Center (Vienna, Austria). All other fly stocks were provided by the Drosophila Stock Center (Bloomington, IN).

4.2.2 Push antibody production

The push fragment (named as push3499), which was used for antibody production, was from amino acids 3499 to 3894 within the push C-terminus, and its molecular weight is about 45.8 kDa. The gene fragment encoding push3499 was cloned from a bacteria artificial chromosome (BAC) BACR08I01 (Berkeley Drosophila Genome Project, Berkeley, CA) with the following pair of primers (5'-CAT ATG GCC TCC GGA AAA CTT CGA ACA GAT CG-3' and 5'-CTC GAG TTA CTC CAG CAT TTG CTT GTT GGT CAG CAG-3'). NdeI and XhoI restriction enzymes sites were used to clone push3499 gene fragments into E. coli expression vector pET19A (Invitogen). The recombinant plasmids

(pET19A-push3499) were transformed into E. coli stain BL21(DE3) for protein expression. The cells were grown overnight in LB medium. The overnight culture was inoculated in the TB medium with 1000X dilution. When the cell population reached 0.6 in O.D. 360, the push3499 cells were induced by adding IPTG to a final concentration of 1 mM at 37°C. The expression level of push3499 was tested by collecting 2 and 4 hours induction cultures and detecting protein on 15% SDS-PAGE. After induction, the cells were broken and total protein was extracted in Hepes buffer (25 mM HEPES, 100 mM KCl, 10% (w/v) glycerol, pH 7.4) with cOmplete ULTRA Protease Inhibitor Tablets (Roche). Push3499 was purified by Ni-NTA under Hepes buffer with gradient imidazole (0-500 mM) and concentrated to 1mg/ml. The antibody production of push3499 was carried out by COCALICO BIOLOGICAL, INC. (Reamstown, PA) using the following procedure (Table 4.1.1).

Day 0	Primary injection of 200 µg/rabbit in complete Freund's adjuvant
Day 21	Secondary injection of 100µg /rabbit in incomplete Freund's adjuvant
Day 42	Boost injection of 100µg /rabbit in incomplete Freund's adjuvant
Day 52	Test Bleed rabbit
Day 63	Boost injection of 100µg /rabbit in incomplete Freund's adjuvant
Day 73	Production Bleed rabbit #1
Day 84	Boost injection of 100µg /rabbit in incomplete Freund's adjuvant
Day 94	Production Bleed rabbit #2
Day 105	Boost injection of 100µg /rabbit in incomplete Freund's adjuvant
Day 115	Production Bleed rabbit #3
Day 126	Boost injection of 100µg /rabbit in incomplete Freund's adjuvant
Day 136	Production Bleed rabbit #4
Day 147	Boost injection of 100µg /rabbit in incomplete Freund's adjuvant
Day 157	Production Bleed rabbit #5
Day 168	Boost injection of 100µg /rabbit in incomplete Freund's adjuvant
Day 178	Production Bleed rabbit #6

Table 4.1.1: The procedure of push3499 production

4.2.3 Immunohistochemistry

Larvae were grown to the wandering third-instar stage in uncrowded half-pint bottles. Larvae were collected for experimentation only during the first and second days after the initial wandering third-instar larvae appeared. For push immunostaining, larvae were dissected in standard Phosphate Buffered saline

(PBS, 0.128 M NaCl, 2.0 mM KCl, 4.0 mM $MgCl_2$, 0.34 M sucrose, 5.0 mM HEPES, pH 7.1, and 0.15 mM $CaCl_2$) and fixed in PBS containing 4% paraformaldehyde. Fixed larval tissues were incubated with a rabbit anti-Drosophila push (push3499) polyclonal primary antibody (1:500 dilution). Larvae were then incubated with Rhodamine Red conjugated goat anti-rabbit IgG (1:500 dilution, Jackson ImmunoResearch), and Cy-2 conjugated antibodies against horseradish peroxidase (1:200 dilution, Jackson ImmunoResearch). Immuno-labeled larval tissues in PBS containing 50% glycerol were mounted onto slides. Larval tissues including brain, ventral ganglion, and muscle were imaged on a Zeiss LSM 510 confocal microscope system (Zeiss, Oberkochen, Germany) with a 20X and 63X objective lens. Optical sections were 1 or 2 μm thick. Optical parameters, including pinhole, gain, contrast, and brightness, were held constant for each experimental set. The protocol of Drosophila S2 cells immunostaining was the same as larvae immunostaining. For phosphorylated Mad (p-Mad) immunostaining, larvae were dissected in Schneider's Drosophila media (Gibco) and fixed in Schneider's Drosophila media containing 4% paraformaldehyde. Fixed larval tissues were incubated with a rabbit anti-p-Mad polyclonal primary antibody (1:500 dilution) (provided by Peter ten Dijke, Ph.D., Leiden, The

Netherlands) (Persson et al., 1998). Larvae were then incubated with Rhodamine Red conjugated goat anti-rabbit IgG (1:500 dilution, Jackson ImmunoResearch), and Cy-2 conjugated antibodies against horseradish peroxidase (1:200 dilution, Jackson ImmunoResearch). Mounting procedures are as described above. Neuromuscular junctions (NMJs) from muscles 6 and 7 in segments A2 to A5 were imaged on a Zeiss LSM 510 confocal microscope system (Zeiss, Oberkochen, Germany) with a 63X objective. Optical sections were 1 μm thick. Optical parameters, including pinhole, gain, contrast, and brightness, were held constant for each experimental set.

4.2.4 Electrophysiology

Larvae were grown and selected as described above and dissected in HL3 buffer (70 mM NaCl, 5.0 mM KCl, 20 mM $MgCl_2$, 10 mM $NaHCO_3$, 5 mM Trehalose, 115 mM sucrose, 5 mM HEPES, pH 7.2, and $CaCl_2$ concentration as specified in the text). Peripheral nerves were cut immediately posterior to their exit from the ventral ganglion, and were stimulated with a suction electrode at a 5V

stimulus intensity. Muscle recordings were taken from muscle 6 in abdominal sections 3–5. Stimulus duration, approximately 0.05 msec, was adjusted to 1.5 times threshold which reproducibly stimulates both axons innervating muscle 6. Intracellular recording electrodes for muscle potentials were pulled with a Flaming/Brown micropipette puller to a tip resistance of 10–40 MΩ and filled with 3M KCl. Excitatory junction potential (EJP) amplitude are reported as geometric means because the data show a positive skew.

4.2.5 2D-Difference in gel electrophoresis (2D-DIGE) and protein identificaiton

The total protein samples were extracted from Drosophila heads of wild type and push null mutants. The protein concentration of each fraction was determined by 2-D Quant (GE lifescience). 25 μg of the wild type protein sample was labeled with Cy2 and 25 μg of the *push null* mutant sample was labeled with Cy3. The fluorophore-labeling and gel electrophoresis were performed by Applied Biomics, Inc. (Hayward, CA). 96 potential protein spots showing differential expression were collected for protein identification. The in-gel digestion and protein identification were also carried out by Applied Biomics, Inc.

4.3 Results

4.3.1 Push is a membrane protein and may also associate with microtubule.

Previous studies have suggested that Push may be a membrane protein based on computational prediction (Yager et al., 2001). However, there was no experimental evidence to confirm this prediction. To address this question, I produced the polyclonal α-push antibody (push3499), which recognizes the region from amino acid 3499 to 3894. Stack images of Push immunostaining on Drosophila early embryos showed that Push existed only on the membranes. Furthermore, three dimensional image reconstructions indicated that push is specifically present on the membrane (Figure 4.3.1).

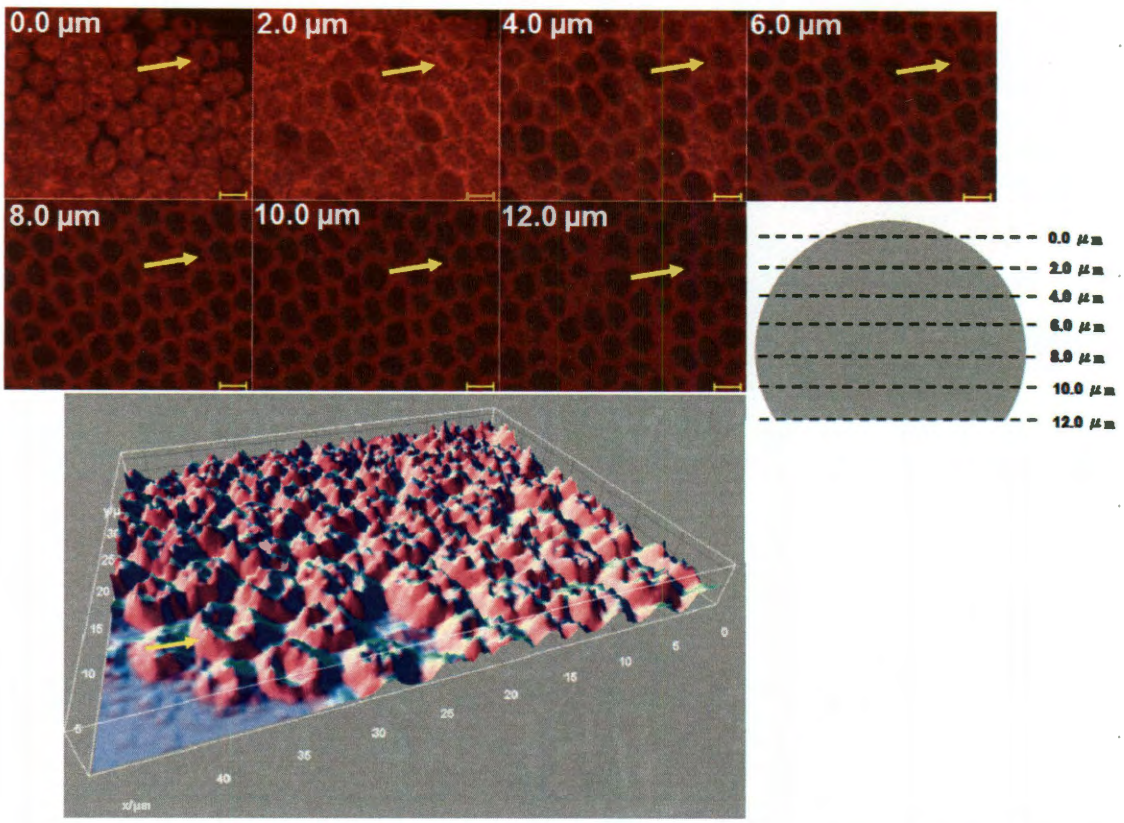

Figure 4.3.1: Push is present on the membrane of Drosophila early embryo. Top panel: Representative stack confocal images of a Drosophila early embryo stained with anti-Push. The stack images were 2 µm serial sections. Scale bar is 5 µm. Bottom panel: 3D image of Drosophila early embryo are reconstructed from the stack confocal images showed on the top panel. The semicircle was a 2D model to represent a single cell, marked by yellow arrow.

To confirm this result, I applied the same immunostaining protocol, except in the absence of nonionic surfactant Triton X-100, on Drosophila S2 Cells. Simultaneously, the cytosolic housekeeping protein, β-tubulin, was stained as the control. I hypothesized that the immunoreaction of β-tubulin will not occur

because the α-β-tubulin antibody can not penetrate into the cytoplasm. In contrast the immunoreaction of push will not be affected if push is present on the membrane. As shown in Figure 4.3.2, Push, but not β-tubulin, is detected, these confirming my prediction (Figure 4.3.2). I conclude that push is a membrane protein.

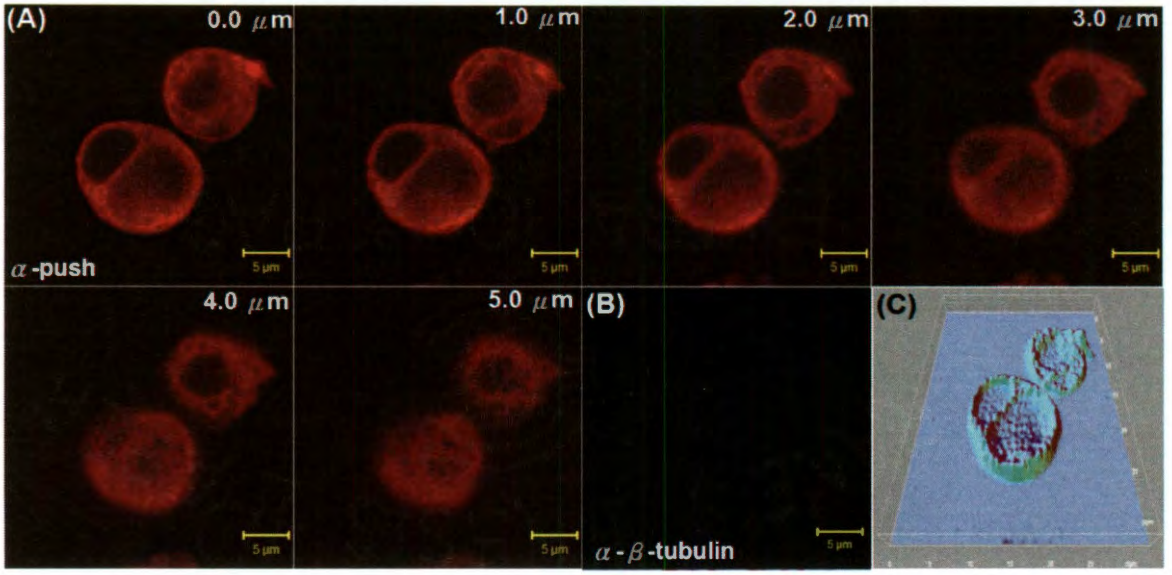

Figure 4.3.2: Push is present on the membrane of Drosophila S2 cells. (A) Representative stack confocal images of Drosophila S2 cell stained with anti-Push. The stack images were 1 μm serial sections to a depth. Scale bar is 5 μm. (B) Representative stack confocal images of Drosophila S2 cells stained with anti-β-tubulin. Scale bar is 5 μm. (C) 3D image of Drosophila S2 cells are reconstructed from the stack confocal images of Push immunostaining.

The mammalian P600 protein, which is an ortholog of Drosophila push, has

been reported as a novel microtubule-associated protein (MAP) and maintains ER stability (Shim et al., 2008). Therefore, I applied both α-push and α-β-tubulin antibodies to S2 cells and also used pre-immune serum (RCM3, the same serum before producing α-push antibody) as a control to examine whether push is also a MAP. We found that the push is colocalized with β-tubulin (Figure 4.3.3). These results indicated that push may also be a microtubule-associated protein in *Drosophila melanogaster*.

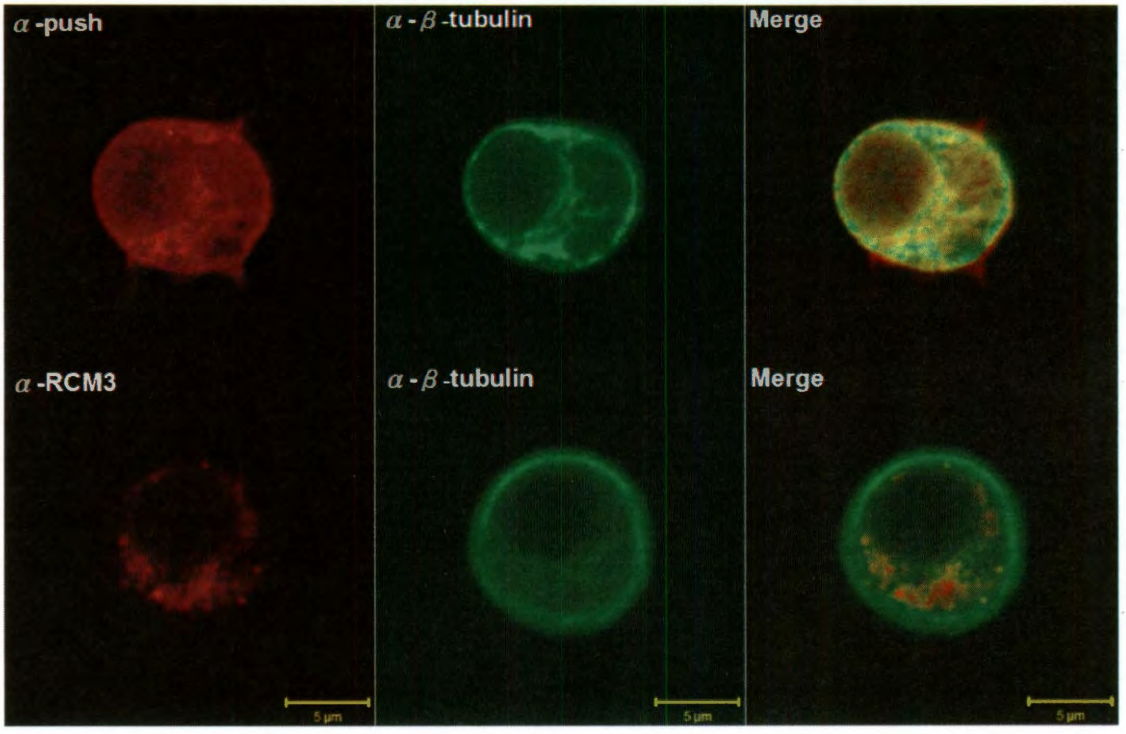

Figure 4.3.3: Push is colocalized with microtubules. Representative confocal images of S2 cells stained with anti-Push (left panels), anti-β-tubulin (center panels), and merged images (right panels). Scale bar is 5 µm.

4.3.2 Push is highly expressed in the Drosophila nervous and muscular systems

Drosophila Push has been implicated in the regulation of neurotransmitter release (Richards et al., 1996), spermatogenesis (Richards et al., 1996), and perineurial glial growth (Yager et al., 2001). The mammalian orthologue, p600, is characterized as a chromatin scaffold in the nucleus (Nakatani et al., 2005; Sakai et al., 2011). In the cytoplasm, p600 was also reported to be involved in the regulation of several events. First, p600 accompanies clathrin to regulate cytoskeletal organization and membrane morphogenesis (Nakatani et al., 2005). Second, p600 interacts with the endoplasmic reticulum (ER) and microtubules to maintain stability of the ER (Shim et al., 2008). Third, p600 is an E3-ubiqitin ligase, also called mammalian UBR4, and is tightly associated with the 26S proteasome (Besche et al., 2009; Tasaki et al., 2005). Fourth, p600 is implicated in the prevention on anoikis, a type of programmed cell death that is induced by improper cell-matrix interactions (Nakatani et al., 2005; Sakai et al., 2011). Therefore, p600 may also be important in the regulation of cell-cell and cell-matrix interactions. Because Drosophila Push and its mammalian ortholog perform several functions, this suggested that Push may be expressed in many types of

tissue. However, the global pattern of push in the *Drosophila melanogaster* remains unclear.

Here, because our lab is focusing on the Drosophila nervous and muscular systems, I chose the Drosophila third instar larva as a model organism to study the expression pattern of Push in nerves and muscles. First, I checked the expression of push in the Drosophila nervous system. As figure 4.3.4 shown, Push is highly expressed in both neurons and glia in the Drosophila brain and ventral ganglion (Figure 4.3.4A and Figure 4.3.4B). Moreover, I found that Push may also be expressed in perineurial glia (Figure 4.3.4C). Second, in the Drosophila muscle, Push is highly expressed and the expression pattern of push seems to be dispersed among the actin filaments (Figure 4.3.4C). Therefore, push may also interact with actin filaments. In conclusion of section 4.3.1 and 4.3.2, Push is expressed in both nervous and muscular systems. Moreover, because push seems to colocalize with cytoskeletal elements, including microtubules and actin filaments, these results may further indicate the importance of push in the regulation of vesicle trafficking, cell mobility, and muscle contraction.

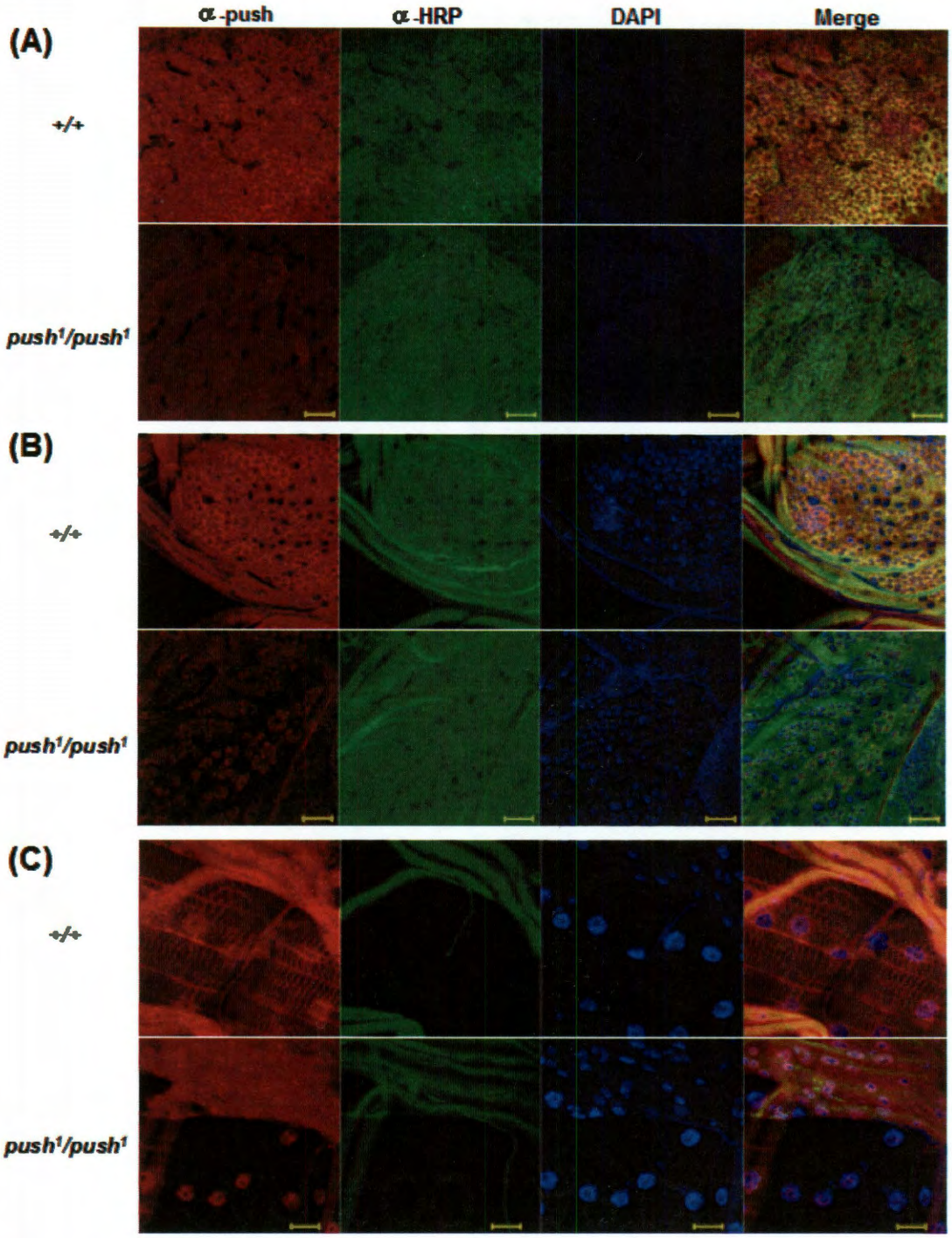

Figure 4.3.4: Push is highly expressed in the Drosophila brain, ventral ganglion, glia, and muscle. (A) Representative confocal images of Drosophila brain stained with anti-Push (left panels), anti-HRP (middle left panels), DAPI (middle right panels), and merged images (right panels). Scale bar is 20 μm. (B) Representative confocal images of Drosophila ventral ganglion stained with

anti-Push (left panels), anti-HRP (middle left panels), DAPI (middle right panels), and merged images (right panels). Scale bar is 20 μm. (C) Representative confocal images of Drosophila nerve and muscle stained with anti-Push (left panels), anti-HRP (middle left panels), DAPI (middle right panels), and merged images (right panels). Scale bar is 20 μm.

4.3.3 Push is required for maintaining proper neurotransmitter release at the Drosophila neuromuscular junction

As mentioned above, push is highly expressed in the nervous system and previous studies showed defects of neurotransmitter release in *push null* mutants. To understand whether this defect is caused by lack of push solely in the nervous system, I combined RNA interference (*UAS-push^{RNAi}*) with central neuron driver *Elav-gal4* to knock down the expression level of push in neurons. However, as shown in Figure 4.3.5, the expression level of push in *Elav > push^{RNAi}* larval brains still remained similar to that of wild type. Therefore, the overexpression of Dicer (Dcr), an endoribonuclease which mediates the cleavage of double-stranded RNA (dsRNA) and pre-microRNA (miRNA) into short double-stranded RNA fragments, was introduced to enhance the efficacy of disruption of *push* mRNA and prevent push translation. By introducing Dcr together with *push^{RNAi}* (*Elav >Dcr, push^{RNAi}*), I was able to knock down the expression level of push dramatically in neurons (Figure 4.3.5).

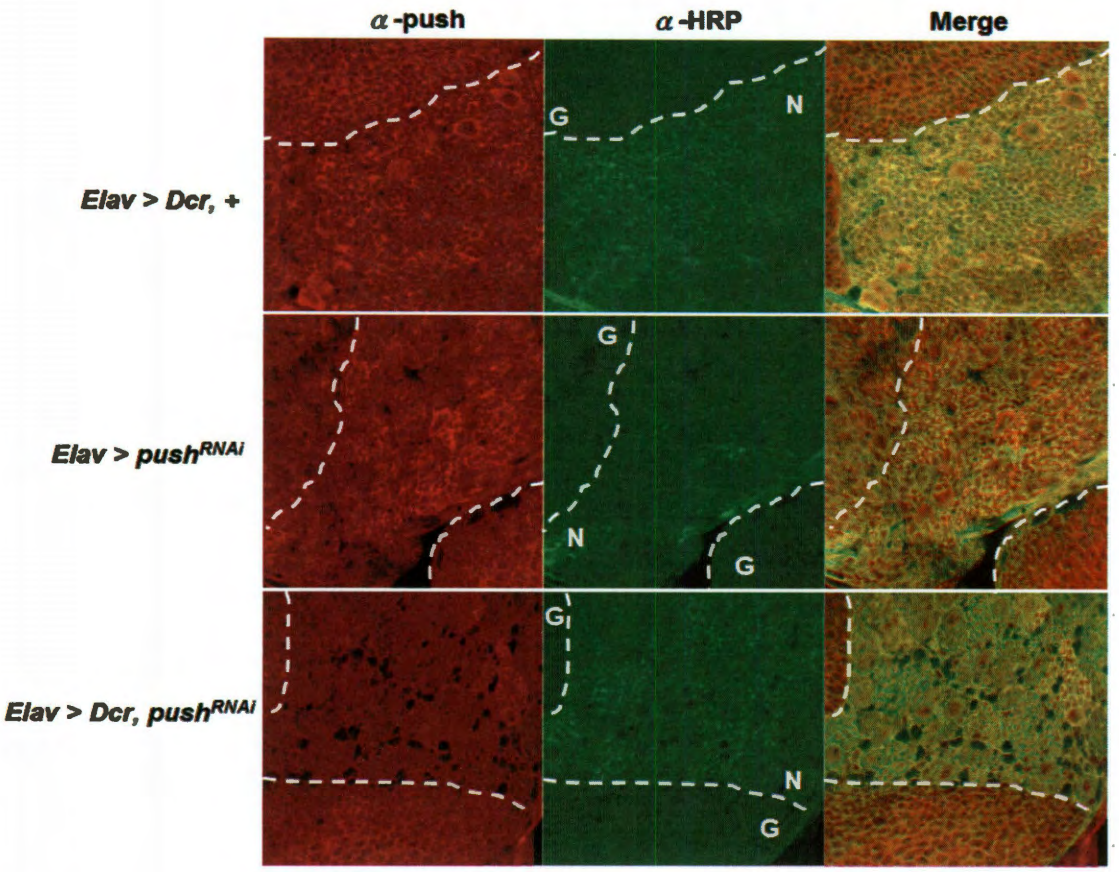

Figure 4.3.5: *Elva > Dcr, push^{RNAi}* can effectively knock down the expression of Push in Drosophila neuron cell. Representative confocal images of of third instar larval brains of *Elav > Dcr, +*, *Elav > push^{RNAi}*,and *Elav > Dcr, push^{RNAi}* stained with anti-Push (left panels), anti-HRP (middle panels), and merged images (right panels). N indicated neuron cells. G indicated glia cells. Scale bar is 20 μm.

Since I was able to knock down push expression by genetic manipulation, next I asked if decreasing in push expression in neurons also increases neurotransmitter release similar to the *push null* mutation. To address this question, I performed electrophysiological recording on third instar neuromuscular

junctions. First, I compared the amplitude of excitatory junction potentials (EJPs) between wild type and *push null* mutants in HL3 solution. The EJP amplitudes of *push null* mutants were increased about 70% in both 0.4 mM and 0.6 mM [Ca^{2+}]. These results confirmed the previous studies in our lab (Richards et al., 1996) (Figure 4.3.6A). Furthermore, the Elav > Dcr, pushRNAi also recaptured the same behaviors both in EJP amplitude and mEJP frequencies as well as push null mutants (Richards et al., 1996) (Figure 4.3.6B and Figure 4.3.6C). The results suggested that the defects of *push* mutants on neurotransmitter release result from loss of Push in neuron.

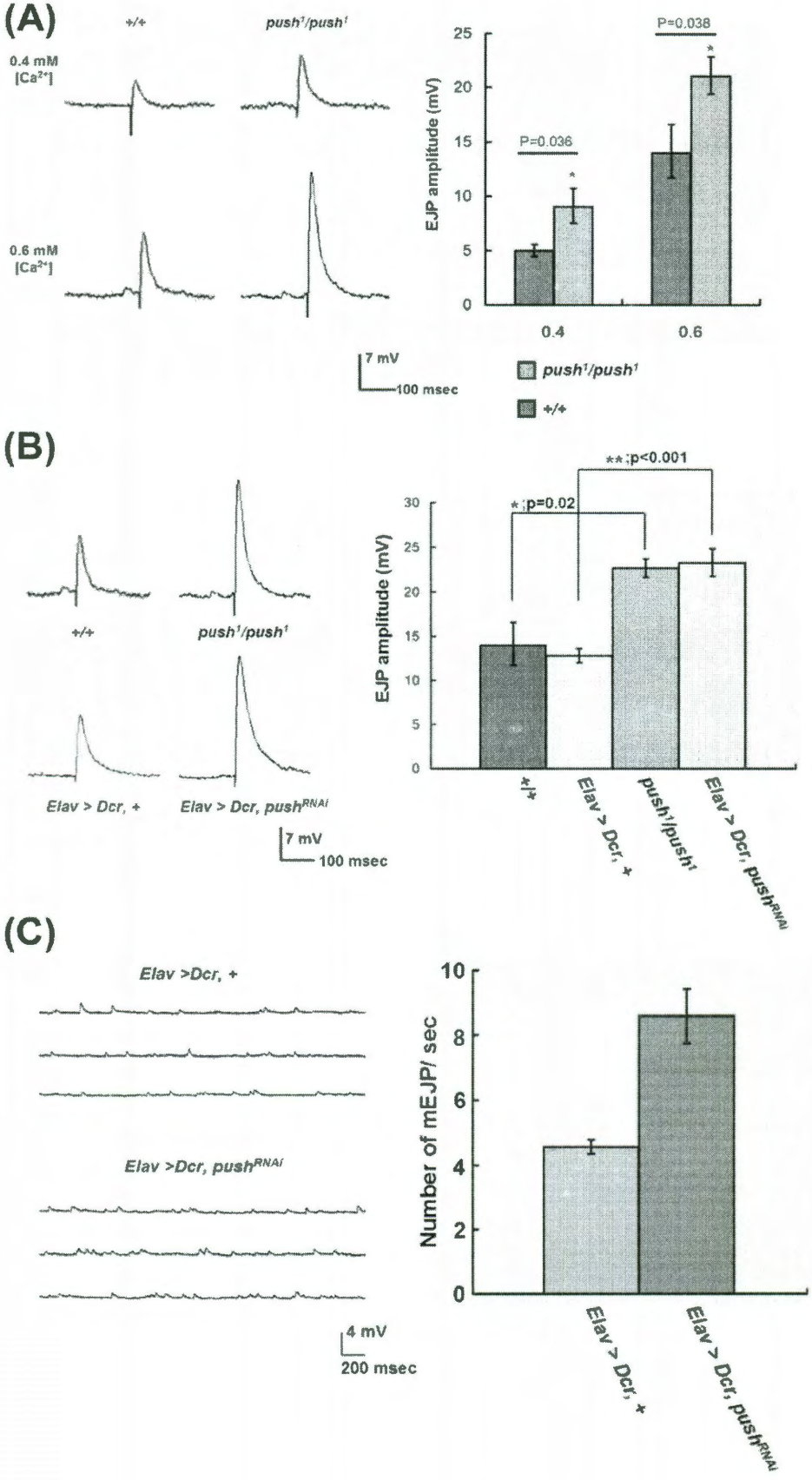
(A)
+/+
push1/push1
0.4 mM [Ca2+]
0.6 mM [Ca2+]
7 mV
100 msec
EJP amplitude (mV)
P=0.036
P=0.038
0.4
0.6
push1/push1
+/+
(B)
+/+
push1/push1
Elav > Dcr, +
Elav > Dcr, pushRNAi
7 mV
100 msec
EJP amplitude (mV)
**:p<0.001
*:p=0.02
+/+
Elav > Dcr, +
push1/push1
Elav > Dcr, pushRNAi
(C)
Elav >Dcr, +
Elav >Dcr, pushRNAi
4 mV
200 msec
Number of mEJP/ sec
Elav > Dcr, +
Elav > Dcr, pushRNAi

Figure 4.3.6: Loss of Push in neuron increase the EJP amplitude and mEJP frequency in the Drosophila NMJ. (A) Left panel: representative traces showing the increased excitatory junction potential (EJP) amplitude in *push*^{1} larvae at bath [Ca^{2+}] of 0.4 and 0.6 mM in HL3 solution. Right panel: mean EJP amplitudes +/- SEMs (Y axis) at the indicated [Ca^{2+}] (X axis), from the following genotypes: *wild type* and *push*^{1}. Larval nerves were stimulated at a frequency of 1 Hz, and 30 responses were measured and averaged from each nerve. n = 4, 4, 6, 6, respectively, for each genotype and [Ca^{2+}] (0.4 mM and 0.6 mM). One-way ANOVA and Fisher's LSD gave significant differences at bath [Ca^{2+}] as indicated on the figure. (B) Left panel: representative traces showing the increased excitatory junction potential (EJP) amplitude in *push*^{1} and *Elav > Dcr, push*^{RNAi} larvae at a bath [Ca^{2+}] of 0.6 mM in HL3 solution. Right panel: mean EJP amplitudes +/- SEMs (Y axis) at the of 0.6 mM [Ca^{2+}] (X axis), from the following genotypes: *wild type*, *Elav > Dcr, +*, *push*^{1}, and *Elav > Dcr, push*^{RNAi}. Larval nerves were stimulated at a frequency of 1 Hz, and 30 responses were measured and averaged from each nerve. n = 6, 11, 6, 6, respectively, for each genotype in 0.6 mM [Ca^{2+}]. One-way ANOVA and Fisher's LSD gave significant differences at 0.6 mM [Ca^{2+}] as indicated on the figure. (C) Left panel: representative traces showing mini EJPs in *Elav > Dcr, +* and *Elav > Dcr, push*^{RNAi}. The three traces from each genotype are from three different larvae. Right panel: Mean mEJP frequency +/- SEMs (Y axis) for the indicated genotypes (X axis): *Elav > Dcr, +* and *Elav > Dcr, push*^{RNAi}. Recordings were collected from six different larvae from each genotype in HL3 solution with a bath [Ca^{2+}] of 0.6 mM, and total number of responses within a one minute period were measured and averaged for each larva. Student T-test gave the following difference; *Elav > Dcr, +* vs. *Elav > Dcr, push*^{RNAi}, $p<0.001$. *P* values <0.05 were considered statistically significant.

To understand the molecular mechanism in which Push is involved, I tried to identify the molecules which are up-regulated or down-regulated in the absence of Push. To identify proteins, I made protein extracts from wild type and *push null* mutant heads and performed 2D-DIGE and mass spectrometry to identify these molecules (Figure 4.3.7A). One protein identified is Drosophila cuticular protein 72Ec (Cpr72Ec, CG4784) (Figure 4.3.6B, and table 4.3.1). In comparison between wild type and push null mutants, Cpr72Ec is decreased about 64% in push null mutants (Figure 4.3.7C). Previous studies have reported that the mRNA level of Cpr72Ec is regulated by the calmodulin-binding transcription activator Camta (Han et al., 2006). Camta has been implicated in the regulation of Ca^{2+} homeostasis by controlling gene transcription (Han et al., 2006) as follows: The Ca^{2+}/Calmodulin activation process is mediated by PLCβ/ IP3R mediating cytoplasmic Ca^{2+} increase from intracellular Ca^{2+} storage from the endoplasmic reticulum (ER). The increase of intracellular [Ca^{2+}] induces Ca^{2+} to bind to calmodulin and become an active Ca^{2+}/calmodulin complex. Next, Ca^{2+}/ calmodulin activates Camta and increase Camta-mediated gene transcription. The gene products of Camta will return the intracellular [Ca^{2+}] back to normal and reduce the Ca^{2+}-dependent excitotoxicity. Therefore, Camta-mediated

transcriptional regulation serves as a negative feedback to maintain Ca^{2+} homeostasis (Han et al., 2006). In Drosophila head protein extracts, Cpr72Ec showed a strong decrease in *push* mutants; this observation implies that protein expression of Camta was decreased in *push null* mutants, further suggesting that intracellular [Ca^{2+}] in *push* mutants may be lower than wild type, or the ability of intracellular [Ca^{2+}] is blocked. Therefore, Push may be required for Ca^{2+} release from ER, and that the cytoplasmic [Ca^{2+}] in the neuson is important for the regulation of proper neurotransmitter release.

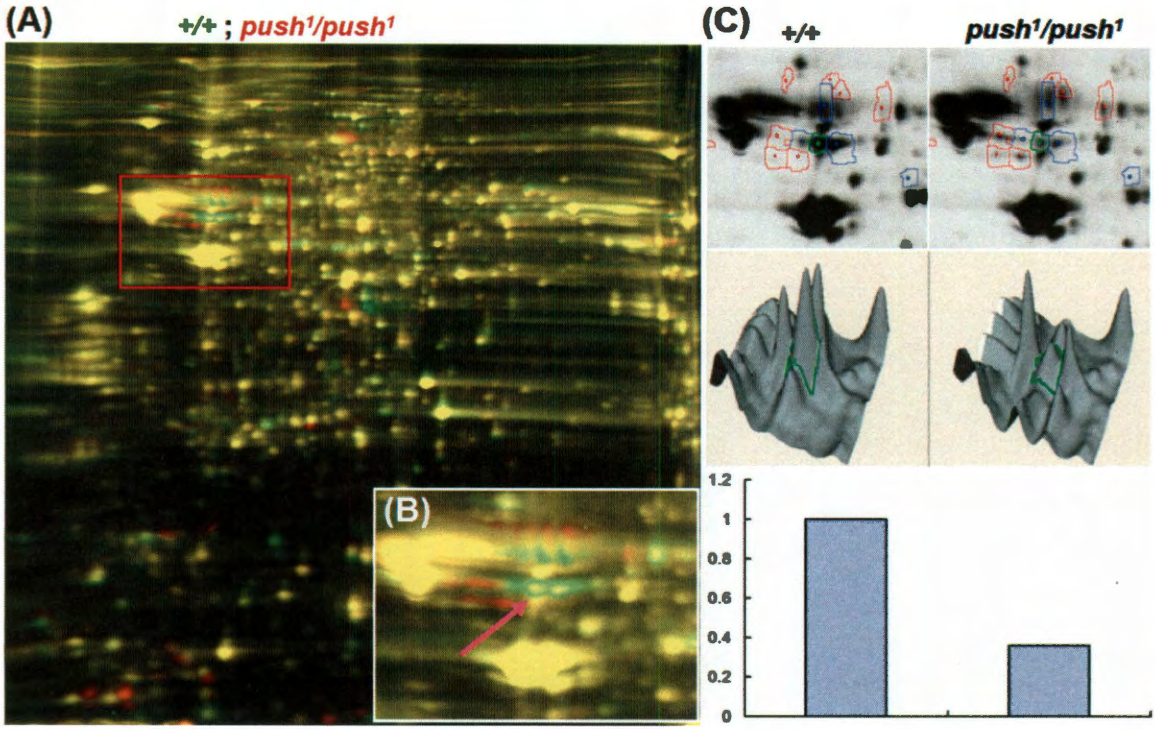

Figure 4.3.7: Drosophila cuticle protein Cpr72Ec (CG4874) is down regulated in *push[1]/push[1]*. (A) The 2D-Difference in gel electrophoresis (2D-DIGE) image of Drosophila head protein extracts of *+>+*, and *push[1]> push[1]*. (B) The close view of region of interest (red box in (A)). Purple arrow indicated Cpr72Ec. (C) The analytical results that showed the different expression of Cpr72Ec between *+>+*, and *push[1]> push[1]* in Drosophila heads.

cuticular protein 72Ec [Drosophila melanogaster]					PI	M.W.
Peptide Information					5.4	50536.3
Calc. Mass	Actual Mass	± da	± ppm	Start Seq.	End Seq.	Sequence
945.4496	945.521	0.0714	76	239	245	QNQREDR
950.553	950.5222	-0.0308	-32	118	125	LNHLNALR
950.553	950.5222	-0.0308	-32	118	125	LNHLNALR
1012.6262	1012.5949	-0.0313	-31	413	421	TLRPVALSR
1025.5851	1025.5592	-0.0259	-25	185	192	QRELNLPR
1026.4679	1026.4391	-0.0288	-28	37	44	AFYSYGYR
1057.575	1057.5415	-0.0335	-32	309	316	QELRQDLR
1092.5354	1092.5028	-0.0326	-30	175	184	AELSAMLADR
1166.6052	1166.5677	-0.0375	-32	403	412	YSVTTPTELR
1221.5422	1221.4979	-0.0443	-36	62	72	GFYSYVDADGK
1331.6914	1331.6462	-0.0452	-34	131	142	ALATSLREEADR
1347.705	1347.6572	-0.0478	-35	173	184	VRAELSAMLADR
1376.64	1376.5955	-0.0445	-32	338	349	QISSDRDGDDLR
1458.7546	1458.7042	-0.0504	-35	376	387	LLEDRLDNSDLR
1622.8788	1622.8179	-0.0609	-38	388	402	VPIGAYYTLVSPNTK
1633.8319	1633.7732	-0.0587	-36	352	366	TVYSLADLSSSSYLK
1653.8442	1653.7872	-0.057	-34	103	117	APLPVTDTEEVQQAR
1682.7557	1682.6956	-0.0601	-36	37	50	AFYSYGYRDENAAR
1682.7557	1682.6956	-0.0601	-36	37	50	AFYSYGYRDENAAR
1818.9021	1818.8391	-0.063	-35	62	77	GFYSYVDADGKLQTVR
1838.9607	1838.8951	-0.0656	-36	101	117	GKAPLPVTDTEEVQQAR
2436.2769	2436.1743	-0.1026	-42	381	402	LDNSDLRVPIGAYYTLVS

Table 4.3.1: The Mass data of Cpr72Ec identification.

Taken together, I hypothesized that push may affect neuronal transmitter release by blocking the elevation of intracellular calcium and altering the intracellular [Ca^{2+}] in the neurons. To test this hypothesis, RNAi-mediated PLCβ, IP3R, or Camta inhibition in neuron were performed to test the level of neurotransmitter release. As I expected, the EJP amplitudes were increased when the protein expression of PLCβ, IP3R, and Camta were decreased (Figure 4.3.8). However, the defects of knocking down the expression of PLCβ, IP3R, and Camta are not as extreme as knocking down the expression of Push (Figure

4.3.8). These results indicated that push may affect neurotransmitter release through other regulatory mechanism, such as the PI3K and MAPK pathway. Therefore, characterization of other Push-mediated signaling pathways that affect neurotransmitter release will be the next objective.

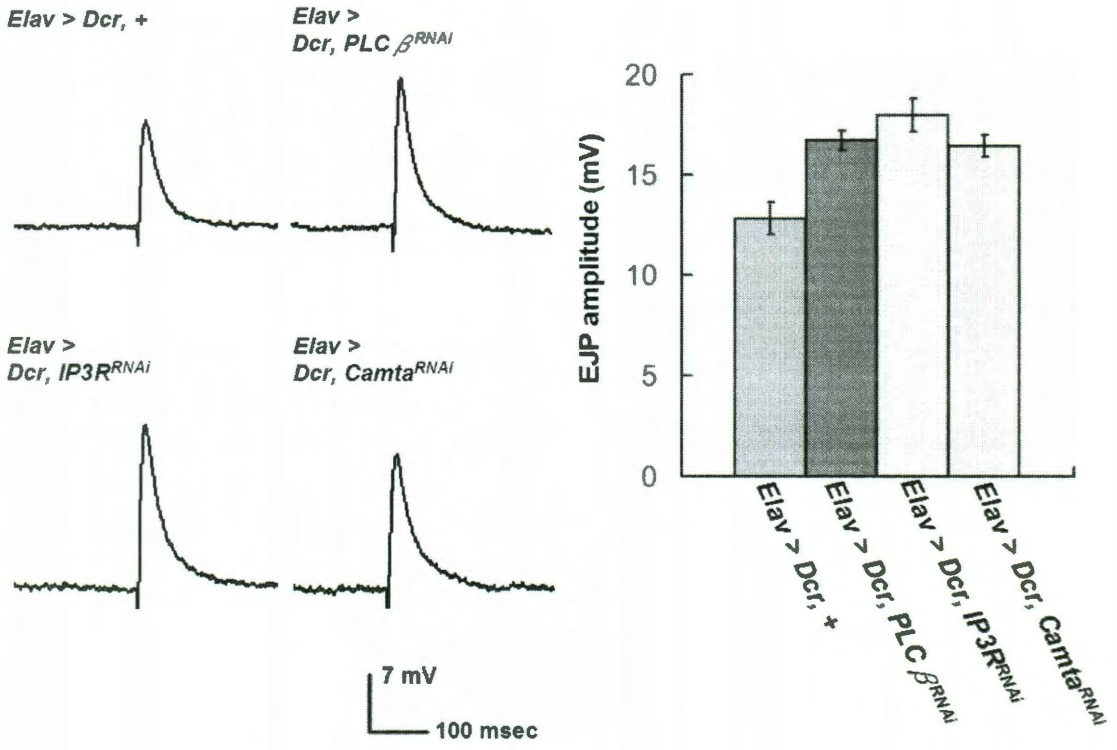

Figure 4.3.8: Knocking down the expression of PLCβ, IP3R, and Camta increased neurotransmitter release in NMJ. Left panel: representative traces showing the increased excitatory junction potential (EJP) amplitude in *Elav > Dcr, PLCβ^{RNAi}*, *Elav > Dcr, IP3R^{RNAi}*, and *Elav > Dcr, Camta^{RNAi}* larvae at a bath [Ca^{2+}] of 0.6 mM in HL3 solution. Right panel: mean EJP amplitudes +/- SEMs (Y axis) at the bath of 0.6 mM [Ca^{2+}] (X axis), from the following genotypes: *Elav > Dcr, +*, *Elav > Dcr, PLCβ^{RNAi}*, *Elav > Dcr, IP3R^{RNAi}*, and *Elav > Dcr, Camta^{RNAi}*. Larval nerves were stimulated at a frequency of 1 Hz, and 30 responses were measured and averaged from each nerve. n = 11, 5, 6, 6, respectively, for each genotype in 0.6 mM [Ca^{2+}]. One-way ANOVA and Fisher's LSD gave the following differences at 0.6 mM [Ca^{2+}], respectively: for *Elav > Dcr, +* vs. *Elav > Dcr, PLCβ^{RNAi}*, p=0.012; vs. *Elav > Dcr, IP3R^{RNAi}*, p=0.003; *Elav > Dcr, Camta^{RNAi}*, p=0.011. *P* values <0.05 were considered statistically significant.

4.3.4 Push-mediated regulation of retrograde signaling may be Ca^{2+}-dependent

push null mutants exhibit strong phenotypes including inability to fly and an increase of neurotransmitter release at the larvae NMJ at low bath [Ca^{2+}] (Richards et al., 1996). In section 4.3.3, I previously examined if the defect of neurotransmitter release was due to the loss of push-mediated intracellular [Ca^{2+}] elevation. However, neuronal knockdowns of Push, PLCβ, IP3R, and Camta did not result in a lack of flight. Therefore, I suggest that the loss of flight ability may not be caused solely by neurological defects but that loss of Push in glia and muscle might also contribute. As described above, I found that push is highly expressed in the Drosophila muscle and the expression pattern of Push in muscle is similar to that of actin filaments (Figure 4.3.4C). From these two observations, I hypothesize that the Drosophila flightless phenotype in *push* mutants may be a muscular defect. To test this hypothesis, we used the muscle driver *Mef2* to express *Dcr* and $push^{RNAi}$ to test whether *Mef2 > Dcr,* $push^{RNAi}$ was able to knock down the protein expression of push in muscle. As shown on Figure 4.3.9, *Mef2 > Dcr,* $push^{RNAi}$ was efficient in knocking down Push expression in muscle (Figure 4.3.9).

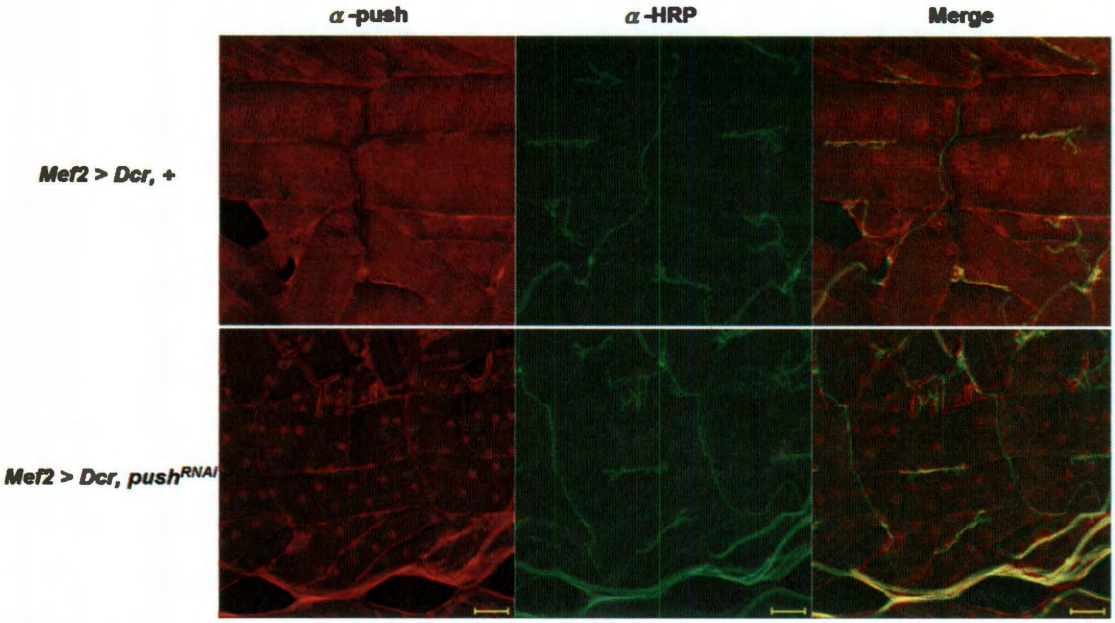

Figure 4.3.9: *Mef2 > Dcr, push*^{RNAi} can effectively knock down the expression of Push in Drosophila muscle. Representative confocal images of third instar larval muscle of *Mef2 > Dcr, +*, and *Mef2 > Dcr, push*^{RNAi} stained with anti-Push (left panels), anti-HRP (middle panels), and merged images (right panels). Scale bar is 20 μm.

Next, we found *Mef2 > Dcr, push*^{RNAi} adult flies exhibited the flightless phenotype (Table 4.3.2). These results illustrated that the flightless phenotype of *push null* mutants is due to muscular defects. Therefore, I would like to examine further the possible mechanism for the flightless phenotype.

Genotype	Flight Ability
Mef2 > Dcr, +	+
Mef2 > Dcr, push^{RNAi}	-
Mef2 > Dcr, PLC β^{RNAi}	-
Mef2 > Dcr, IP3R^{RNAi}	-
Mef2 > Dcr, Camta^{RNAi}	-
Mef2 > Dcr, mGluR^{RNAi}	+

Table 4.3.2: The flight ability in the adult flies of *Mef2 > Dcr, +*, *Mef2 > Dcr, push*^{RNAi} , *Mef2 > Dcr, PLCβ*^{RNAi}, *Mef2 > Dcr, IP3R*^{RNAi}, *Mef2 > Dcr, Camta*^{RNAi}, and *Mef2 > Dcr, mGluR*^{RNAi}. Flight ability is determined by following criteria. If flies can not escape from a plane surface within 90 sec and flies land within a circle of 15 cm radius after being dropped from a height of 1 meter, it was scored as flight defective (Richards et al., 1996). + indicated normal flight ability and - indicated flightless.

When a neuron stimulates a target muscle, this stimulus induces calcium release from the muscular Ca^{2+} storage known as the Sarcoplasmic reticulum (SR). The increase of cytoplasmic [Ca^{2+}] in muscle subsequently triggers the interaction of the myosin filaments and actin filaments to promote muscle contraction (Herranz et al., 2005). In addition, in section 4.3.3, I examined if Push is required in the regulation of Ca^{2+} release in neurons. In summary, I hypothesize that Push is similarly required in the regulation of Ca^{2+} release from the muscle SR and the alteration of the molecules that are affected by the cytoplasmic [Ca^{2+}] in muscle including PLCβ, IP3R, and Camta. These same molecules may also

regulate Drosophila flight ability. To test the possibility, I used the same muscle driver, *Mef2-gal4*, and overexpressed Dcr with *DmGluRA*^{RNAi}, *PLCβ*^{RNAi}, *IP3R*^{RNAi}, or *Camta*^{RNAi}. I found that *Mef2 > Dcr, PLCβ*^{RNAi}, *Mef2 > Dcr, IP3R*^{RNAi}, and *Mef2 > Dcr, Camta*^{RNAi} adults were all flightless (Table 4.3.2). However, *Mef2 > Dcr, DmGluRA*^{RNAi} did not show the defect in flight. These results suggested that PLCβ, IP3R, and Camta are required for assisting the Ca^{2+} release from the SR required for the muscle contraction and flight, but DmGluRA is not necessary for muscle contraction.

Push, PLCβ, IP3R, and Camta have been showed above that they are required for assisting the SR to release Ca^{2+} in muscle and this alteration of cytoplasmic [Ca^{2+}] in muscle can also affect the presynaptic neurotransmitter release through a retrograde signaling pathway (Carrillo et al., 2010; Kazama et al., 2007). Therefore, I suggested that knocking down protein expression of Push, PLCβ, IP3R, and Camta would decrease the Ca^{2+}–dependent retrograde signaling and neurotransmitter release at the Drosophila NMJ. To test this prediction, I performed electrophysiological analysis and measured the EJP amplitudes in *Mef2 > Dcr, push*^{RNAi}, *Mef2 > Dcr, PLCβ*^{RNAi}, *Mef2 > Dcr, IP3R*^{RNAi}, and *Mef2 > Dcr, Camta*^{RNAi} larval NMJs. As shown in figure 4.3.9, *Mef2 > Dcr,*

push^{RNAi} severely reduced neurotransmitter release by about 70% compared to wild type (Figure 4.3.10). This result implied that Push strongly regulates retrograde signaling in the NMJ. I also found that the EJP amplitude in *Mef2 > Dcr, PLCβ*^{RNAi}, *Mef2 > Dcr, IP3R*^{RNAi}, and *Mef2 > Dcr, Camta*^{RNAi} larva NMJ are decreased about 30%. However, the effects of knocking down protein expression of PLCβ, IP3R, and Camta are not as severe as knocking down protein expression of Push. Therefore, these results suggested that push may partially control retrograde signaling, muscle contraction, and flight through the PLCβ /IP3R-mediated Ca^{2+} signaling pathway but remain further characterized. Furthermore, EJP amplitude in *Mef2 > Dcr, DmGluRA*^{RNAi} larvae remains the same as wild type for the supporting the hypothesis that DmGluRA does not participate in retrograde signaling (Figure 4.3.10). For the supporting the hypothesis that DmGluRA does not participate in retrograde signaling.

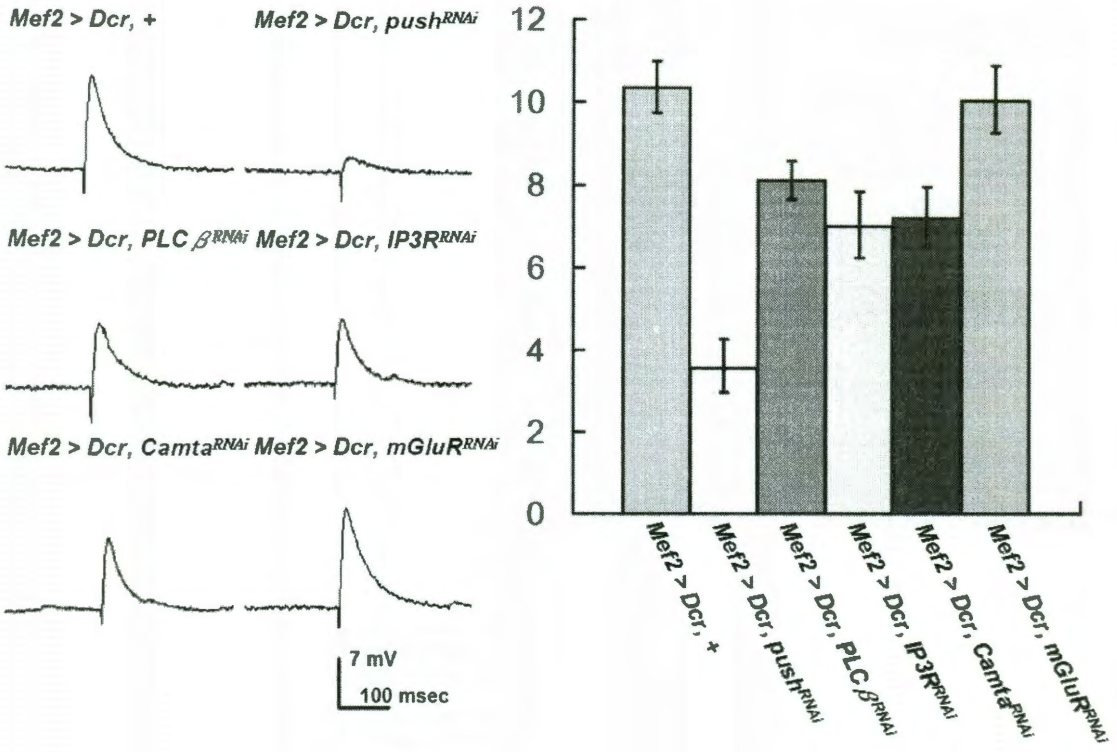

Figure 4.3.10: Knocking down the expression of Push, PLCβ, IP3R, and Camta in Drosophila muscle decreased neurotransmitter release. Left panel: representative traces showing the decreased excitatory junction potential (EJP) amplitude in *Mef2 > Dcr, push^{RNAi}*, *Mef2 > Dcr, PLCβ^{RNAi}*, *Mef2 > Dcr, IP3R^{RNAi}*, and *Mef2 > Dcr, Camta^{RNAi}* larvae at a bath [Ca^{2+}] of 0.6 mM in HL3 solution. Right panel: mean EJP amplitudes +/- SEMs (Y axis) at the bath of 0.6 mM [Ca^{2+}] (X axis), from the following genotypes: *Mef2 > Dcr, +*, *Mef2 > Dcr, PLCβ^{RNAi}*, *Mef2 > Dcr, PLCβ^{RNAi}*, *Mef2 > Dcr, IP3R^{RNAi}*, and *Mef2 > Dcr, Camta^{RNAi}*. Larval nerves were stimulated at a frequency of 1 Hz, and 30 responses were measured and averaged from each nerve. n = 12, 8, 7, 5, 7, 6, respectively, for each genotype in 0.6 mM [Ca^{2+}]. One-way ANOVA and Fisher's LSD gave the following differences at 0.6 mM [Ca^{2+}], respectively: for *Mef2 > Dcr, +* vs. *Mef2 > Dcr, push^{RNAi}*, $p<0.001$; vs. *Mef2 > Dcr, PLCβ^{RNAi}*, $p=0.015$; vs. *Mef2 > Dcr, IP3R^{RNAi}*, $p=0.004$; vs. *Elav > Dcr, Camta^{RNAi}*, $p=0.004$; vs. *Elav > Dcr, mGluR^{RNAi}*, $p=0.77$. *P* values <0.05 were considered statistically significant.

Because *Mef2 > Dcr, push*^{RNAi} exhibited severe decreases in retrograde signaling and neurotransmitter release compared to the of PLCβ, IP3R, and Camta knockdown (Figure 4.3.10), Push may regulate retrograde signaling through PLCβ/IP3R-independent pathway. Therefore, I tested if Push regulated retrograde signaling through the bone morphogenetic protein (BMP) signaling pathway. As mentioned in Section 1.9, the BMP signaling pathway is the most well-established system for regulating retrograde signaling in Drosophila NMJ. If Push regulates retrograde signaling through the BMP signaling pathway in addition to Ca^{2+} pathway, level of phosphorylated Smad in motor neuron will be altered. As shown on Figure 4.3.11, the basal phospho-Smad (p-Smad) level in *Mef2 > Dcr, +* and *Mef2 > Dcr, push*^{RNAi} exhibited no significant differences. These results suggested that Push does not regulate retrograde signaling through the BMP signaling pathway. Therefore, the retrograde signaling pathways affected by Push remain unidentified.

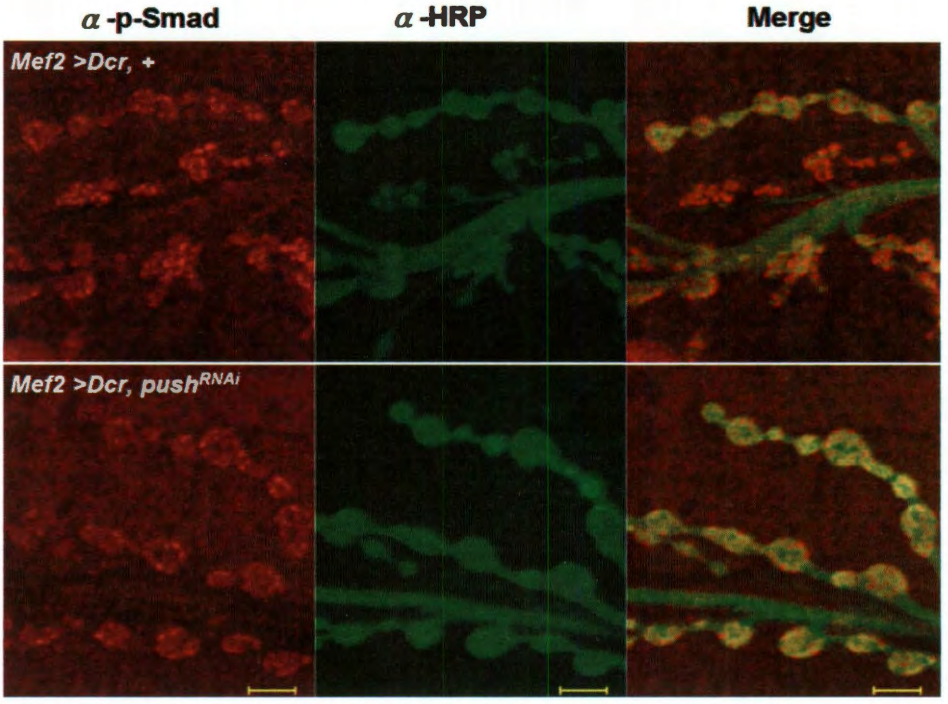

Figure 4.3.11: *Mef2 > Dcr, push*^{RNAi} did not affect p-Smad level in Drosophila nerve terminal. Representative confocal images of of third instar larval muscle of *Mef2 > Dcr, +* and *Mef2 > Dcr, push*^{RNAi} stained with anti-p-Smad (left panels), anti-HRP (middle panels), and merged images (right panels). Scale bar is 5 μm.

4.4 Summary

In both Drosophila and mammalian system, push has been implicated in the regulation of neurotransmitter release (Richards et al., 1996), chromatin scaffolding, spermatogenesis (Richards et al., 1996), and perineurial glia growth (Yager et al., 2001). However, mechanisms by which Push affects these processes have not been elucidated. Here I reported several novel observations.

First, I found that push is highly expressed in neurons, muscle, and glia cells. Second, I find that push acts both in neuron and muscle to regulate neurotransmitter release. Third, the flightless phenotype of *push* mutants can be phenocopied by RNAi knockdown of PLC β /IP3R-mediated Ca^{2+} signaling molecules. Fourth, from immunostaining of Drosophila S2 cells and muscles, I found that push is localized similar to microtubules and actin filaments. Finally, the mammalian ortholog of push, P600, has been regulated to be an ER-associated and 26S proteasome-associated protein (Besche et al., 2009; Shim et al., 2008). Taken together, these results suggest that push may function as a platform that connects the cytoskeleton (microtubules and actin filaments), Ca^{2+} storage (ER and SR), and the proteasome in the nervous and muscular system (Figure 4.4.1). This biological setting of Push may provide several advantages: 1) ERs or SRs can be located close to the regions that utilize changes in [Ca^{2+}] as signals; 2) Ca^{2+} can diffuse to target faster and be utilized more efficiently; 3) push may also act as a Ca^{2+} sensor because of the Ca^{2+}/CaM binding property of Push and negative regulator to control the intracellular Ca^{2+} homeostasis; 4) abnormal Ca^{2+} concentration can be rectified faster by UPS-mediated protein degradation and no transcriptional and translational machinery is needed. These results provide novel

insights into the observation by which push may control the intracellular [Ca^{2+}] release in Drosophila motor neurons and muscle. Here, I propose a possible working mechanism of Drosophila Push (Figure 4.4.1). Under normal conditions, Push and its UPS machinery negatively regulate the unknown protein which inhibits Ca^{2+} release. When PLCβ/IP3R-mediated Ca^{2+} signaling pathway induces Ca^{2+} release and increases intracellular [Ca^{2+}], the active Ca^{2+}/CaM binds to Push directly and inhibits the Push-mediated UPS machinery. This inhibition prevents the degradation of the unknown protein and allows this protein to inhibit Ca^{2+} release from Ca^{2+} storage. Then, the cell can adjust intracellular [Ca^{2+}] back to normal by pumping Ca^{2+} back to Ca^{2+} storage (Figure 4.4.1). In addition, in Camta knockdown mutants, the Camta-mediated negative feedback control of [Ca^{2+}] is damaged and results in the elevation of intracellular [Ca^{2+}]. The elevation of intracellular [Ca^{2+}] inhibits of Push activity and prevents of the degradation of unknown protetin. Therefore, the unknown protein may block the elevation of [Ca^{2+}] and result lower intracellular [Ca^{2+}]. In conclusion, the Push-mediated UPS machinery may play as negative feedback in the regulation of intracellular [Ca^{2+}] in neuron and muscle.

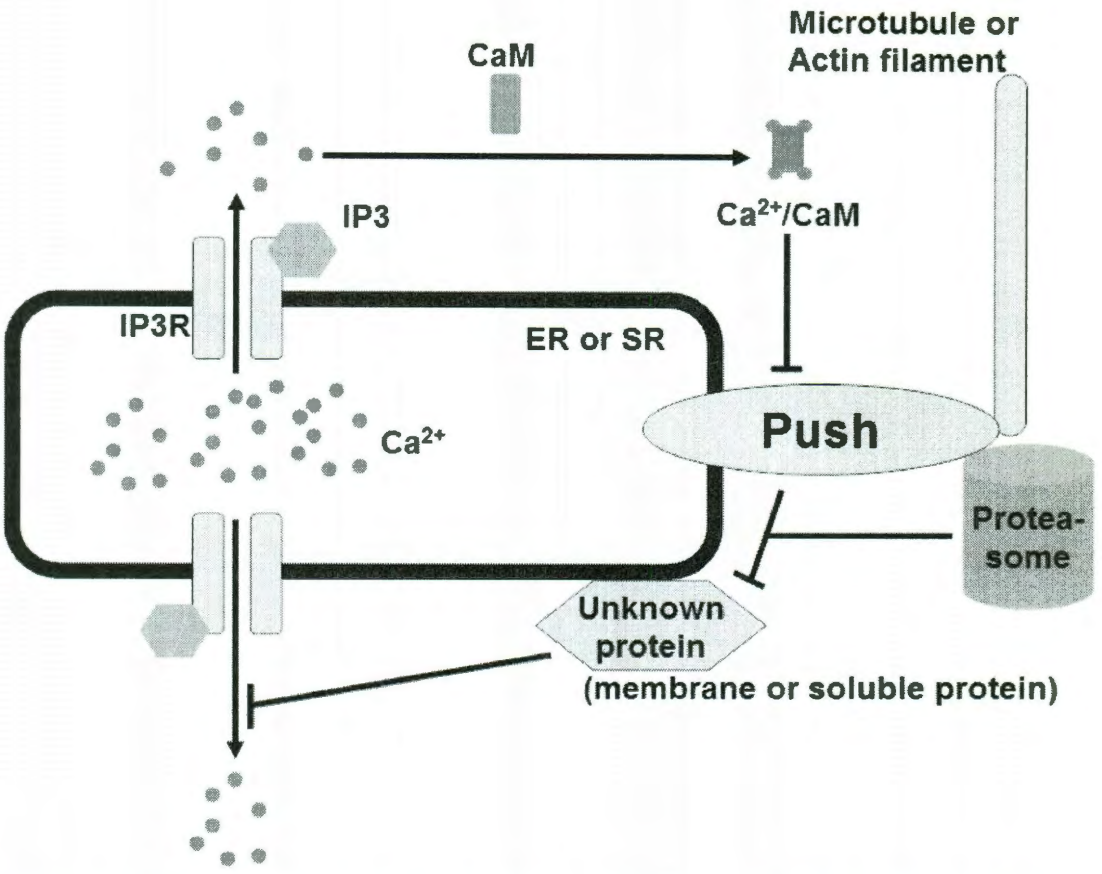

Figure 4.4.1: The role of Push in the regulation of intracellular [Ca^{2+}]. When intracellular [Ca^{2+}] is increased, the active Ca^{2+}/CaM will bind to Push directly and inhibit Push-mediated UPS machinery to prevent the degradation of unknown protein. This inhibition allows unknown protein to inhibit more Ca^{2+} release form Ca^{2+} storage. Then, the cell can adjust intracellular [Ca^{2+}] back to normal and maintain Ca^{2+} homeostasis.

4.5 Future Work

4.5.1 Identify any Push-related protein degradation substrates

E3-ubiquitin ligases, collaborating with E1-ubiquitin activating and E2-ubquitin conjugating enzymes, can label specific proteins with a ubiquitin degradation signal and further degrade those proteins via the proteasome-mediated degradation pathway (Glickman and Ciechanover, 2002; Hershko and Ciechanover, 1998). Push has been predicted to be an E3-ubiquitin ligase (Yager et al., 2001), but Push-mediated protein degradation still remains unknown. To understand this degradation mechanism, the E1-ubiquitin activating, E2-ubquitin conjugating, and target proteins need to be identified. Therefore, I will perform Tandem affinity purification (TAP) (details are described in Chapter 6) and mass spectrometry to identify Push substrates. To carry out the TAP experiment on Push, generating a transgenic fly which possesses a *TAP-tagged push* is required (details are described in Chapter 6).

Chapter 5: References

Aberle, H., Haghighi, A. P., Fetter, R. D., McCabe, B. D., Magalhaes, T. R., and Goodman, C. S. (2002). wishful thinking encodes a BMP type II receptor that regulates synaptic growth in Drosophila. Neuron 33, 545-558.

Altier, C., Garcia-Caballero, A., Simms, B., You, H., Chen, L., Walcher, J., Tedford, H. W., Hermosilla, T., and Zamponi, G. W. (2010). The Cavbeta subunit prevents RFP2-mediated ubiquitination and proteasomal degradation of L-type channels. Nat Neurosci 14, 173-180.

Avraham, H., Park, S. Y., Schinkmann, K., and Avraham, S. (2000). RAFTK/Pyk2-mediated cellular signalling. Cell Signal 12, 123-133.

Bear, M. F., Huber, K. M., and Warren, S. T. (2004). The mGluR theory of fragile X mental retardation. Trends Neurosci 27, 370-377.

Bear, M. F., and Malenka, R. C. (1994). Synaptic plasticity: LTP and LTD. Curr Opin Neurobiol 4, 389-399.

Berridge, M. J. (1993). Inositol trisphosphate and calcium signalling. Nature 361, 315-325.

Berridge, M. J., Lipp, P., and Bootman, M. D. (2000). The versatility and universality of calcium signalling. Nat Rev Mol Cell Biol 1, 11-21.

Besche, H. C., Haas, W., Gygi, S. P., and Goldberg, A. L. (2009). Isolation of mammalian 26S proteasomes and p97/VCP complexes using the ubiquitin-like domain from HHR23B reveals novel proteasome-associated proteins. Biochemistry 48, 2538-2549.

Beumer, K., Matthies, H. J., Bradshaw, A., and Broadie, K. (2002). Integrins regulate DLG/FAS2 via a CaM kinase II-dependent pathway to mediate synapse elaboration and stabilization during postembryonic development. Development 129, 3381-3391.

Bogdanik, L., Mohrmann, R., Ramaekers, A., Bockaert, J., Grau, Y., Broadie, K., and Parmentier, M. L. (2004). The Drosophila metabotropic glutamate receptor DmGluRA regulates activity-dependent synaptic facilitation and fine synaptic morphology. J Neurosci 24, 9105-9116.

Brand, A. H., and Perrimon, N. (1993). Targeted gene expression as a means of altering cell fates and generating dominant phenotypes. Development 118, 401-415.

Budnik, V., Zhong, Y., and Wu, C. F. (1990). Morphological plasticity of motor axons in Drosophila mutants with altered excitability. J Neurosci 10, 3754-3768.

Burgering, B. M., and Medema, R. H. (2003). Decisions on life and death: FOXO Forkhead transcription factors are in command when PKB/Akt is off duty. J Leukoc Biol 73, 689-701.

Butler, M. G., Dasouki, M. J., Zhou, X. P., Talebizadeh, Z., Brown, M., Takahashi, T. N., Miles, J. H., Wang, C. H., Stratton, R., Pilarski, R., and Eng, C. (2005). Subset of individuals with autism spectrum disorders and extreme macrocephaly associated with germline PTEN tumour suppressor gene mutations. J Med Genet 42, 318-321.

Cardnell, R. J., Nogare, D. E., Ganetzky, B., and Stern, M. (2006). In vivo analysis of a gain-of-function mutation in the Drosophila eag-encoded K+ channel. Genetics 172, 2351-2358.

Carrillo, R. A., Olsen, D. P., Yoon, K. S., and Keshishian, H. (2010). Presynaptic activity and CaMKII modulate retrograde semaphorin signaling and synaptic refinement. Neuron 68, 32-44.

Chang, I. F. (2006). Mass spectrometry-based proteomic analysis of the epitope-tag affinity purified protein complexes in eukaryotes. Proteomics 6, 6158-6166.

Chen, H. C., Appeddu, P. A., Isoda, H., and Guan, J. L. (1996). Phosphorylation of tyrosine 397 in focal adhesion kinase is required for binding phosphatidylinositol 3-kinase. J Biol Chem 271, 26329-26334.

Chen, H. C., Appeddu, P. A., Parsons, J. T., Hildebrand, J. D., Schaller, M. D., and Guan, J. L. (1995). Interaction of focal adhesion kinase with cytoskeletal protein talin. J Biol Chem 270, 16995-16999.

Chen, H. C., and Guan, J. L. (1994). Association of focal adhesion kinase with its potential substrate phosphatidylinositol 3-kinase. Proc Natl Acad Sci U S A 91, 10148-10152.

Chin, D., and Means, A. R. (2000). Calmodulin: a prototypical calcium sensor. Trends Cell Biol 10, 322-328.

Colombani, J., Bianchini, L., Layalle, S., Pondeville, E., Dauphin-Villemant, C., Antoniewski, C., Carre, C., Noselli, S., and Leopold, P. (2005). Antagonistic actions of ecdysone and insulins determine final size in Drosophila. Science 310, 667-670.

Curran, S. P., Wu, X., Riedel, C. G., and Ruvkun, G. (2009). A soma-to-germline transformation in long-lived Caenorhabditis elegans mutants. Nature 459, 1079-1084.

Cusco, I., Medrano, A., Gener, B., Vilardell, M., Gallastegui, F., Villa, O., Gonzalez, E., Rodriguez-Santiago, B., Vilella, E., Del Campo, M., and Perez-Jurado, L. A. (2009). Autism-specific copy number variants further implicate the phosphatidylinositol signaling pathway and the glutamatergic synapse in the etiology of the disorder. Hum Mol Genet 18, 1795-1804.

Dasgupta, B., Yi, Y., Chen, D. Y., Weber, J. D., and Gutmann, D. H. (2005). Proteomic analysis reveals hyperactivation of the mammalian target of rapamycin pathway in neurofibromatosis 1-associated human and mouse brain tumors. Cancer Res 65, 2755-2760.

Davis, G. W. (2006a). Homeostatic Control of Neural Activity: From Phenomenology to Molecular Design. Annu Rev Neurosci.

Davis, G. W. (2006b). Homeostatic control of neural activity: from phenomenology to molecular design. Annu Rev Neurosci 29, 307-323.

Davis, G. W., and Bezprozvanny, I. (2001). Maintaining the stability of neural function: a homeostatic hypothesis. Annu Rev Physiol 63, 847-869.

Davis, G. W., and Goodman, C. S. (1998). Synapse-specific control of synaptic efficacy at the terminals of a single neuron. Nature 392, 82-86.

Della Rocca, G. J., van Biesen, T., Daaka, Y., Luttrell, D. K., Luttrell, L. M., and Lefkowitz, R. J. (1997). Ras-dependent mitogen-activated protein kinase activation by G protein-coupled receptors. Convergence of Gi- and Gq-mediated pathways on calcium/calmodulin, Pyk2, and Src kinase. J Biol Chem 272, 19125-19132.

Demontis, F., and Perrimon, N. FOXO/4E-BP signaling in Drosophila muscles

regulates organism-wide proteostasis during aging. Cell 143, 813-825.

Demontis, F., and Perrimon, N. (2010). FOXO/4E-BP signaling in Drosophila muscles regulates organism-wide proteostasis during aging. Cell 143, 813-825.

Desai, N. S., Rutherford, L. C., and Turrigiano, G. G. (1999). Plasticity in the intrinsic excitability of cortical pyramidal neurons. Nat Neurosci 2, 515-520.

DiAntonio, A., Haghighi, A. P., Portman, S. L., Lee, J. D., Amaranto, A. M., and Goodman, C. S. (2001). Ubiquitination-dependent mechanisms regulate synaptic growth and function. Nature 412, 449-452.

Dikic, I., Tokiwa, G., Lev, S., Courtneidge, S. A., and Schlessinger, J. (1996). A role for Pyk2 and Src in linking G-protein-coupled receptors with MAP kinase activation. Nature 383, 547-550.

Dionne, M. S., Pham, L. N., Shirasu-Hiza, M., and Schneider, D. S. (2006). Akt and FOXO dysregulation contribute to infection-induced wasting in Drosophila. Curr Biol 16, 1977-1985.

Engelman, J. A., Luo, J., and Cantley, L. C. (2006). The evolution of phosphatidylinositol 3-kinases as regulators of growth and metabolism. Nat Rev Genet 7, 606-619.

Enz, R. (2007). The trick of the tail: protein-protein interactions of metabotropic glutamate receptors. Bioessays 29, 60-73.

Erondu, N. E., and Kennedy, M. B. (1985). Regional distribution of type II Ca2+/calmodulin-dependent protein kinase in rat brain. J Neurosci 5, 3270-3277.

Fan, R. S., Jacamo, R. O., Jiang, X., Sinnett-Smith, J., and Rozengurt, E. (2005). G protein-coupled receptor activation rapidly stimulates focal adhesion kinase phosphorylation at Ser-843. Mediation by Ca2+, calmodulin, and Ca2+/calmodulin-dependent kinase II. J Biol Chem 280, 24212-24220.

Fong, Y. L., Taylor, W. L., Means, A. R., and Soderling, T. R. (1989). Studies of the regulatory mechanism of Ca2+/calmodulin-dependent protein kinase II. Mutation of threonine 286 to alanine and aspartate. J Biol Chem 264, 16759-16763.

Fu, A. K., Hung, K. W., Fu, W. Y., Shen, C., Chen, Y., Xia, J., Lai, K. O., and Ip, N. Y. (2010). APC(Cdh1) mediates EphA4-dependent downregulation of AMPA receptors in homeostatic plasticity. Nat Neurosci 14, 181-189.

Ganetzky, B., and Wu, C. F. (1982). Drosophila mutants with opposing effects on nerve excitability: genetic and spatial interactions in repetitive firing. J Neurophysiol 47, 501-514.

Ganong, W.F. (2005). The general & cellular basis of medical physiology. Review of Medical Physiology, Chapter 1, 6-8.

Gao, X., Zhang, Y., Arrazola, P., Hino, O., Kobayashi, T., Yeung, R. S., Ru, B., and Pan, D. (2002). Tsc tumour suppressor proteins antagonize amino-acid-TOR signalling. Nat Cell Biol 4, 699-704.

Gericke, A., Munson, M., and Ross, A. H. (2006). Regulation of the PTEN phosphatase. Gene 374, 1-9.

Gingras, A. C., Aebersold, R., and Raught, B. (2005). Advances in protein complex analysis using mass spectrometry. J Physiol 563, 11-21.

Giniger, E., Varnum, S. M., and Ptashne, M. (1985). Specific DNA binding of GAL4, a positive regulatory protein of yeast. Cell 40, 767-774.

Glickman, M. H., and Ciechanover, A. (2002). The ubiquitin-proteasome proteolytic pathway: destruction for the sake of construction. Physiol Rev 82, 373-428.

Grabbe, C., Zervas, C. G., Hunter, T., Brown, N. H., and Palmer, R. H. (2004). Focal adhesion kinase is not required for integrin function or viability in Drosophila. Development 131, 5795-5805.

Griffith, L. C. (2004). Regulation of calcium/calmodulin-dependent protein kinase II activation by intramolecular and intermolecular interactions. J Neurosci 24, 8394-8398.

Griffith, L. C., Wang, J., Zhong, Y., Wu, C. F., and Greenspan, R. J. (1994). Calcium/calmodulin-dependent protein kinase II and potassium channel subunit eag similarly affect plasticity in Drosophila. Proc Natl Acad Sci U S A 91, 10044-10048.

Guinebault, C., Payrastre, B., Racaud-Sultan, C., Mazarguil, H., Breton, M., Mauco, G., Plantavid, M., and Chap, H. (1995). Integrin-dependent translocation of phosphoinositide 3-kinase to the cytoskeleton of thrombin-activated platelets involves specific interactions of p85 alpha with actin filaments and focal adhesion kinase. J Cell Biol 129, 831-842.

Han, J., Gong, P., Reddig, K., Mitra, M., Guo, P., and Li, H. S. (2006). The fly CAMTA transcription factor potentiates deactivation of rhodopsin, a G protein-coupled light receptor. Cell 127, 847-858.

Hanks, S. K., Ryzhova, L., Shin, N. Y., and Brabek, J. (2003). Focal adhesion kinase signaling activities and their implications in the control of cell

survival and motility. Front Biosci 8, d982-996.

Heidinger, V., Manzerra, P., Wang, X. Q., Strasser, U., Yu, S. P., Choi, D. W., and Behrens, M. M. (2002). Metabotropic glutamate receptor 1-induced upregulation of NMDA receptor current: mediation through the Pyk2/Src-family kinase pathway in cortical neurons. J Neurosci 22, 5452-5461.

Herranz, R., Mateos, J., Mas, J. A., Garcia-Zaragoza, E., Cervera, M., and Marco, R. (2005). The coevolution of insect muscle TpnT and TpnI gene isoforms. Mol Biol Evol 22, 2231-2242.

Hershko, A., and Ciechanover, A. (1998). The ubiquitin system. Annu Rev Biochem 67, 425-479.

Hildebrand, J. D., Schaller, M. D., and Parsons, J. T. (1993). Identification of sequences required for the efficient localization of the focal adhesion kinase, pp125FAK, to cellular focal adhesions. J Cell Biol 123, 993-1005.

Hou, L., and Klann, E. (2004). Activation of the phosphoinositide 3-kinase-Akt-mammalian target of rapamycin signaling pathway is required for metabotropic glutamate receptor-dependent long-term depression. J Neurosci 24, 6352-6361.

Howlett, E., Lin, C. C., Lavery, W., and Stern, M. (2008). A PI3-kinase-mediated negative feedback regulates neuronal excitability. PLoS Genet 4, e1000277.

Hsu, A. L., Murphy, C. T., and Kenyon, C. (2003). Regulation of aging and age-related disease by DAF-16 and heat-shock factor. Science 300, 1142-1145.

Huang, Y., and Stern, M. (2002). In vivo properties of the Drosophila inebriated-encoded neurotransmitter transporter. J Neurosci 22, 1698-1708.

Huber, K. M., Gallagher, S. M., Warren, S. T., and Bear, M. F. (2002). Altered synaptic plasticity in a mouse model of fragile X mental retardation. Proc Natl Acad Sci U S A 99, 7746-7750.

Hudmon, A., and Schulman, H. (2002). Neuronal CA2+/calmodulin-dependent protein kinase II: the role of structure and autoregulation in cellular function. Annu Rev Biochem 71, 473-510.

Inoki, K., Li, Y., Zhu, T., Wu, J., and Guan, K. L. (2002). TSC2 is phosphorylated and inhibited by Akt and suppresses mTOR signalling. Nat Cell Biol 4, 648-657.

Ito, M. (2001). Cerebellar long-term depression: characterization, signal transduction, and functional roles. Physiol Rev 81, 1143-1195.

Jan, L. Y., and Jan, Y. N. (1976). Properties of the larval neuromuscular junction in Drosophila melanogaster. J Physiol 262, 189-214.

Jan, Y. N., and Jan, L. Y. (1978). Genetic dissection of short-term and long-term facilitation at the Drosophila neuromuscular junction. Proc Natl Acad Sci U S A 75, 515-519.

Jin, P., Griffith, L. C., and Murphey, R. K. (1998). Presynaptic calcium/calmodulin-dependent protein kinase II regulates habituation of a simple reflex in adult Drosophila. J Neurosci 18, 8955-8964.

Joiner MI, A., and Griffith, L. C. (1997). CaM kinase II and visual input modulate memory formation in the neuronal circuit controlling courtship

conditioning. J Neurosci 17, 9384-9391.

Kantamneni, S., Wilkinson, K. A., and Henley, J. M. (2011). Ubiquitin regulation of neuronal excitability. Nat Neurosci 14, 126-128.

Kazama, H., Nose, A., and Morimoto-Tanifuji, T. (2007). Synaptic components necessary for retrograde signaling triggered by calcium/calmodulin-dependent protein kinase II during synaptogenesis. Neuroscience 145, 1007-1015.

Kelleher, R. J., 3rd, and Bear, M. F. (2008). The autistic neuron: troubled translation? Cell 135, 401-406.

Kemp, B. E., Barden, J. A., Kobe, B., House, C., and Parker, M. W. (1996). Intrasteric regulation of calmodulin-dependent protein kinases. Adv Pharmacol 36, 221-249.

Klann, E., and Sweatt, J. D. (2008). Altered protein synthesis is a trigger for long-term memory formation. Neurobiol Learn Mem 89, 247-259.

Koekkoek, S. K., Yamaguchi, K., Milojkovic, B. A., Dortland, B. R., Ruigrok, T. J., Maex, R., De Graaf, W., Smit, A. E., VanderWerf, F., Bakker, C. E., et al. (2005). Deletion of FMR1 in Purkinje cells enhances parallel fiber LTD, enlarges spines, and attenuates cerebellar eyelid conditioning in Fragile X syndrome. Neuron 47, 339-352.

Koh, Y. H., Gramates, L. S., and Budnik, V. (2000). Drosophila larval neuromuscular junction: molecular components and mechanisms underlying synaptic plasticity. Microsc Res Tech 49, 14-25.

Koh, Y. H., Popova, E., Thomas, U., Griffith, L. C., and Budnik, V. (1999). Regulation of DLG localization at synapses by CaMKII-dependent

phosphorylation. Cell 98, 353-363.

Kolb, S. J., Hudmon, A., Ginsberg, T. R., and Waxham, M. N. (1998). Identification of domains essential for the assembly of calcium/calmodulin-dependent protein kinase II holoenzymes. J Biol Chem 273, 31555-31564.

Kops, G. J., Dansen, T. B., Polderman, P. E., Saarloos, I., Wirtz, K. W., Coffer, P. J., Huang, T. T., Bos, J. L., Medema, R. H., and Burgering, B. M. (2002). Forkhead transcription factor FOXO3a protects quiescent cells from oxidative stress. Nature 419, 316-321.

Kwon, C. H., Luikart, B. W., Powell, C. M., Zhou, J., Matheny, S. A., Zhang, W., Li, Y., Baker, S. J., and Parada, L. F. (2006). Pten regulates neuronal arborization and social interaction in mice. Neuron 50, 377-388.

Lavery, W., Hall, V., Yager, J. C., Rottgers, A., Wells, M. C., and Stern, M. (2007). Phosphatidylinositol 3-kinase and Akt nonautonomously promote perineurial glial growth in Drosophila peripheral nerves. J Neurosci 27, 279-288.

Leevers, S. J., Weinkove, D., MacDougall, L. K., Hafen, E., and Waterfield, M. D. (1996). The Drosophila phosphoinositide 3-kinase Dp110 promotes cell growth. Embo J 15, 6584-6594.

Li, H., Velasco-Miguel, S., Vass, W. C., Parada, L. F., and DeClue, J. E. (2002). Epidermal growth factor receptor signaling pathways are associated with tumorigenesis in the Nf1:p53 mouse tumor model. Cancer Res 62, 4507-4513.

Libina, N., Berman, J. R., and Kenyon, C. (2003). Tissue-specific activities of C. elegans DAF-16 in the regulation of lifespan. Cell 115, 489-502.

Lou, L. L., and Schulman, H. (1989). Distinct autophosphorylation sites sequentially produce autonomy and inhibition of the multifunctional Ca2+/calmodulin-dependent protein kinase. J Neurosci 9, 2020-2032.

Luscher, C., and Huber, K. M. (2010). Group 1 mGluR-dependent synaptic long-term depression: mechanisms and implications for circuitry and disease. Neuron 65, 445-459.

Ma, S., Yang, Y., Wang, C., Hui, N., Gu, L., Zhong, H., Cai, Z., Wang, Q., Zhang, Q., Li, N., and Cao, X. (2009). Endogenous human CaMKII inhibitory protein suppresses tumor growth by inducing cell cycle arrest and apoptosis through down-regulation of the phosphatidylinositide 3-kinase/Akt/HDM2 pathway. J Biol Chem 284, 24773-24782.

Macdonald, P. M. (1992). The Drosophila pumilio gene: an unusually long transcription unit and an unusual protein. Development 114, 221-232.

Mackay, T. F. (2009). The genetic architecture of complex behaviors: lessons from Drosophila. Genetica 136, 295-302.

MacLean, J. N., Zhang, Y., Goeritz, M. L., Casey, R., Oliva, R., Guckenheimer, J., and Harris-Warrick, R. M. (2005). Activity-independent coregulation of IA and Ih in rhythmically active neurons. J Neurophysiol 94, 3601-3617.

Malenka, R. C., and Bear, M. F. (2004). LTP and LTD: an embarrassment of riches. Neuron 44, 5-21.

Mallart, A., Angaut-Petit, D., Bourret-Poulain, C., and Ferrus, A. (1991). Nerve terminal excitability and neuromuscular transmission in T(X;Y)V7 and Shaker mutants of Drosophila melanogaster. J Neurogenet 7, 75-84.

Marder, E., and Prinz, A. A. (2002). Modeling stability in neuron and network function: the role of activity in homeostasis. Bioessays 24, 1145-1154.

Marques, G. (2005). Morphogens and synaptogenesis in Drosophila. J Neurobiol 64, 417-434.

Marques, G., Bao, H., Haerry, T. E., Shimell, M. J., Duchek, P., Zhang, B., and O'Connor, M. B. (2002). The Drosophila BMP type II receptor Wishful Thinking regulates neuromuscular synapse morphology and function. Neuron 33, 529-543.

Martin-Pena, A., Acebes, A., Rodriguez, J. R., Sorribes, A., de Polavieja, G. G., Fernandez-Funez, P., and Ferrus, A. (2006). Age-independent synaptogenesis by phosphoinositide 3 kinase. J Neurosci 26, 10199-10208.

McCabe, B. D., Hom, S., Aberle, H., Fetter, R. D., Marques, G., Haerry, T. E., Wan, H., O'Connor, M. B., Goodman, C. S., and Haghighi, A. P. (2004). Highwire regulates presynaptic BMP signaling essential for synaptic growth. Neuron 41, 891-905.

McCabe, B. D., Marques, G., Haghighi, A. P., Fetter, R. D., Crotty, M. L., Haerry, T. E., Goodman, C. S., and O'Connor, M. B. (2003). The BMP homolog Gbb provides a retrograde signal that regulates synaptic growth at the Drosophila neuromuscular junction. Neuron 39, 241-254.

McGuire, S. E., Roman, G., and Davis, R. L. (2004). Gene expression systems in Drosophila: a synthesis of time and space. Trends Genet 20, 384-391.

McLean, G. W., Carragher, N. O., Avizienyte, E., Evans, J., Brunton, V. G., and Frame, M. C. (2005). The role of focal-adhesion kinase in cancer - a new therapeutic opportunity. Nat Rev Cancer 5, 505-515.

Medema, R. H., Kops, G. J., Bos, J. L., and Burgering, B. M. (2000). AFX-like

Forkhead transcription factors mediate cell-cycle regulation by Ras and PKB through p27kip1. Nature 404, 782-787.

Mee, C. J., Pym, E. C., Moffat, K. G., and Baines, R. A. (2004). Regulation of neuronal excitability through pumilio-dependent control of a sodium channel gene. J Neurosci 24, 8695-8703.

Menon, K. P., Andrews, S., Murthy, M., Gavis, E. R., and Zinn, K. (2009). The translational repressors Nanos and Pumilio have divergent effects on presynaptic terminal growth and postsynaptic glutamate receptor subunit composition. J Neurosci 29, 5558-5572.

Menon, K. P., Sanyal, S., Habara, Y., Sanchez, R., Wharton, R. P., Ramaswami, M., and Zinn, K. (2004). The translational repressor Pumilio regulates presynaptic morphology and controls postsynaptic accumulation of translation factor eIF-4E. Neuron 44, 663-676.

Miller, S. G., Patton, B. L., and Kennedy, M. B. (1988). Sequences of autophosphorylation sites in neuronal type II CaM kinase that control Ca2(+)-independent activity. Neuron 1, 593-604.

Mills, J. L., Hediger, M. L., Molloy, C. A., Chrousos, G. P., Manning-Courtney, P., Yu, K. F., Brasington, M., and England, L. J. (2007). Elevated levels of growth-related hormones in autism and autism spectrum disorder. Clin Endocrinol (Oxf) 67, 230-237.

Miron, M., Lasko, P., and Sonenberg, N. (2003). Signaling from Akt to FRAP/TOR targets both 4E-BP and S6K in Drosophila melanogaster. Mol Cell Biol 23, 9117-9126.

Mitra, S. K., Hanson, D. A., and Schlaepfer, D. D. (2005). Focal adhesion kinase: in command and control of cell motility. Nat Rev Mol Cell Biol 6, 56-68.

Montiel, M., Quesada, J., and Jimenez, E. (2007). Activation of calcium-dependent kinases and epidermal growth factor receptor regulate muscarinic acetylcholine receptor-mediated MAPK/ERK activation in thyroid epithelial cells. Cell Signal 19, 2138-2146.

Moore, J. W., and Adelman, W. J., Jr. (1961). Electronic measurement of the intracellular concentration and net flux of sodium in the squid axon. J Gen Physiol 45, 77-92.

Muraro, N. I., Weston, A. J., Gerber, A. P., Luschnig, S., Moffat, K. G., and Baines, R. A. (2008). Pumilio binds para mRNA and requires Nanos and Brat to regulate sodium current in Drosophila motoneurons. J Neurosci 28, 2099-2109.

Murata, Y., and Wharton, R. P. (1995). Binding of pumilio to maternal hunchback mRNA is required for posterior patterning in Drosophila embryos. Cell 80, 747-756.

Murphy, C. T., McCarroll, S. A., Bargmann, C. I., Fraser, A., Kamath, R. S., Ahringer, J., Li, H., and Kenyon, C. (2003). Genes that act downstream of DAF-16 to influence the lifespan of Caenorhabditis elegans. Nature 424, 277-283.

Nakae, J., Kitamura, T., Silver, D. L., and Accili, D. (2001). The forkhead transcription factor Foxo1 (Fkhr) confers insulin sensitivity onto glucose-6-phosphatase expression. J Clin Invest 108, 1359-1367.

Nakatani, Y., Konishi, H., Vassilev, A., Kurooka, H., Ishiguro, K., Sawada, J., Ikura, T., Korsmeyer, S. J., Qin, J., and Herlitz, A. M. (2005). p600, a unique protein required for membrane morphogenesis and cell survival. Proc Natl Acad Sci U S A 102, 15093-15098.

Neves-Pereira, M., Muller, B., Massie, D., Williams, J. H., O'Brien, P. C., Hughes, A., Shen, S. B., Clair, D. S., and Miedzybrodzka, Z. (2009). Deregulation of EIF4E: a novel mechanism for autism. J Med Genet 46, 759-765.

Ogawa, S., Kwon, C. H., Zhou, J., Koovakkattu, D., Parada, L. F., and Sinton, C. M. (2007). A seizure-prone phenotype is associated with altered free-running rhythm in Pten mutant mice. Brain Res 1168, 112-123.

Onodera, H., Hara, H., Kogure, K., Fukunaga, K., Ohta, Y., and Miyamoto, E. (1990). Ca2+/calmodulin-dependent protein kinase II immunoreactivity in the rat hippocampus after forebrain ischemia. Neurosci Lett 113, 134-138.

Palomero, T., Sulis, M. L., Cortina, M., Real, P. J., Barnes, K., Ciofani, M., Caparros, E., Buteau, J., Brown, K., Perkins, S. L., et al. (2007). Mutational loss of PTEN induces resistance to NOTCH1 inhibition in T-cell leukemia. Nat Med 13, 1203-1210.

Pan, L., Woodruff, E., 3rd, Liang, P., and Broadie, K. (2008). Mechanistic relationships between Drosophila fragile X mental retardation protein and metabotropic glutamate receptor A signaling. Mol Cell Neurosci 37, 747-760.

Park, D., Coleman, M. J., Hodge, J. J., Budnik, V., and Griffith, L. C. (2002). Regulation of neuronal excitability in Drosophila by constitutively active CaMKII. J Neurobiol 52, 24-42.

Parkes, T. L., Elia, A. J., Dickinson, D., Hilliker, A. J., Phillips, J. P., and Boulianne, G. L. (1998). Extension of Drosophila lifespan by overexpression of human SOD1 in motorneurons. Nat Genet 19, 171-174.

Perroy, J., Gutierrez, G. J., Coulon, V., Bockaert, J., Pin, J. P., and Fagni, L. (2001). The C terminus of the metabotropic glutamate receptor subtypes 2 and 7 specifies the receptor signaling pathways. J Biol Chem 276, 45800-45805.

Persson, U., Izumi, H., Souchelnytskyi, S., Itoh, S., Grimsby, S., Engstrom, U., Heldin, C. H., Funa, K., and ten Dijke, P. (1998). The L45 loop in type I receptors for TGF-beta family members is a critical determinant in specifying Smad isoform activation. FEBS Lett 434, 83-87.

Phelps, C. B., and Brand, A. H. (1998). Ectopic gene expression in Drosophila using GAL4 system. Methods 14, 367-379.

Pin, J. P., Joly, C., Heinemann, S. F., and Bockaert, J. (1994). Domains involved in the specificity of G protein activation in phospholipase C-coupled metabotropic glutamate receptors. Embo J 13, 342-348.

Porter, J. A., Minke, B., and Montell, C. (1995). Calmodulin binding to Drosophila NinaC required for termination of phototransduction. Embo J 14, 4450-4459.

Poulain, C., Ferrus, A., and Mallart, A. (1994). Modulation of type A K+ current in Drosophila larval muscle by internal Ca2+; effects of the overexpression of frequenin. Pflugers Arch 427, 71-79.

Prokop, A. (2006). Organization of the efferent system and structure of neuromuscular junctions in Drosophila. Int Rev Neurobiol 75, 71-90.

Puig, O., Caspary, F., Rigaut, G., Rutz, B., Bouveret, E., Bragado-Nilsson, E., Wilm, M., and Seraphin, B. (2001). The tandem affinity purification (TAP) method: a general procedure of protein complex purification. Methods 24, 218-229.

Puig, O., Marr, M. T., Ruhf, M. L., and Tjian, R. (2003). Control of cell number by Drosophila FOXO: downstream and feedback regulation of the insulin receptor pathway. Genes Dev 17, 2006-2020.

Rawson, J. M., Lee, M., Kennedy, E. L., and Selleck, S. B. (2003). Drosophila neuromuscular synapse assembly and function require the TGF-beta type I receptor saxophone and the transcription factor Mad. J Neurobiol 55, 134-150.

Richards, S., Hillman, T., and Stern, M. (1996). Mutations in the Drosophila pushover gene confer increased neuronal excitability and spontaneous synaptic vesicle fusion. Genetics 142, 1215-1223.

Riedel, G., and Reymann, K. G. (1996). Metabotropic glutamate receptors in hippocampal long-term potentiation and learning and memory. Acta Physiol Scand 157, 1-19.

Rocic, P., Govindarajan, G., Sabri, A., and Lucchesi, P. A. (2001). A role for PYK2 in regulation of ERK1/2 MAP kinases and PI 3-kinase by ANG II in vascular smooth muscle. Am J Physiol Cell Physiol 280, C90-99.

Rodriguez-Viciana, P., Warne, P. H., Dhand, R., Vanhaesebroeck, B., Gout, I., Fry, M. J., Waterfield, M. D., and Downward, J. (1994). Phosphatidylinositol-3-OH kinase as a direct target of Ras. Nature 370, 527-532.

Ronesi, J. A., and Huber, K. M. (2008). Homer interactions are necessary for metabotropic glutamate receptor-induced long-term depression and translational activation. J Neurosci 28, 543-547.

Ruest, P. J., Roy, S., Shi, E., Mernaugh, R. L., and Hanks, S. K. (2000).

Phosphospecific antibodies reveal focal adhesion kinase activation loop phosphorylation in nascent and mature focal adhesions and requirement for the autophosphorylation site. Cell Growth Differ 11, 41-48.

Sakai, H., Ohuchida, K., Mizumoto, K., Cui, L., Nakata, K., Toma, H., Nagai, E., and Tanaka, M. (2011). Inhibition of p600 Expression Suppresses Both Invasiveness and Anoikis Resistance of Gastric Cancer. Ann Surg Oncol.

Salazar, A. M., Silverman, E. J., Menon, K. P., and Zinn, K. (2010). Regulation of synaptic Pumilio function by an aggregation-prone domain. J Neurosci 30, 515-522.

Salih, D. A., and Brunet, A. (2008). FoxO transcription factors in the maintenance of cellular homeostasis during aging. Curr Opin Cell Biol 20, 126-136.

Sanyal, S. (2009). Genomic mapping and expression patterns of C380, OK6 and D42 enhancer trap lines in the larval nervous system of Drosophila. Gene Expr Patterns 9, 371-380.

Schaller, M. D. (2001). Biochemical signals and biological responses elicited by the focal adhesion kinase. Biochim Biophys Acta 1540, 1-21.

Schlaepfer, D. D., Hanks, S. K., Hunter, T., and van der Geer, P. (1994). Integrin-mediated signal transduction linked to Ras pathway by GRB2 binding to focal adhesion kinase. Nature 372, 786-791.

Schlaepfer, D. D., Hauck, C. R., and Sieg, D. J. (1999). Signaling through focal adhesion kinase. Prog Biophys Mol Biol 71, 435-478.

Schlaepfer, D. D., and Hunter, T. (1997). Focal adhesion kinase overexpression enhances ras-dependent integrin signaling to ERK2/mitogen-activated

protein kinase through interactions with and activation of c-Src. J Biol Chem 272, 13189-13195.

Schlaepfer, D. D., Mitra, S. K., and Ilic, D. (2004). Control of motile and invasive cell phenotypes by focal adhesion kinase. Biochim Biophys Acta 1692, 77-102.

Schoepp, D. D. (2001). Unveiling the functions of presynaptic metabotropic glutamate receptors in the central nervous system. J Pharmacol Exp Ther 299, 12-20.

Schweers, B. A., Walters, K. J., and Stern, M. (2002). The Drosophila melanogaster translational repressor pumilio regulates neuronal excitability. Genetics 161, 1177-1185.

Serajee, F. J., Nabi, R., Zhong, H., and Mahbubul Huq, A. H. (2003). Association of INPP1, PIK3CG, and TSC2 gene variants with autistic disorder: implications for phosphatidylinositol signalling in autism. J Med Genet 40, e119.

Shakiryanova, D., Klose, M. K., Zhou, Y., Gu, T., Deitcher, D. L., Atwood, H. L., Hewes, R. S., and Levitan, E. S. (2007). Presynaptic ryanodine receptor-activated calmodulin kinase II increases vesicle mobility and potentiates neuropeptide release. J Neurosci 27, 7799-7806.

Shen, K., and Meyer, T. (1998). In vivo and in vitro characterization of the sequence requirement for oligomer formation of Ca2+/calmodulin-dependent protein kinase IIalpha. J Neurochem 70, 96-104.

Shim, S. Y., Wang, J., Asada, N., Neumayer, G., Tran, H. C., Ishiguro, K., Sanada, K., Nakatani, Y., and Nguyen, M. D. (2008). Protein 600 is a

microtubule/endoplasmic reticulum-associated protein in CNS neurons. J Neurosci 28, 3604-3614.

Shizuya, H., Birren, B., Kim, U. J., Mancino, V., Slepak, T., Tachiiri, Y., and Simon, M. (1992). Cloning and stable maintenance of 300-kilobase-pair fragments of human DNA in Escherichia coli using an F-factor-based vector. Proc Natl Acad Sci U S A 89, 8794-8797.

Sieg, D. J., Hauck, C. R., Ilic, D., Klingbeil, C. K., Schaefer, E., Damsky, C. H., and Schlaepfer, D. D. (2000). FAK integrates growth-factor and integrin signals to promote cell migration. Nat Cell Biol 2, 249-256.

Soltoff, S. P. (1998). Related adhesion focal tyrosine kinase and the epidermal growth factor receptor mediate the stimulation of mitogen-activated protein kinase by the G-protein-coupled P2Y2 receptor. Phorbol ester or [Ca2+]i elevation can substitute for receptor activation. J Biol Chem 273, 23110-23117.

Sonoda, J., and Wharton, R. P. (1999). Recruitment of Nanos to hunchback mRNA by Pumilio. Genes Dev 13, 2704-2712.

Sonoda, J., and Wharton, R. P. (2001). Drosophila Brain Tumor is a translational repressor. Genes Dev 15, 762-773.

Spassov, D. S., and Jurecic, R. (2003). The PUF family of RNA-binding proteins: does evolutionarily conserved structure equal conserved function? IUBMB Life 55, 359-366.

Stern, M., and Ganetzky, B. (1989). Altered synaptic transmission in Drosophila hyperkinetic mutants. J Neurogenet 5, 215-228.

Stern, M., Kreber, R., and Ganetzky, B. (1990). Dosage effects of a Drosophila

sodium channel gene on behavior and axonal excitability. Genetics 124, 133-143.

Tasaki, T., Mulder, L. C., Iwamatsu, A., Lee, M. J., Davydov, I. V., Varshavsky, A., Muesing, M., and Kwon, Y. T. (2005). A family of mammalian E3 ubiquitin ligases that contain the UBR box motif and recognize N-degrons. Mol Cell Biol 25, 7120-7136.

Teleman, A. A., Hietakangas, V., Sayadian, A. C., and Cohen, S. M. (2008). Nutritional control of protein biosynthetic capacity by insulin via Myc in Drosophila. Cell Metab 7, 21-32.

Toutant, M., Costa, A., Studler, J. M., Kadare, G., Carnaud, M., and Girault, J. A. (2002). Alternative splicing controls the mechanisms of FAK autophosphorylation. Mol Cell Biol 22, 7731-7743.

Turrigiano, G. G., and Nelson, S. B. (2004). Homeostatic plasticity in the developing nervous system. Nat Rev Neurosci 5, 97-107.

Ueda, A., Grabbe, C., Lee, J., Lee, J., Palmer, R. H., and Wu, C. F. (2008). Mutation of Drosophila focal adhesion kinase induces bang-sensitive behavior and disrupts glial function, axonal conduction and synaptic transmission. Eur J Neurosci 27, 2860-2870.

Venken, K. J., and Bellen, H. J. (2005). Emerging technologies for gene manipulation in Drosophila melanogaster. Nat Rev Genet 6, 167-178.

Venken, K. J., He, Y., Hoskins, R. A., and Bellen, H. J. (2006). P[acman]: a BAC transgenic platform for targeted insertion of large DNA fragments in D. melanogaster. Science 314, 1747-1751.

Wild, J., Hradecna, Z., and Szybalski, W. (2002). Conditionally amplifiable BACs:

switching from single-copy to high-copy vectors and genomic clones. Genome Res 12, 1434-1444.

Wreden, C., Verrotti, A. C., Schisa, J. A., Lieberfarb, M. E., and Strickland, S. (1997). Nanos and pumilio establish embryonic polarity in Drosophila by promoting posterior deadenylation of hunchback mRNA. Development 124, 3015-3023.

Xu, G. F., Lin, B., Tanaka, K., Dunn, D., Wood, D., Gesteland, R., White, R., Weiss, R., and Tamanoi, F. (1990). The catalytic domain of the neurofibromatosis type 1 gene product stimulates ras GTPase and complements ira mutants of S. cerevisiae. Cell 63, 835-841.

Yager, J., Richards, S., Hekmat-Scafe, D. S., Hurd, D. D., Sundaresan, V., Caprette, D. R., Saxton, W. M., Carlson, J. R., and Stern, M. (2001). Control of Drosophila perineurial glial growth by interacting neurotransmitter-mediated signaling pathways. Proc Natl Acad Sci U S A 98, 10445-10450.

Ye, B., Petritsch, C., Clark, I. E., Gavis, E. R., Jan, L. Y., and Jan, Y. N. (2004). Nanos and Pumilio are essential for dendrite morphogenesis in Drosophila peripheral neurons. Curr Biol 14, 314-321.

Yi, J. J., and Ehlers, M. D. (2005). Ubiquitin and protein turnover in synapse function. Neuron 47, 629-632.

Yi, T. M., Huang, Y., Simon, M. I., and Doyle, J. (2000). Robust perfect adaptation in bacterial chemotaxis through integral feedback control. Proc Natl Acad Sci U S A 97, 4649-4653.

Zwick, E., Wallasch, C., Daub, H., and Ullrich, A. (1999). Distinct calcium-dependent pathways of epidermal growth factor receptor

transactivation and PYK2 tyrosine phosphorylation in PC12 cells. J Biol Chem 274, 20989-20996.

Chapter 6: Appendices

6.1 The *push-CTAG* transgenic fly.

Tandem affinity purification (TAP) is a tool that uses a target protein as bait to fish out substrate proteins under native conditions (Chang, 2006; Gingras et al., 2005). The TAP tag contains other IgG binding domain of Staphylococcus aureus protein A (ProtA) and a calmodulin binding peptide (CBP) (Chang, 2006; Gingras et al., 2005). This method involves the fusion of the TAP tag to the target protein and expression of this fusion protein in the cell or organism. The protein complex is purified by two different affinity columns; the first one is IgG and the second one is calmodulin. Then, the bound proteins are analyzed by electrophoresis and identified by mass spectrometry (Puig et al., 2001). As mentioned in Section 4.5, I want to identify the Push binding substrates. Therefore, generating transgenic flies which possess a TAP-tagged Push is required.

To make the TAP-tagged Push construct, we used the *P[acman]* plasmid (provided by Hugo Bellen, Ph.D. , BCM) (Venken et al., 2006). The *P[acman]* plasmid contains two origins of replication. One origin, *oriS*, which is of

low-copy-number can stabilize a large cloned DNA fragment, such as the bacteria artificial chromosome (BAC) and prevent the errors of DNA replication (Shizuya et al., 1992). The other origin ,*oriV*, which is of high-copy-number, provides the capacity for sequencing, embryo injection, and other manipulations requiring large amounts of plasmid DNA (Venken and Bellen, 2005; Venken et al., 2006; Wild et al., 2002). Therefore, P[acman] is capable to carry large *push* genomic DNA and 20 kb upstream region, which equates to 45 kb. In addition, we wanted to keep the N-terminal signal sequence of Push to ensure that Push can be properly inserted into the membrane. Therefore, I cloned the C-terminal TAP tag (*CTAG*) DNA fragment from *pFA-6A-CTAP* plasmid (provided by Kathy L. Gould, Ph.D, Vanderbilt University) and I cloned two DNA fragments of *push* (LA and RA, each is about 500 bp) from BAC clone (*BACR08I01*, CHORI) which carries *push* (Figure 6.1.1). Then, LA, RA, and *CTAG* were cloned into *P[acman] (called P[acman]-LRC)*. *P[acman]-LRC* was co-transformed with *BACR08I01* into the E. coli strain SW102 (provided by NCI). This transformation in SW102 induced phage-mediated recombination and generated *P[acman]* with *push* and *CTAG* (*P[acman]-push-CTAG*). The *P[acman]-push-CTAG* was further characterized by plasmid size, PCR, and restriction enzyme digestion mapping to ensure the

construct was correct (Figure 6.1.2). The correct *P[acman]-push-CTAG* was injected into Drosophila embryo (*white*$^{-}$). The successful transgenic *push-CTAG* flies were screened and selected according to their red eye color (*white*$^{+}$) (Figure 6.1.1).

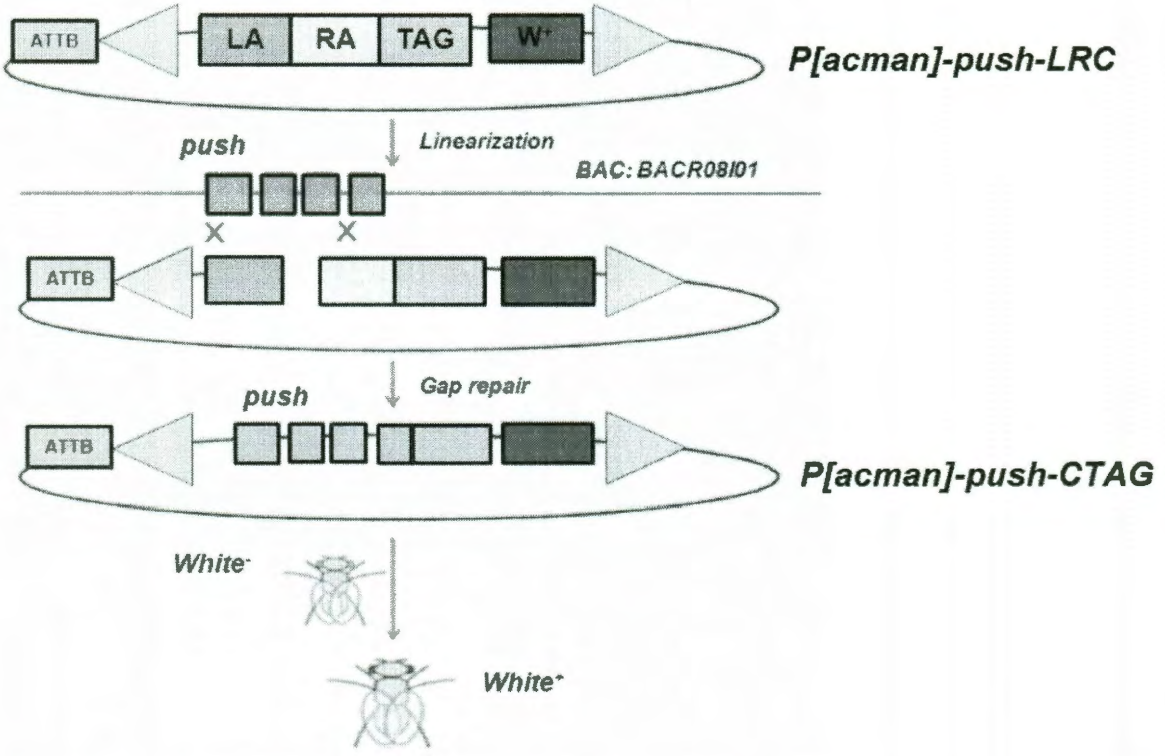

Figure 6.1.1: The cloning strategy of *P[acman]-push-CTAG*. LA, RA, and *CTAG* were cloned into *P[acman] (called P[acman]-LRC)*. Linear *P[acman]-LRC* was co-transformed with *BACR08I01* into the E. coli strain SW102. The phage-mediated homologous recombination (gap repair) in SW102 generated *P[acman]* with *push* and *CTAG* (*P[acman]-push-CTAG*). The *P[acman]-push-CTAG* was injected into Drosophila embryo with *white*$^{-}$ background. The successful transgenic *push-CTAG* flies were screened and selected according to their red eye color (*white*$^{+}$)

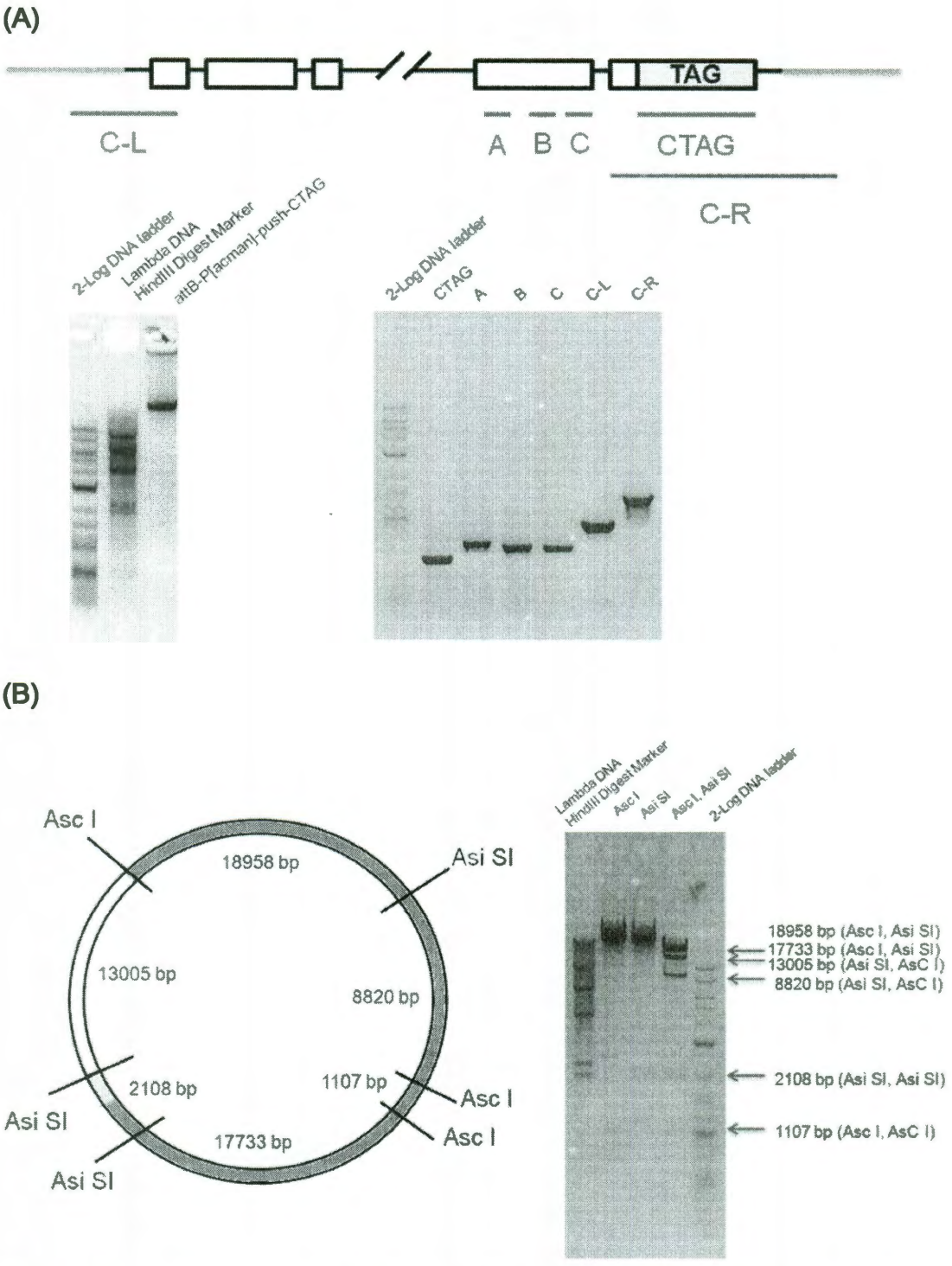

Figure 6.1.2: The characterization of *P[acman]-push-CTAG*. (A) Top: the simple picture shows the region of push-CTAG in *P[acman]-push-CTAG*. Bottom left: the DNA electrophoresis shows the size of *P[acman]-push-CTAG*. Bottom right: the

DNA electrophoresis shows the PCR products (CTAG, A, B, C, C-L, and C-R) were amplified from different region of *P[acman]-push-CTAG*. These DNA fragments (CTAG, A, B, C, C-L, and C-R) are indicated on Top picture. (B) Left: the simple picture shows the size of DNA fragments after restriction enzymes (Asc I and Asi SI) digestion. Right: the Asc I/Asi SI digestion map of *P[acman]-push- CTAG*. Each arrow indicated the fragment size and parentheses represent the related pair of restriction enzymes. 2-Log DNA ladder and Lambda DNA HindIII digest are DNA markers.